

## ABSTRACT

Title of Dissertation: Investigation of the *Tetrahymena Pyriformis*  
2-Aminoethylphosphonic Acid Biosynthetic  
Pathway and the P-C Bond Forming Enzyme  
Phosphoenolpyruvate Mutase

Michael Scott McQueney, Doctor of Philosophy, 1991

Dissertation directed by: Dr. Debra Dunaway-Mariano  
Professor  
Department of Chemistry and Biochemistry

The biosynthetic pathway leading to 2-aminoethylphosphonate in *Tetrahymena pyriformis* was determined. A cell-free homogenate of *T. pyriformis* converted phosphoenolpyruvate to AEP in 37 %yield, phosphonopyruvate to AEP in a 11% yield and phosphonoacetaldehyde to AEP in an 83% yield. The *Tetrahymena pyriformis* enzyme, PEP mutase was purified. The PEP Mutase catalyzes the rearrangement of phosphoenolpyruvate to phosphonopyruvate and the equilibrium constant is >500:1 in favor of phosphoenolpyruvate. To distinguish between an intra-and intermolecular reaction pathway for this process an equimolar mixture of [P=<sup>18</sup>O, C(2)-<sup>18</sup>O]thiophosphonopyruvate and (all-<sup>16</sup>O)thiophosphonopyruvate was reacted with the PEP mutase and the resulting products were analyzed by <sup>31</sup>P-NMR. The absence of the cross-

over product [C(2)-<sup>18</sup>O]thiophosphoenolpyruvate in the product mixture was interpreted as evidence for an intramolecular reaction pathway. To distinguish between a concerted and stepwise intramolecular reaction pathway the pure enantiomers of the chiral substrate [P=<sup>18</sup>O]thiophosphonopyruvate were prepared and the stereochemical course of their conversion to chiral [P=<sup>18</sup>O]thiophosphoenolpyruvate was determined. Based on the observed conversion of (S<sub>P</sub>)-[P=<sup>18</sup>O]thiophosphonopyruvate to (S<sub>P</sub>)-[P=<sup>18</sup>O]thiophosphoenolpyruvate and (R<sub>P</sub>)-[P=<sup>18</sup>O]thiophosphonopyruvate to (R<sub>P</sub>)-[P=<sup>18</sup>O]thiophosphoenolpyruvate it was concluded that the PEP phosphomutase reaction proceeds with retention of the phosphorus configuration and therefore by a stepwise mechanism. The similar reactivity of the oxo and thio substituted phosphonopyruvate substrates (*i. e.*, nearly equal V<sub>max</sub>) was interpreted to suggest that addition to the phosphorus atom is not rate limiting among the reaction steps. Lastly, single turnover experiments failed to trap a pyruvate in the PEP mutase reaction.

Investigation of the *Tetrahymena Pyriformis* 2-Aminoethylphosphonic Acid  
Biosynthetic Pathway and the P-C Bond Forming Enzyme,  
Phosphoenolpyruvate Mutase

by

Michael S. McQueney

Dissertation submitted to the Faculty of the Graduate School  
of the University of Maryland in partial fulfillment  
of the requirements for the degree of  
Doctor of Philosophy  
1991

Cl.  
MD

Dept. of Chemistry and Biochemistry

Advisory Committee:

Professor	Debra Dunaway-Mariano, Chairman/Advisor
Professor	Patrick S. Mariano
Professor	John A. Gerlt
Assistant Professor	Daniel E. Falvey
Professor	James Herndon

Maryland  
LD  
3231  
.M70d  
McQueney,  
M.S.

## **DEDICATION**

To my parents  
John Robert McQueney Sr.  
and  
Helen Boyles McQueney

## ACKNOWLEDGEMENTS

I want to express my deepest gratitude to my advisor Professor Debra Dunaway-Mariano for her guidance patience and help. I also want to thank Professor Patrick S. Mariano for his advice and teaching in the methods of organic synthesis. Additionally, I thank Dr. Yui-Fai Lam for his assistance in NMR experiments and Dr. Herman Ammon for the X-ray analysis.

I must give special thanks to Elise Bowman and Sheng-Lian Lee, for insightful discussions and friendship and to William Swartz for technical assistance. I also thank all my colleagues in both Professor Dunaway-Mariano's and Professor Mariano's labs, especially Sara Thrall and Linda Yankie for proofreading this dissertation. I thank Jae-Bong Kim for his work and wish him luck in continuing the research.

I am indebted to my family and friends for all their encouragement and support, especially my parents, my sisters Carol and Patricia and my brother John; Fr. Tom Kalita; Tom Peightel; and my fraternity, the Alpha Beta Chapter of Phi Sigma Pi National Honor Fraternity.

## TABLE OF CONTENTS

<u>Section</u>	<u>Page</u>
<b>List of Tables</b> .....	x
<b>List of Figures</b> .....	xi
<b>List of Abbreviations</b> .....	xv
<b>INTRODUCTION</b> .....	1
<b>BACKGROUND</b> .....	3
I. Biological Pathways of P-C Bond Clavage.....	9
A. The AEP Degradation Pathway.....	10
B. The C-P Lyase Pathway.....	11
C. Enzymology of P-C Bond Cleavage.....	11
1. Chemical Models for P-C bond Cleavage.....	11
2. The Mechanism of Phosphonatase.....	16
3. Mechanism of C-P Lyase.....	21
II. P-C Bond Formation in Nature.....	23
A. AEP Biosynthetic Pathway.....	24
B. Phosphonate Antibiotic Biosynthetic Pathways.....	29
C. Enzymology of P-C Bond formation.....	32
1. Chemical Models for P-C Bond formation via Nucleophilic Phosphorus.....	33
2. Chemical Models of P-C Bond Formation via Electophilic Phosphorus.....	34
<b>RESEARCH PROPOSAL</b> .....	39
I. Verification of the PEP $\leftrightarrow$ P-pyr Mode of P-C Bond Formation.....	39
II. Examination of the Catalytic Mechanism of the PEP $\leftrightarrow$ P-pyr Rearrangement.....	40

<b>RESULTS AND DISCUSSION</b> .....	42
I. Verification of the PEP $\leftrightarrow$ P-pyr Mode of P-C Bond Formation.....	42
A. Evidence for the PEP $\Rightarrow$ AEP Conversion in <i>T. pyriformis</i> .....	43
1. Cell-free Homogenate Conversion of PEP to AEP.....	44
2. TPP-Enhanced Conversion of PEP to AEP.....	44
B. Cell-free Homogenate Conversion of P-pyr to AEP.....	45
C. Cell-free Homogenate Conversion of P-ald to AEP.....	46
D. Discovery of PEP Mutase.....	46
1. Relative Conversions of PEP, P-pyr, and P-ald to AEP.....	46
2. Determining the In Vitro Fate of P-pyr in the Cell- Free Homogenate.....	48
E. Purification and Characterization of PEP Mutase.....	48
1. Purification of PEP Mutase.....	51
2. Determination of the External Equilibrium of PEP Mutase .....	54
3. Discussion of the Internal and External Equilibria of PEP Mutase.....	57
I. Studies of the Catalytic Mechanism of the PEP $\leftrightarrow$ P-pyr Rearrangement Catalyzed by PEP Mutase.....	59
1. Synthesis of Thiophosphonopyruvate.....	59
2. Substrate Activity of Thiophosphonopyruvate with PEP Mutase.....	60
A. Determination of the Intramolecularity of the PEP Mutase Rearrangement of PEP.....	62

1. Precedence for Intra- and Intermolecular Mechanisms in Phosphomutases.....	62
2. Does the PEP Mutase Reaction Proceed Intramolecularly?.....	65
a. [ <sup>18</sup> O]Thiophosphonopyruvate <sup>31</sup> P NMR Shift Standards.....	68
b. PEP Mutase Crossover Experiment.....	69
B. Is the PEP Mutase-Catalyzed Intramolecular Rearrangement Concerted or Stepwise?.....	72
1. Analysis of Possible Mechanisms.....	72
a. Precedence for a Concerted Mechanism.....	75
b. Precedence for Stepwise Mechanisms.....	75
2. Stereochemical Analysis to Probe the Concerted vs Stepwise Mechanism.....	76
a. Stereochemical Course of the Concerted Reaction.....	76
b. Stereochemical Course of the Stepwise Pathways.....	77
3. Design of the Phosphorus Stereochemical Analysis.....	80
a. Synthesis of Chiral Thiophosphonopyruvate.....	81
b. Stereochemical Analysis .....	84
4. Direct Evidence for Carboxyl-Assisted P-N Bond Hydrolysis with Retention of Phosphorus Stereochemistry.....	88
a. Kinetic Evidence for Carboxyl-Assisted P-N Bond Hydrolysis.....	88

b. Stereochemical Evidence for Carboxyl-Assisted P-N Bond Hydrolysis.....	92
C. The Search for the Intermediate in the PEP $\leftrightarrow$ P-pyr Rearrangement.....	105
1. Rapid Quench Experiments with PEP Mutase.....	107
a. Synthesis of [ $^3\text{H}$ ]P-pyr.....	109
b. Single Turnover Experiment with [ $^3\text{H}$ ]P-pyr and Mg $^{2+}$ Activated PEP Mutase.....	111
2. Single Turnover Experiment with [ $^3\text{H}$ ]P-pyr and Mn $^{2+}$ Activated PEP Mutase.....	115
3. Rapid Quench of the Mg $^{2+}$ -Activated PEP Mutase Reaction at 4 $^\circ\text{C}$ .....	118
4. Determination of the Internal Equilibrium of PEP and P-pyr Bound to PEP Mutase.....	121
<b>CONCLUSION</b> .....	126
<b>METHODS</b> .....	129
<b>General</b> .....	129
Phosphonoacetaldehyde (P-ald).....	130
Phosphonoalanine (P-ala) .....	131
Phosphonopyruvate (P-pyr).....	132
Tetrahymena pyriformis Media and Stock Cultures.....	133
Large Scale Growth and Lysis.....	133
Reactions with Tetrahymena pyriformis Homogenate and Homogenate Fractions.....	134
PEP Phosphomutase Assay and Isolation.....	135

Thiophosphonopyruvate and Racemic	
[P= <sup>18</sup> O]Thiophosphonopyruvate.....	136
Kinetic Constants for Thiophosphonopyruvate vs.	
Phosphonopyruvate.....	137
[P= <sup>18</sup> O, C(2)- <sup>18</sup> O]Thiophosphonopyruvate (26) and [C(2)- <sup>18</sup> O]Thio-	
phosphonopyruvate (32).....	137
PEP Phosphomutase Catalyzed Reactions of [P= <sup>18</sup> O, C(2)-	
<sup>18</sup> O]Thiophos-phonopyruvate (26) and	
[C(2)- <sup>18</sup> O]Thiophosphonopyruvate (32) to the Corresponding	
Thiophosphoenolpyruvates.....	137
PEP Phosphomutase Catalyzed Reaction of an Equimolar Mixture	
of Thiophosphonopyruvate and [P= <sup>18</sup> O, C(2)- <sup>18</sup> O]	
Thiophosphonopyruvate (32).....	138
OP-(2-Trimethylsilylethyl) Methylphosphonochloridothioate (20).....	139
Synthesis of (2-Trimethylsilylethyl)oxalyl Chloride.....	139
Synthesis of (S)-(-)-N-Methyl-N-(1-Phenylethyl)amine (21).....	140
(S <sub>p</sub> ,S <sub>c</sub> )- and (R <sub>p</sub> ,S <sub>c</sub> )-N,P-Dimethyl-N-(1-Phenylethyl)-O-[2-	
(Trimethylsilyl)ethyl Phosphonamidothioate (22a and 22b).....	141
(S <sub>p</sub> ,S <sub>c</sub> )-N,P-Dimethyl-N-(1-Phenylethyl)-S-[2-(4-Nitrophenyl)-	
2-Oxoethyl] Phosphonamidothioate (40) for X-Ray Analysis.....	143
X-Ray Analysis of (S <sub>p</sub> ,S <sub>c</sub> )-N,P-Dimethyl-N-(1-Phenylethyl)-	
S-[2-(4-Nitrophenyl)-2-Oxoethyl] Phosphonamidothioate (40).....	144
(S <sub>p</sub> ,S <sub>c</sub> )- and (R <sub>p</sub> ,S <sub>c</sub> )-3-[[Methyl(1-Phenylethyl)amino][2-	
(trimethylsilyl)ethoxy]phosphinothioyl]-2-Oxo-2-(Trimethylsilyl)ethyl	
Propanoate (23a and 23b).....	145

(SP,SC)- and (RP,SC)-3-[[Methyl(1-Phenylethyl)amino]phosphinothioyl]-2-Oxo-2-Propanoic Acid (24a and 24b).....	147
Preparation of the (Rp)- and (Sp)-[P= <sup>18</sup> O]Thiophosphonopyruvates (31a and 31b) by Hydrolysis of 24a and 24b in [ <sup>18</sup> O]H <sub>2</sub> O.....	148
Selective OP-De(trimethyl)silylethylation of 23a.....	148
[P= <sup>18</sup> O]Thiophosphonopyruvates (31a and 31b) by Hydrolysis of OP-Desilylethyl-23a (42a) in [ <sup>18</sup> O]H <sub>2</sub> O.....	149
(Sp,Sc)- and (Rp,Sc)-3-[[Methyl(1-Phenylethyl)amino][2-(Trimethylsilyl)ethoxy]phosphinothioyl]-2-Oxo-(2-Propyl)propanoate (45a and 45b).....	149
(SP, SC)- and (RP,SC)-3-[[Methyl(1-Phenylethyl)amino]phosphinothioyl]-2-Oxo-(2-Propyl)propanoate (46a and 46b).....	151
Formation of the [P= <sup>18</sup> O]Thiophosphonopyruvates (31a and 31b) by Hydrolysis of 46a and 46b in H <sub>2</sub> <sup>18</sup> O.....	152
Enzymatic Conversion of the (Rp)- and (Sp)-[P= <sup>18</sup> O, <sup>18</sup> O]Thiophosphonopyruvates (31a and 31b) to the [P= <sup>18</sup> O]Thiophosphoenolpyruvates (29a and 29b).....	153
Enzymatic Conversion of [P= <sup>18</sup> O]Thiophosphoenolpyruvates 29a and/or 29b to [ $\gamma$ - <sup>18</sup> O-P]ATPS.....	153
Rapid Quench\Experiments.....	156
<b>APPENDIX</b> .....	158
<b>REFERENCES</b> .....	162

## LIST OF TABLES

<b>Table 1.</b> Conversion of proposed intermediates to AEP.....	47
<b>Table 2.</b> Purification of Phosphoenolpyruvate Mutase.....	54
<b>Table 3.</b> Amount of radioactivity associated with each product formed in the experiment determining the on-enzyme equilibrium of PEP mutase.....	123

## LIST OF FIGURES

- Figure 1.**  $^{31}\text{P}$  NMR of the products formed from 47  $\mu\text{mol}$  of P-pyr in the cell-free homogenate, and 23.5  $\mu\text{mol}$  of added ADP. b) The same reaction mixture 20 min after the addition of 54 units of pyruvate kinase  
.....50
- Figure 2.** SDS-PAGE of the column chromatographic purification of PEP mutase. Lanes 2-8 are tubes 90 to 96 from the phenyl Sepharose column and lanes 9 -19 are tubes 31-41 from the Biogel. column. Columns 1 and 20 display molecular weight markers.  
.....52
- Figure 3.** HPLC elution profile of a reaction of 10mM PEP and 10mM P-pyr in 50 mM  $\text{K}^+$ HEPES buffer containing 10 mM  $\text{MgCl}_2$  **a)** before addition of PEP mutase and **b)** after a 30 min reaction with PEP mutase. Inset is magnified 10-fold.  
.....55
- Figure 4.** The  $^{31}\text{P}$  NMR spectrum of the mixture of isotopically labelled thiophosphoenolpyruvates obtained by PEP mutase catalyzed reaction of a mixture of  $[\text{P}=\text{}^1\text{}^8\text{O}, \text{C}(2)\text{-}\text{}^1\text{}^8\text{O}]$ thiophosphonopyruvate (**26**) and  $[\text{all-}\text{}^1\text{}^6\text{O}]$ thiophosphonopyruvate (Scheme 2). The observed resonances correspond to the thiophosphoenolpyruvate isotopomers **27**, **29**, and **30** as labelled.  
.....71
- Figure 5.** X-Ray Structure of the Crystalline Derivative of **40** Derived from the Methylphosphonamidate **22a**

**Figure 6.** The  $\gamma$ -P region(a) and  $\beta$ -P region (b) of the  $^{31}\text{P}$  NMR spectra of a mixture of (SP)-(all- $^{16}\text{O}$ )ATP $\beta\text{S}$  and (SP)-[P( $\beta$ )= $^{18}\text{O}$ ]ATP $\beta\text{S}$  (**41a**) isotopomers derived from (RP)-[P= $^{18}\text{O}$ ]thiophosphoenolpyruvate enantiomer **29a** formed *via* PEP phosphomutase reaction of the (RP)-thiophosphonopyruvate enantiomer **31a**; the  $\gamma$ -P region(c) and  $\beta$ -P region (d) of the  $^{31}\text{P}$  NMR spectra of a mixture of (SP)-[ $^{16}\text{O}_3\text{-P}$ ]ATP $\beta\text{S}$  and (SP)-[P( $\beta$ )= $^{18}\text{O}$ ]ATP $\beta\text{S}$  (**41b**) isotopomers derived from (SP)-[P= $^{18}\text{O}$ ]thiophosphoenolpyruvate enantiomer **29b** formed *via* PEP phosphomutase reaction of the (SP)-thiophosphonopyruvate enantiomer **31b**.

**Figure 7.** The  $\beta$ -P region of the  $^{31}\text{P}$  NMR spectra of a mixture of (SP)-(all- $^{16}\text{O}$ )ATP $\beta\text{S}$  and (SP)-[P( $\beta$ )= $^{18}\text{O}$ ]ATP $\beta\text{S}$  (**41a and 41b**) isotopomers derived from (SP)- and (RP)-[P= $^{18}\text{O}$ ]thiophosphoenolpyruvate enantiomers **29a** and **29b** formed *via* PEP mutase reaction of a mixture of (SP)-and (RP)-thiophosphonopyruvate enantiomers **31a** and **31b**.produced from the hydrolysis of **42a**.

**Figure 8.** The  $\beta$ -P region of the  $^{31}\text{P}$  NMR spectra of a mixture of (SP)-(all- $^{16}\text{O}$ )ATP $\beta\text{S}$  and (SP)-[P( $\beta$ )= $^{18}\text{O}$ ]ATP $\beta\text{S}$  (**41a and 41b**) isotopomers derived from (SP)- and (RP)-[P= $^{18}\text{O}$ ]thiophosphoenolpyruvate enantiomers **29a** and **29b** formed *via* PEP mutase reaction of a mixture of (SP)-and (RP)-

thiophosphonopyruvate enantiomers **31a** and **31b** produced from the hydrolysis of **46a**.

.....101

**Figure 9.** Idealized hypothetical time course of the PEP mutase reaction with [<sup>3</sup>H]P-pyr under single turnover conditions.

.....106

**Figure 10.** Kinetic equation of the PEP mutase-catalyzed rearrangement of P-pyr

.....107

**Figure 11.** Flowchart of the rapid quench experiments.

.....108

**Figure 12.** HPLC elution profiles of a) [<sup>3</sup>H]P-lac derived from a reaction of [<sup>3</sup>H]P-pyr and b) [<sup>3</sup>H]PEP derived from a reaction of [<sup>3</sup>H]P-pyr with a catalytic amount of PEP mutase

.....110

**Figure 13.** Time course for a single turnover of P-pyr in the active site of Mg<sup>2+</sup>-activated PEP mutase at 25°C. The reaction contained ca. 13 μM [<sup>3</sup>H]P-pyr, 46 μM PEP mutase (subunit Mol. Wt. 39000 Daltons), 5 mM MgCl<sub>2</sub> and 50 mM K<sup>+</sup>HEPES (pH 7.5).

.....112

**Figure 14.** Time course for a single turnover of P-pyr in the active site of Mg<sup>2+</sup>-activated PEP mutase at 25°C. The reaction contained 5 μM [<sup>3</sup>H]P-pyr, 50 μM PEP mutase (subunit Mol. Wt. 39000 Daltons), 5 mM MgCl<sub>2</sub> and 50 mM K<sup>+</sup>HEPES (pH 7.5).

.....114

**Figure 15.** Time course for a single turnover of P-pyr in the active site of Mn<sup>2+</sup>-activated PEP mutase at 25°C. The reaction contained 5 μM [<sup>3</sup>H]P-pyr, 50 μM PEP mutase (subunit Mol. Wt. 39000 Daltons), 5 mM MgCl<sub>2</sub> and 50 mM K<sup>+</sup>HEPES (pH 7.5)  
.....117

**Figure 16.** Time course for a single turnover of P-pyr in the active site of Mg<sup>2+</sup>-activated PEP mutase at 4°C. The reaction contained 5 μM [<sup>3</sup>H]P-pyr, 50μM PEP mutase (subunit Mol. Wt. 39000 Daltons), 5 mM MgCl<sub>2</sub> and 50 mM K<sup>+</sup>HEPES (pH 7.50).  
.....120

**Figure 17.** Plot of % substrates and products vs PEP mutase (subunit Molec Wt. 39000 daltons) concentration of 86 μL reactions consisting of 5 μM [<sup>3</sup>H]P-pyr 5 mM MgCl<sub>2</sub> in 50 mM K<sup>+</sup>HEPES buffer (pH 7.5) at 25°C, for 50 msec.  
.....124

## LIST OF ABBREVIATIONS

ADP	adenosine 5'-diphosphate
ADP $\beta$ S	adenosine 5'-(2-thiodiphosphate)
AEP	(2-aminoethyl)phosphonate
AMP	adenosine 5'-monophosphate
ATP	adenosine 5'-triphosphate
ATP $\gamma$ S	adenosine 5'-(1-thiotriphosphate)
ATP $\beta$ S	adenosine 5'-(2-thiotriphosphate)
C <sub>i</sub>	Currie
CPM	Counts per minute
DTT	dithiothreitol
EDTA	(ethylenedinitrilo)tetraacetic acid
HEPES	N-(2-hydroxyethyl)piperazine-N'-2-ethane sulfonic acid
HPLC	high-pressure liquid chromatography
LDH	lactate dehydrogenase
NAD <sup>+</sup>	nicotinamide adenine dinucleotide
NADH	dihyronicotinamide adenine dinucleotide
NMR	nuclear magnetic resonance
P-ala	phosphonalanine
P-ald	phosphonoacetaldehyde
P-pyr	phosphonopyruvate
p-TsOH	p-toluenesulfonic acid
PEP	phosphoenolpyruvate
PK	pyruvate kinase
PLP	pyridoxal phosphate

P-lac	phosphonolactate
SP-pyr	thiophosphonopyruvate
TEAB	triethanolamine bicarbonate
TMSBr	trimethylsilyl bromide
TMSI	trimethylsilyl iodide
TPP	Thiamine pyrophosphate
Tris	tris(hydroxymethyl)aminomethane
THF	tetrahydrofuran

## INTRODUCTION

Work in our laboratory has focussed on the metabolism of an obscure but important class of natural products, the phosphonates [for reviews on this topic see Hilderband.<sup>1</sup> Unlike the phosphates, which comprise the principal class of naturally occurring phosphorus compounds, phosphonates contain a P-C linkage. The phosphonate P-C bond is resistant to the acid, base and enzyme catalyzed hydrolysis reactions that lead to P-O-C bond cleavage in organophosphates. A diverse group of microbes and invertebrates have retained, or specially developed, the ability to form the P-C bond and hence, the ability to synthesize phosphonates. Because the phosphonyl moiety of the phosphonates resemble, both structurally and electronically, the carboxyl and phosphoryl moieties of cellular metabolites and because the phosphonates are resistant to enzyme catalyzed degradation, phosphonates are effective anti-metabolites. Of the naturally occurring phosphonates discovered thus far, many have been identified as antibiotics, antiviral agents, herbicides or hypertensive agents.

The actual chemistry of P-C bond formation in biological systems has alluded researchers since the discovery of the first phosphonate natural product thirty years ago.<sup>2</sup> This dissertation describes the advances we have made in understanding the enzymology of P-C bond formation which have emerged from our investigation of the biosynthesis of the most ubiquitous of the naturally occurring phosphonates, 2-aminoethylphosphonate (AEP). Elucidation<sup>3</sup> of the AEP forming pathway of *Tetrahymena pyriformis* (see below) ultimately led to the isolation of the

P-C bond forming enzyme, PEP mutase from this organism.<sup>4,5</sup> Also describe herein are studies which examine the chemical mechanism of the PEP mutase catalyzed conversion of PEP to phosphonopyruvate. We first addressed the question of whether the rearrangement occurs intermolecularly or intramolecularly. After demonstrating that an intramolecular pathway is followed, we employed stereochemical techniques to show that the reaction occurs *via* a stepwise as opposed to concerted mechanism.

## BACKGROUND

Phosphorus is found in a variety of compounds and plays crucial roles in the earth's geology, in biological systems, and in modern society. The wide variety of phosphorus compounds is a result of its ability to exist in the +5, +3, and +1 oxidation states and form stable bonds with many elements (H, N, O, S, C, and halides). In the environment phosphorus is predominantly +5 and can be found in over 200 minerals, the most abundant of which is  $\text{Ca}(\text{PO}_4)_6\text{F}_2$ .<sup>6</sup> The earth's geology maintains a delicate balance and supply of phosphorus in the soil and in aquatic systems available for use by biological systems via a process called the phosphorus cycle. Biological systems require phosphorus, and it is often the limiting growth nutrient in aquatic ecosystems. Modern society has recognized the crucial role phosphorus plays in the ecosystem and has used it in a variety of synthetic forms as fertilizers, animal food stuffs, detergents, pesticides and herbicides.

Phosphorus in biological systems originates from phosphate in the soil or water. Biological systems use phosphorus in oxidation states of +5 (phosphates), +3 (phosphonates, phosphites), and +1 (phosphinates). Biophosphates in the +5 oxidation state assume a variety of forms and play many important roles. High energy phosphate ester and anhydride moieties in some biophosphates, like phosphoenol pyruvate (PEP) and adenosine triphosphate (ATP), are important in bioenergetics. Phosphodiester linkages make up the backbone of dideoxyribonucleic acid (DNA) and ribonucleic acid (RNA), molecules which are important in genetic processing. Phospholipids are important constituents of biological

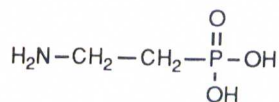
membranes and play important roles in cellular structure. The P-O linkage in biophosphates is kinetically and thermodynamically stable, but can be manipulated by the correct phosphoryl-transfer enzyme catalyst in order to fulfill a given biological function.

Phosphorus also occurs in lower oxidation state in biological systems as phosphonates (+3) and phosphinates (+1). Although the origins of these more reduced biophosphates are less understood, current studies are revealing interesting aspects of their reactivities. Phosphonates and phosphinates contain a P-C bond which give them a different range of reactivity. The P-C bond is thermodynamically less stable than its P-O counterpart.<sup>7</sup> However, the kinetic barrier for P-C bond cleavage is apparently much higher than for P-O bond cleavage. For this reason most phosphonates are inert to hydrolysis by strong base (5 M NaOH, 120°C for 8 h) and strong acid (8M HCl for 48 h).<sup>2</sup> The kinetic stability of the P-C linkage also causes phosphonates and phosphinates to be inert to transfer reactions catalyzed by typical phosphoryl-transfer enzymes. Thus, a class of enzymes different than those which act on phosphates is required to manipulate the P-C bond.

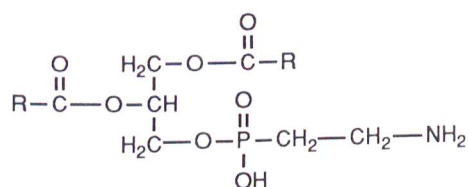
Phosphonates occur in plants, coelentrates, molluscs, echinoderms, arthropods, porifera, and mammals. Since phosphorus is found in its +5 oxidation state in the environment these reduced forms of phosphorus in the biota must be produced biologically. Phosphonates are believed to be produced only by lower organisms. The existence of phosphonates in higher organisms is believed to be the result of dietary intake of exogenous phosphonates. In lower organisms phosphonates can make up a significant amount of the total phosphorus. Phosphonates make up 50% of

the proteinaceous extract of the sea anemone *M. dianthus*,<sup>8</sup> nearly all of the phosphorus in *Helisoma* sp. snail eggs,<sup>9</sup> and 13% of the total phosphorus in the protozoa, *Tetrahymena pyriformis* W.<sup>10</sup> The large amount of phosphonates suggests they play important physiological roles in these organisms.

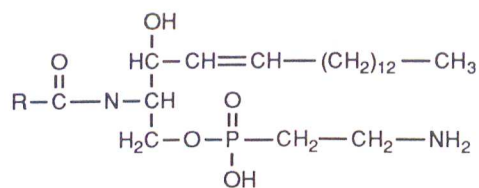
In living organisms phosphonates are found in a variety of forms. In a broad sense, phosphonates can be classified functionally as either structural units, phosphonolipids, or as secondary metabolites, antibiotics. The most abundant and ubiquitous phosphonate is 2-aminoethylphosphonic acid (AEP). AEP is found both in lipids and in the free form.<sup>11</sup> Some examples of phosphonolipids are glycerophosphonolipids and sphingophosphonolipids which occur in nervous tissue of animals<sup>12</sup>, in sea anemone<sup>13</sup>, in rumen protozoa<sup>14</sup>, and in parasitic organisms *Bdellovibrio bacleriovorus*<sup>15</sup> and *Pythium prolatum*.<sup>16</sup> A number of *Streptomyces* species produce phosphonate secondary metabolites. Fosfomycin and forms of 3-N-acyaminopropylphosphonates are produced by strains of *Streptomyces*.<sup>17</sup> Fosfazinomycins A and B, produced by *Streptomyces lavendofoliae*,<sup>18</sup> are potent antifungal agents. Bialaphos is produced by *Streptomyces hygrosopicus*<sup>19</sup> and is unique in that it contains a phosphinate moiety in the form of a novel C-P-C linkage



**AEP**



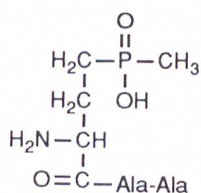
**Diacylglyceryl-AEP**



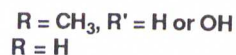
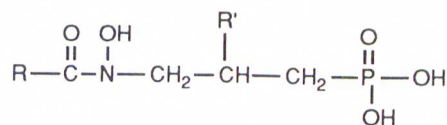
**Ceramide-AEP**

Although the physiological roles of phosphonates are not well understood, some researchers have postulated functions for phosphonates in living systems. The function of phosphonates must be related to the different reactivity of the P-C bond, relative to the P-O bond. AEP is believed to function as a slow-release form of phosphate in maturing eggs of the *Helisinoa* sp. snail eggs.<sup>9</sup> AEP has apparently no active physiological function other than to serve as a precursor to structurally more complex phosphonates. AEP is the phosphonate containing constituent in phosphonolipids. The P-C bond is kinetically more stable than a P-O bond and is resistant to acid and base hydrolysis. Therefore, unlike P-O bond-containing phospholipids, P-C bond-containing phosphonolipids are rather inert to enzymatic hydrolysis, oxidation, and other metabolic processes.<sup>11</sup> Thus, organisms which contain phosphonolipids in their cell membranes may have an advantage over organisms which do not. In light of this, phosphonolipids are thought to bestow parasitic capability on their parent organism, allowing them to survive inside other organisms.<sup>15,16</sup>

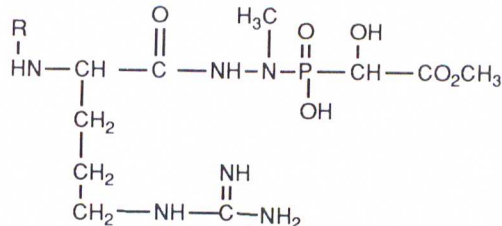
Some organisms produce phosphonates as secondary metabolites which have potent antibiotic activity. Fosfomicin and 3-N-acylamino propylphosphonate derivatives are antibiotics because they inhibit bacterial cell wall biosynthesis.<sup>20</sup> Bialaphos is an effective herbicide. It is not known whether these secondary metabolites are produced intentionally as active antibiotics or are produced for another purpose and have serendipitous antibiotic activity.



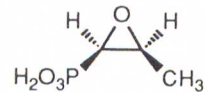
**Bialaphos**



**3-(N-acyl-N-hydroxyamino) propylphosphonates**



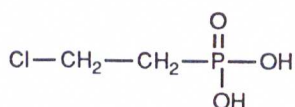
**Fosfazinomycin**



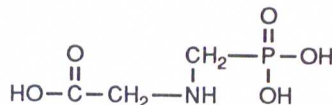
**Fosfomicin**

Many synthetic phosphonates also have potent biological activity. Some phosphonates are essentially phosphorus containing xenobiotics which influence phosphorus metabolism because they are unreactive structural and electronic mimics of physiologically important phosphates.<sup>1</sup> Phosphonates have been used as insecticides (trichloronate), herbicides (glyphosate, fosamin), and plant growth regulators (ethephon). Alkyl- or aryl diesters of phosphonic acids are potent inhibitors of biological

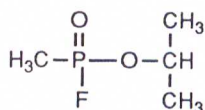
esterases. Trichloronate inhibits acetylcholine esterase and is an effective insecticide. Sarin, Soman, Tabun, and VX are phosphonate containing esters which are used as nerve gases due to their ability to inhibit human acetylcholine esterase.



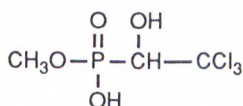
**Ethephon**



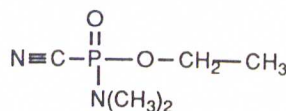
**Glyphosate**



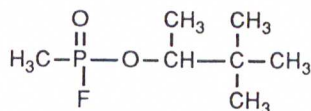
**Sarin**



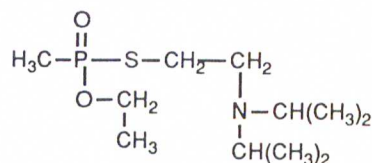
**Trichlorofon**



**Tabun**



**Soman**



**Agent VX**

Synthetic phosphonates are starting to replace phosphates in industrial applications. Phosphonates are now being used in many applications such as adhesives, antioxidants, detergents, flame retardants, and lubricants. For practical reasons phosphonates are considered more attractive than their phosphate counterparts because of their greater hydrolytic stability, lower molecular weight, and lower boiling points.

Man's increasing use of phosphonates instead of phosphates may result in the build-up of phosphonate pollutants if nature does not have a mechanism to catabolize the C-P moiety. The natural occurrence of phosphonates, however, indicates that nature has methods for manipulating C-P bonds. Indeed, researchers have found some organisms which can cleave a P-C bond and some organisms which can form a P-C bond. Studies of both P-C bond cleavage and formation have important practical applications. Studies into P-C biosynthesis have at least one important practical goal, that is the design of a selective agent against phosphonolipid containing parasites. Studies of bacterial C-P bond cleavage may lead to a biological means of controlling potential phosphonate pollutants.

## **II. Biological Pathways of P-C Bond Cleavage**

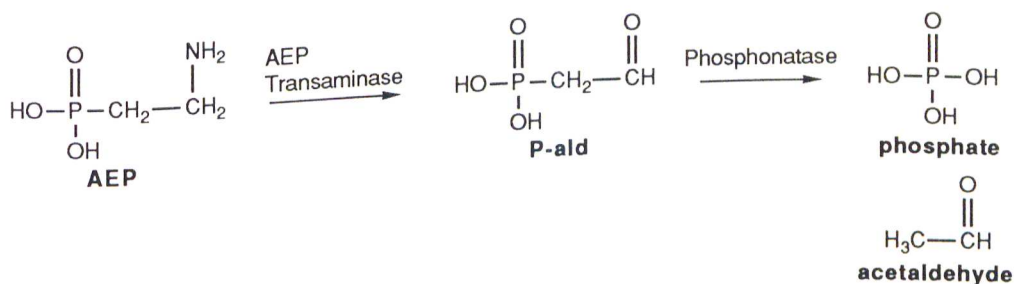
Phosphonates have the potential to be persistent pollutants since the P-C bond is highly resistant to the ecological forces of chemical hydrolysis, photolysis, and oxidation. Fortunately, there are two known biological pathways to P-C bond cleavage in nature. Certain bacteria are able to cleave the P-C bond by either an AEP-specific degradation pathway involving the enzyme phosphonoacetaldehyde hydrolase (hereafter referred to as phosphonatase), or by a substrate-nonspecific system involving the enzyme C-P lyase. Both of these P-C bond cleaving systems are induced in bacteria under phosphate starvation conditions, and the P-C bond cleaving phenotype is not expressed when phosphates are available.<sup>21-23</sup> Since such phosphate starvation conditions are not

typically found in nature, these bacterial systems have limited direct utility as environmental clean-up agents. Hence, there has been an intense research effort to better understand their mode of action in the hope that either purified enzyme catalyst or engineered bacteria can be used to degrade otherwise environmentally persistent phosphonate pollutants.

### A. AEP Biodegradative Pathway

The AEP degrading system was first discovered in *B. cerius* by La Nauze.<sup>24</sup> As illustrated in Scheme 1 the pathway consists of two enzymatic reactions. AEP is first converted to phosphonoacetaldehyde by AEP transaminase. Phosphonoacetaldehyde then serves as the substrate for phosphonatase. AEP transaminase, the first enzyme of the pathway, was purified and characterized by Demora<sup>25</sup> in 1984, and requires pyruvate as an amine acceptor and pyridoxal phosphate as a cofactor. The second enzyme, phosphonatase<sup>26,27</sup>, requires a divalent metal for structural, not catalytic purposes, and converts phosphonoacetaldehyde to phosphate and acetaldehyde.

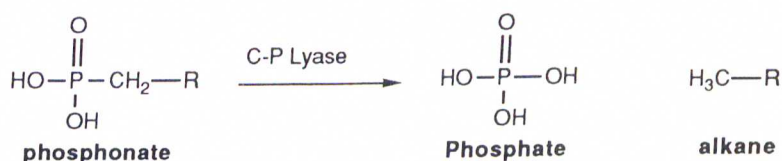
**Scheme 1.** The Biodegradative Pathway of AEP in *B. Cerius*



## B. The C-P Lyase Pathway

C-P lyase is a substrate-nonspecific enzyme system found in several bacteria including *K. pneumoniae*, *A. radiobacter*, *Agrobacterum*, *E. coli*, and *K. ascorbata*. C-P lyase can cleave P-C bonds in which the phosphonate carbon substituent is not functionalized.<sup>28-35</sup> The C-P lyase system converts phosphonates to phosphate and the corresponding alkane (Scheme 2). C-P lyase is far less understood than the AEP degradation system in which the mechanisms of the isolated enzymes are understood in some detail.

**Scheme 2.** The Reaction Catalyzed in the C-P Lyase Pathway



## C. Enzymology of P-C Bond Cleavage

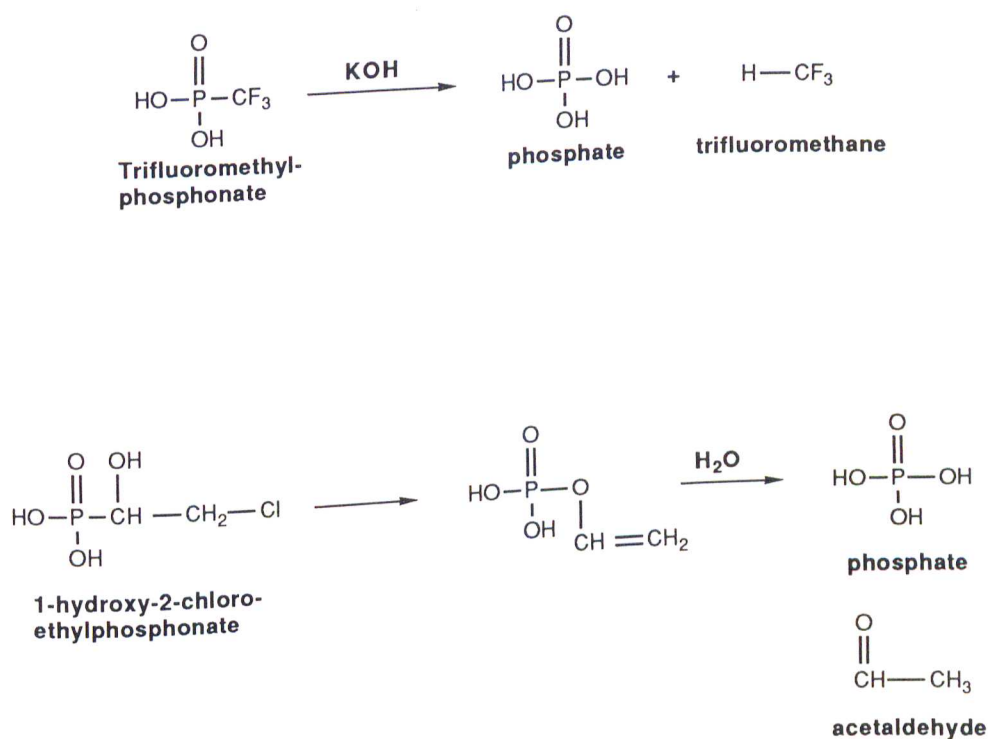
In order to understand the possible mechanisms of P-C bond cleavage by phosphonatase or C-P lyase several chemical models for the cleavage of functionalized and nonfunctionalized phosphonates will be discussed.

### 1. Chemical Models for P-C Bond Cleavage

Phosphonates functionalized on the alpha or beta carbon typically undergo heterolytic P-C bond cleavage. Heterolytic cleavage of the P-C bond produces a carbanion leaving group which must be stabilized by

electron withdrawing substituents. For example, trifluoromethyl phosphonate readily hydrolyzes under alkaline conditions.<sup>36</sup> Phosphonates functionalized on the alpha carbon with a hydroxyl group can undergo P-C bond cleavage under alkaline conditions by migration of the phosphorus atom from carbon to oxygen followed by P-O bond cleavage.<sup>37</sup> These reactions are illustrated in Scheme 3.

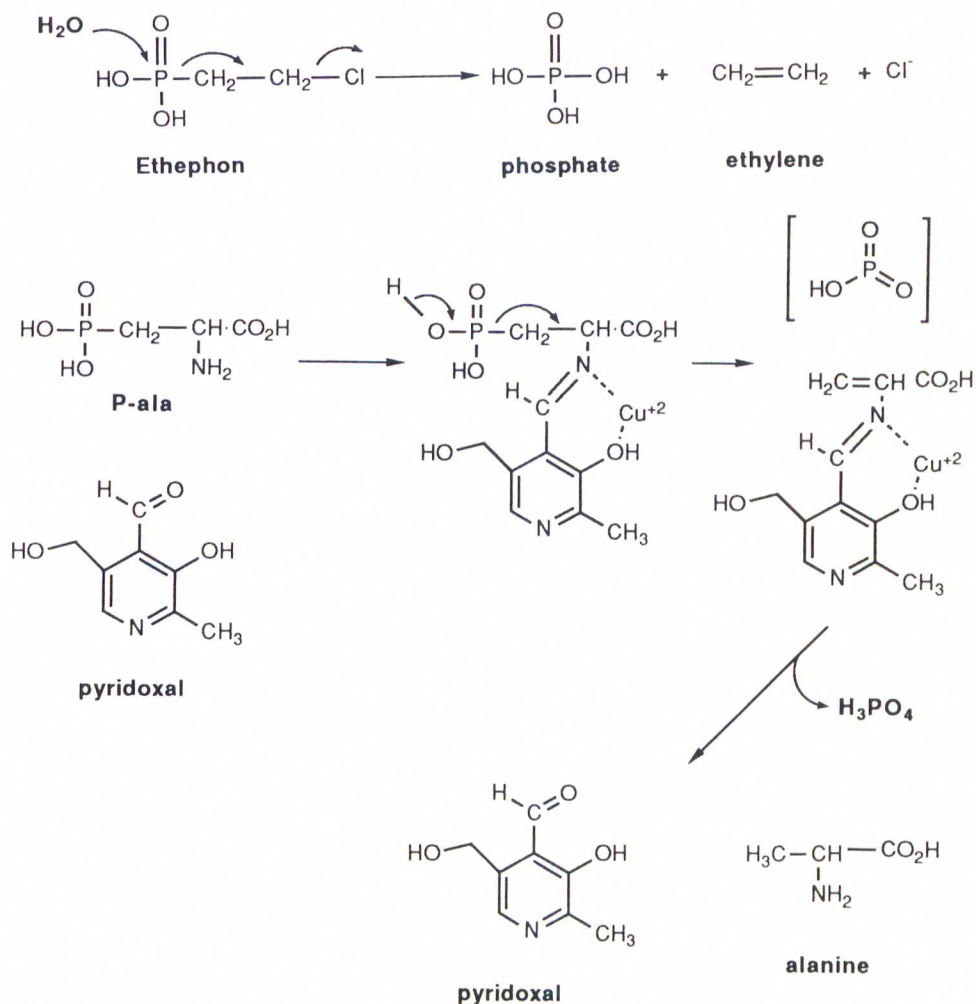
**Scheme 3.** P-C Bond Cleavage of  $\alpha$ -Functionalized Phosphonates



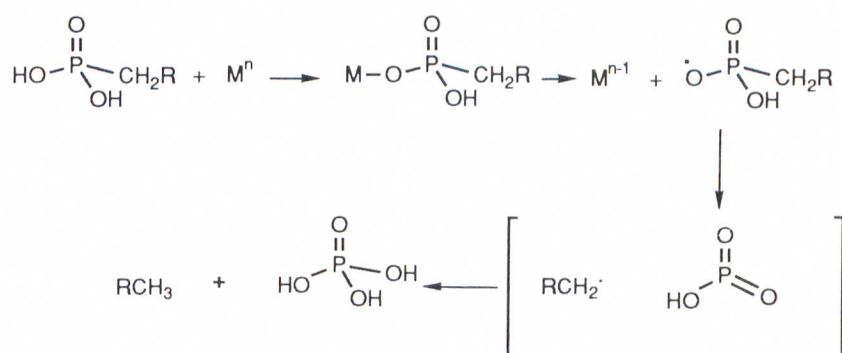
Functionalization at the beta carbon facilitates P-C bond cleavage via a  $\beta$ -elimination process, Scheme 4. The plant growth regulator Ethephon, having a chlorine on the beta carbon, rapidly decomposes in the presence of hydroxide ion to form phosphate, chloride and ethylene.<sup>38</sup>

The hydrolysis of  $\beta$ -keto phosphonates has also been studied. The P-C hydrolysis of  $\beta$ -keto phosphonates is catalyzed by chelation of a divalent metal cation with the ketone. P-C bond hydrolysis is also catalyzed by Schiff base formation at the beta carbon.<sup>24</sup> Martel and coworkers<sup>39</sup> have demonstrated that the pyridoxal Schiff base of 2-amino-3-phosphonopropionic acid (P-ala) undergoes C-P bond cleavage in the presence of  $\text{Cu}^{+2}$  under mild conditions (95°C, pH 7.5).

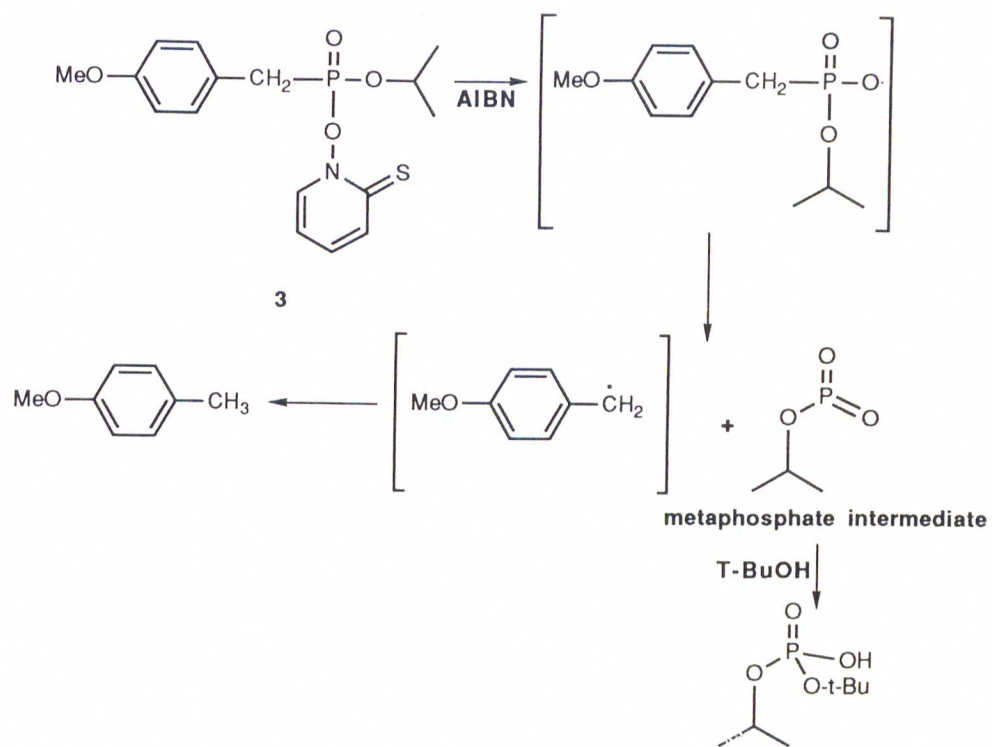
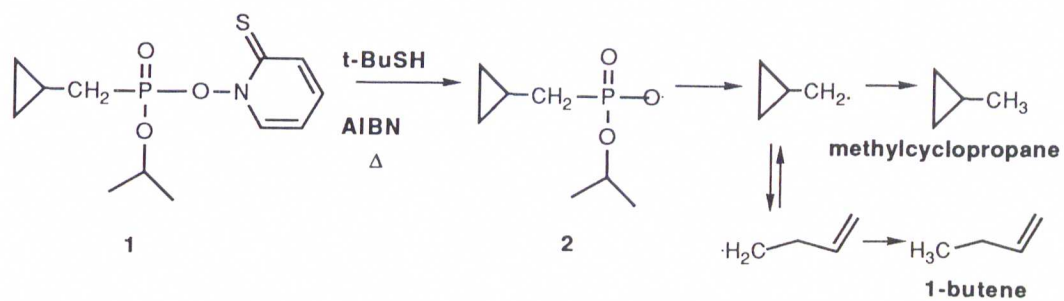
**Scheme 4.** C-P bond Cleavage in  $\beta$ -Functionalized Phosphonates.



Phosphonates which are not functionalized at the alpha or beta carbon can be cleaved via a homolytic P-C bond cleavage, thus avoiding the high energy carbanion intermediate produced by a heterolytic cleavage. A model proposed for this reaction is the lead(IV) tetraacetate transformation of phosphonates to phosphate and the corresponding alkane. Frost and coworkers<sup>40</sup> postulated the mechanism involved formation of an oxyl radical followed by P-C bond cleavage producing a carbon-centered radical and monomeric metaphosphate. The existence of the carbon-centered radical intermediate was evidenced by reacting the cyclopropylmethylphosphonate (1) with *tert*-butylthiol and AIBN (azobisisobutyronitrile) which produced methylcyclopropane and 1-butene.<sup>41</sup> The 1-butene could only be produced from the putative cyclopropylmethyl radical intermediate. Monomeric metaphosphate was trapped as *t*-butylphosphate when 4-methylbenzylphosphate was reacted with tributyltin hydride followed by the addition of *tert*-butanol. These results are summarized in Scheme 5.



**Scheme 5.** Radical-Based Mechanism of C-P Bond Cleavage in Non-functionalized Phosphonates.



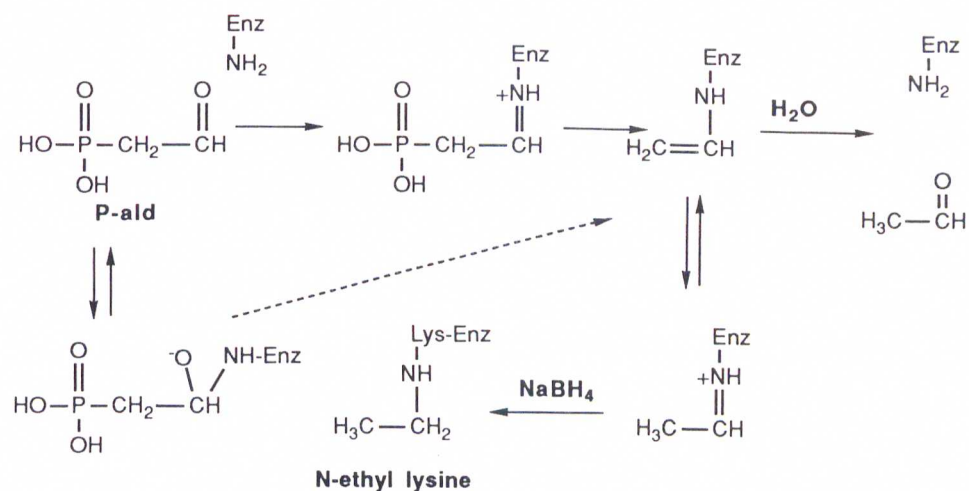
## 2. The Mechanism of Phosphonatase

Dephosphonylation beta to a carbonyl can be considered analogous to a  $\beta$ -keto decarboxylation process (Scheme 6), where the C-C bond is activated for cleavage and the departing enolate is stabilized either by divalent metal cation chelation or by Schiff base formation.<sup>42</sup> La Nauze reported that the required magnesium cofactor did not chelate to P-Ald and therefore probably does not play a direct role in catalysis.<sup>26</sup> The magnesium is postulated to be necessary for maintaining the active dimeric enzyme structure. P-Ald was found to form a Schiff base with the enzyme during catalysis. La Nauze<sup>26</sup> was able to trap the P-Ald/enzyme or acetaldehyde/enzyme Schiff base by reducing it with  $\text{KBH}_4$ , thus irreversibly inactivating the phosphonatase. These results are consistent with the general mechanism for phosphonatase shown in Scheme 7.

**Scheme 6.** Two Modes of Decarboxylation.



**Scheme 7.** Catalytic Mechanism of Phosphonatase.

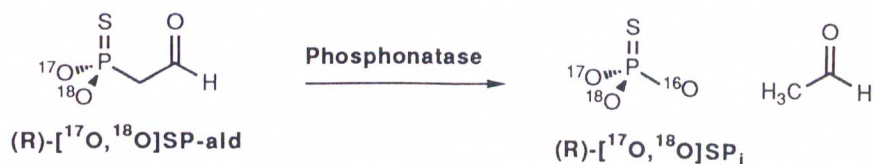


Olsen et al. showed the inactivation event occurred at the active site by demonstrating that inactivation could be blocked by the substrate analog, acetylphosphonate.<sup>43</sup> Furthermore, the active site residue responsible for Schiff base formation was identified as a lysine residue and the active site tryptic peptide was sequenced (Scheme 7).

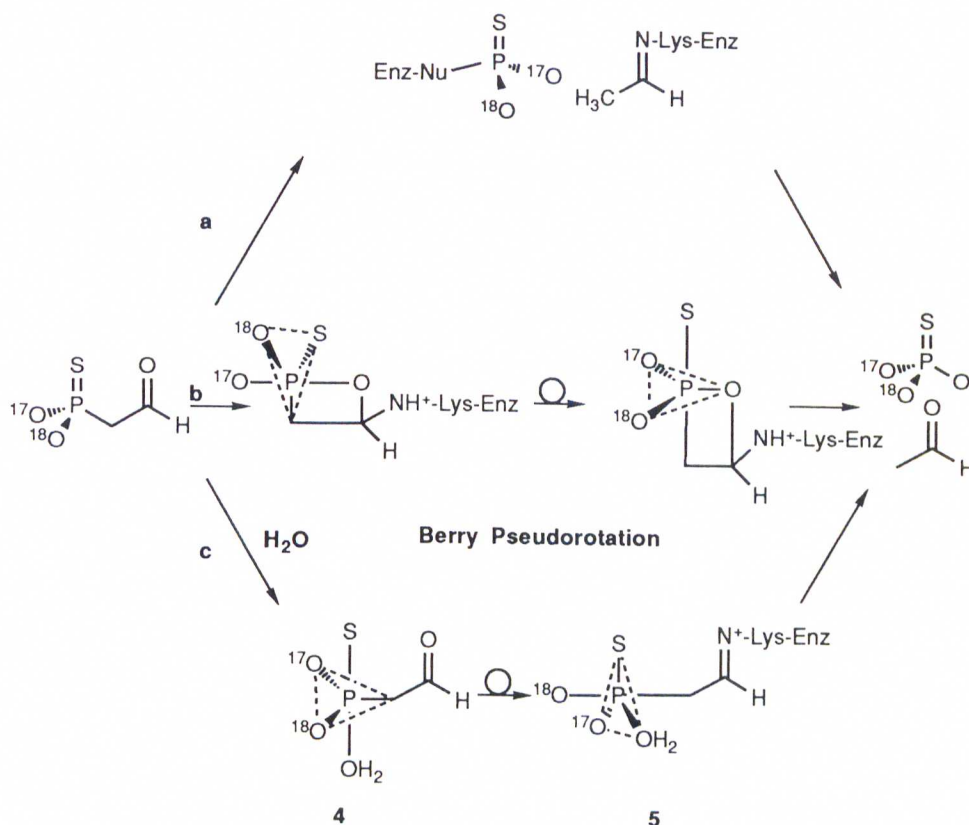
To further detail the C-P cleavage event the stereochemical course of the reaction was determined. The hydrolysis of the C-P bond of [<sup>17</sup>O,<sup>18</sup>O]thiophosphonoacetaldehyde (SP-Ald) in H<sub>2</sub><sup>16</sup>O resulted in the phosphorus stereochemistry being retained in the thiophosphate product (Scheme 8).<sup>44</sup> Two mechanistic possibilities consistent with these results are shown in Scheme 9; two in-line displacements of the thiophosphoryl group (pathway **a**) or adjacent nucleophilic attack followed by pseudorotation (pathways **b** and **c**). To date there is no evidence to

support the existence of a second active site nucleophile which is required for the double displacement mechanism.

**Scheme 8.** The Stereochemical Course of Phosphonoacetaldehyde Hydrolase



**Scheme 9.** Mechanisms Consistent with Retention of Configuration

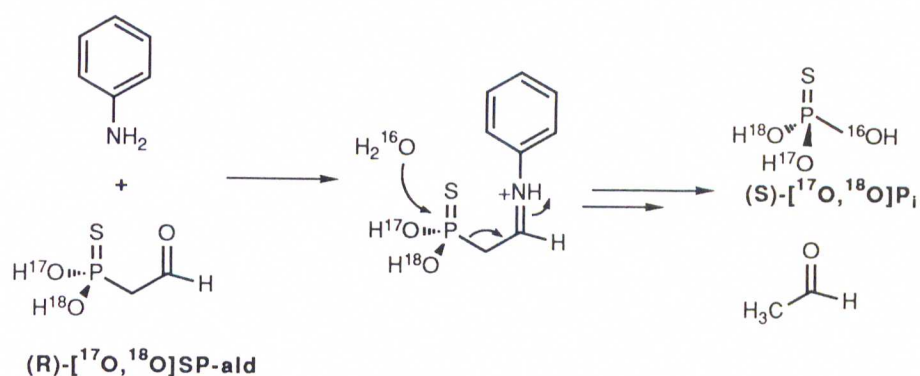


The adjacent attack mechanisms involving either the carbonyl oxygen or a water molecule also seem unlikely. P-Ald with  $^{18}\text{O}$  label in the carbonyl was dephosphonylated with phosphonatease and the phosphate produced did not contain the  $^{18}\text{O}$  of the carbonyl. The adjacent attack by water (pathway **c**) followed by pseudorotation was explored by determining the solution hydrolysis of chiral [ $^{18}\text{O}$ ]TP-Ald.

It was reasoned that if the factors necessitating putative adjacent attack in the enzyme were due only to the Schiff base formation, then Schiff base formation in the solution hydrolysis should produce the same retained stereochemical result. The factors which govern adjacent versus in-line attack are outlined by Westheimer's rules.<sup>45</sup> Westheimer's rules for nucleophilic displacement at phosphorus predicts that the nucleophile must approach in the apical direction opposite the most electronegative group, and the departing ligand must leave from an apical position of the pentavalent trigonal bipyramid intermediate. Since the apical positions are preferentially occupied by the most electronegative groups, the nucleophile must approach opposite the most electronegative group. Using these paradigms, one predicts that the hydrolysis of a P-C bond would occur with water attacking opposite oxygen (or sulfur) and adjacent to carbon to form a pentavalent intermediate. This trigonal bipyramid intermediate (**4**) then must undergo one pseudorotation event to place the carbon leaving group in an apical position for departure (**5**). Following the sequence of steps of pathway **c** in Scheme 9, one can easily see that this adjacent attack/pseudorotation mechanism retains the original phosphorus stereochemistry in the product.

If this adjacent attack mechanism is the cause of the retention of phosphorus stereochemistry observed in the phosphonatase reaction, then the same stereochemical result should be observed in the Schiff base mediated reaction in solution. So, to better interpret the retained phosphorus stereochemistry observed for phosphonatase, Lee et. al.<sup>44</sup> determined the stereochemical course of the solution hydrolysis of chiral SP-Ald. The chiral thiophosphate produced from the aniline catalyzed hydrolysis of chiral SP-Ald was found to have inverted phosphorus stereochemistry (Scheme 10). A single in-line displacement mechanism would invert the stereochemistry.

**Scheme 10.** Aniline-Catalyzed Solution Hydrolysis of P-ald



Therefore, these results are consistent with an in-line attack of water opposite the the Schiff base carbon leaving group. If the solution hydrolysis of a  $\beta$ -iminophosphonate involves an in-line attack, there is no reason to invoke an adjacent attack/pseudorotation mechanism for the phosphonate-catalyzed hydrolysis. Experiments designed to gain evidence for the double-displacement mechanism involving a second enzyme nucleophile are now in progress.

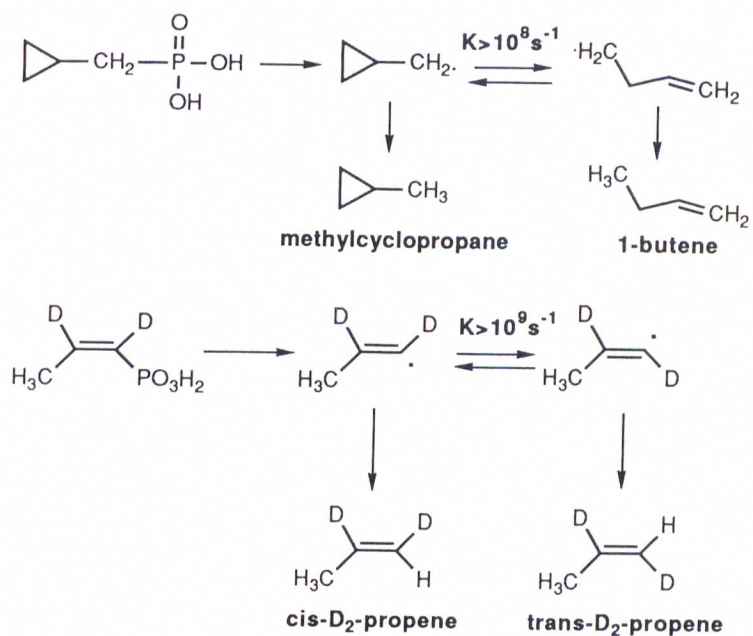
### 3. Mechanism of C-P Lyase

The mechanism of C-P lyase is not well understood. The nonfunctionalized carbon would preclude the operation of a phosphonate-like reaction, since the heterolytic C-P cleavage would result in a very high energy carbanion. Therefore, researchers have postulated a homolytic bond cleavage mechanism consistent with the chemical model studies.

The C-P lyase activity has yet to be demonstrated *in vitro*, therefore all mechanistic details of C-P lyase are based upon *in vivo* studies. Walsh and coworkers have demonstrated that a radical intermediate may be involved in the C-P lyase reaction.<sup>22</sup> Walsh used two radical probes, cyclopropyl methylphosphonate (**6**) and cis-1,2-dideuteropropenylphosphonate (**7**). If homolytic P-C bond cleavage occurs cyclopropyl methylphosphonate should produce a cyclopropylmethyl radical, which rearranges to 1-butene at a rate of  $10^8$  s<sup>-1</sup>. If homolytic bond cleavage of cis-1,2-dideuteropropenylphosphonate occurs, the resulting cis-1,2-dideuteropropyl radical which rearranges to the trans-1,2-dideuteropropyl radical at a rate of  $10^9$  s<sup>-1</sup> would produce

trans-1,2-dideuteropropene. C-P lyase produced 0.3-2% 1-butene from cyclopropyl methylphosphonate and 1.5% trans-1,2-dideuteropropene from cis-1,2-dideuteropropenylphosphonate. These results are summarized in Scheme 11. The small amount of rearranged product indicate either a very short-lived radical intermediate, or radical cleavage is not the major reaction pathway.

**Scheme 11.** Probes for a Radical Mechanism in C-P Lyase



Walsh and coworkers attempted to characterize the C-P lyase gene in the hope that C-P lyase activity could be reconstituted *in vitro*. The C-P lyase operon has 17 open reading frames encoding 17 proteins.<sup>46</sup> Thus the C-P lyase activity is the result of a complex multi-protein system, which remains undefined.

The application of knowledge gained by the research of biological C-P bond cleavage may eventually lead to an efficient means of biodegradation of phosphonates. Thus far the study of C-P bond cleavage has produced intriguing insight into the enzymology of P-C bond manipulation. The cryptic nature of C-P lyase and the still not fully understood detailed mechanism of phosphonate will provide scientists much work in the future.

## **II. P-C Bond Formation in Nature**

The other side of the phosphonate question addresses how naturally occurring phosphonates are formed. How can the knowledge of biological P-C bond formation be utilized in a constructive manner? As mentioned earlier, there are numerous naturally occurring phosphonates, some of which have potent biological activity. Most natural phosphonates are found bound in lipids. Phosphonolipid constituents give a membrane stability against lipases and chemical hydrolysis. Therefore, organisms with phosphonolipid constituents in the cell wall have the ability to exist in somewhat harsh environments. The parasitic capability of some rumen protzoa,<sup>47</sup> *B. bacteriovorus*,<sup>15</sup> and pythea fungus<sup>16</sup> is attributed to their ability to make phosphonolipids. Evidence linking phosphonolipids to

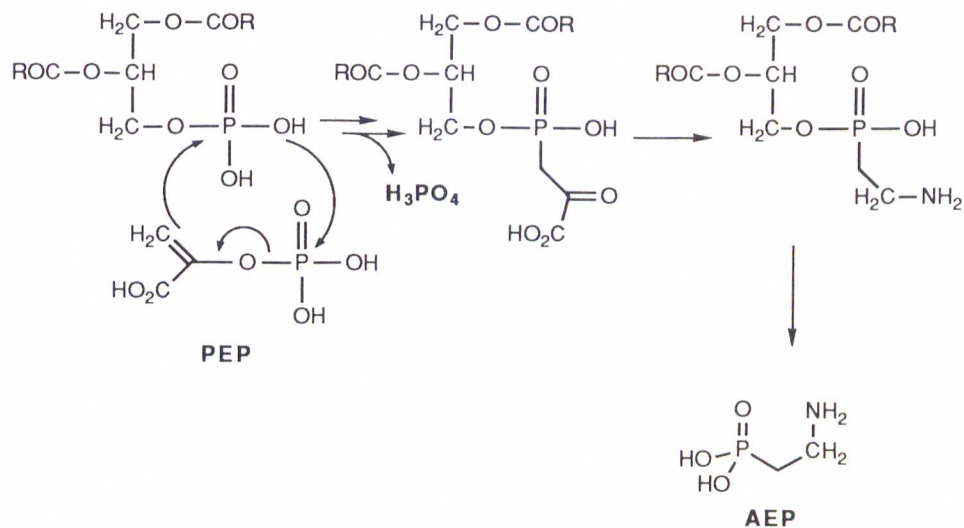
parasitic capability can be found in the case of *B. batrivorius*.<sup>15</sup> This microbe can be either saprophytic or parasitic, having the unique ability to live inside other bacteria. Interestingly, only strains which make phosphonates are parasitic. The phosphonolipid-containing protozoa, *Tetrahymena pyriformis*, are facultatively parasitic and infect a variety of aquatic invertebrates. Another organism in which phosphonate appear to bestow parasitic capability is the fungus *Pythium pratum*. Ceramide AEP is found in both major genera of *Pythiaceae* fungus, the only fungus known to have phosphonolipids. The *Pythiaceae* are plant pathogens of enormous importance to nearly every economic agricultural crop.

Therefore, understanding the mode of phosphonolipid synthesis, especially the mode of P-C bond formation, could lead to the design of specific antiparasite reagents, such as a *Pythiaceae* fungicide. Over the past 25 years several groups have been investigating the mode of P-C bond biosynthesis. The following sections will describe work which has been done in elucidating the biosynthesis of AEP, fosfomycin, and bialaphos.

### **A. AEP Biosynthetic Pathway**

Phosphonates were first discovered in biological systems in 1959 by Horiguchi and Kandatsu<sup>8</sup>. These same workers later identified AEP as the major phosphonic acid unit, existing both in the free form **7** and bound in a lipid form **4**. Free AEP was first proposed to be derived from lipid-bound AEP because [<sup>32</sup>P] phosphate ([<sup>32</sup>P] Pi) was incorporated more rapidly into lipid-bound AEP than free AEP. Lipid-bound AEP would be formed by a mechanism outlined in Scheme 12.

**Scheme 12.** Proposed Synthesis of AEP from Phospholipids



However, subsequent experiments discounted this hypothesis. First, a pulse-chase experiment in which log phase cells were incubated first with [ $^{32}\text{P}$ ]  $\text{P}_i$  for one hour followed by a chase with inorganic phosphate revealed no loss of radioactivity from lipid-bound AEP. Therefore, lipid-bound AEP was not labile and not the precursor to free AEP. Second, a two hour incubation of log phase cells with [ $^{32}\text{P}$ ]  $\text{P}_i$  resulted in [ $^{32}\text{P}$ ] lipid AEP having greater radioactivity than [ $^{32}\text{P}$ ] phosphate lipid<sup>11</sup>. Thus, the phosphoryl group in AEP was not derived from a phospholipid. Finally, Horguchi and coworkers demonstrated the conversion of [ $^{32}\text{P}$ ]  $\text{P}_i$  to AEP in a cell-free homogenate of *Tetrahymena* and showed that AEP was 'free' and not lipid-bound<sup>48</sup>. An explanation for the original observation of [ $^{32}\text{P}$ ]

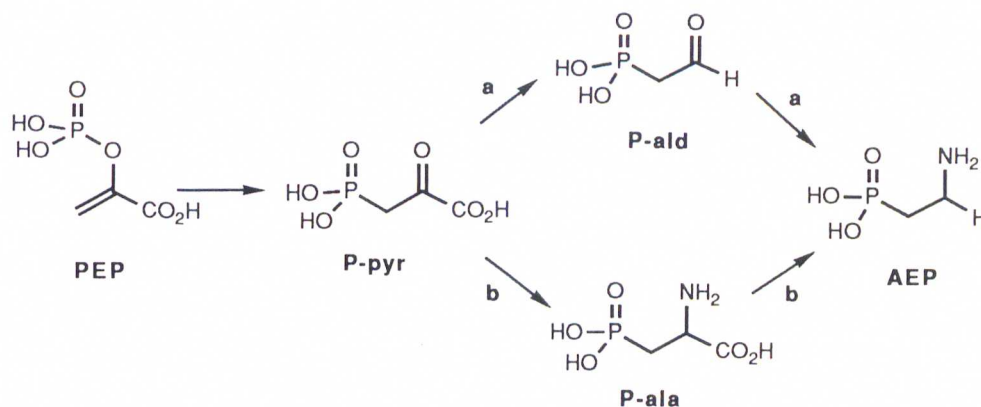
P<sub>i</sub> being incorporated into lipid-AEP faster than into free AEP may be that there is a pool of free AEP and newly synthesized AEP is channeled more directly into lipid synthesis.

Mounting evidence indicated the C-P bond was not derived by the mechanism in Scheme 13, so alternative mechanisms were proposed which incorporated the finding that phosphoenol pyruvate was a direct precursor to AEP. *In vivo* studies carried out by Trebst and Geike implicated PEP was a direct precursor to AEP<sup>49</sup>. Utilizing <sup>14</sup>C glucose the authors showed that C-1 and C-2 of AEP were derived from C-1 and C-2 of glucose, respectively. Laing and Rosenberg showed that *T. pyriformis* converted [<sup>14</sup>C-1 or <sup>14</sup>C-2] glucose into [<sup>14</sup>C-1] AEP<sup>50</sup>. In addition to these results, Warren showed that [<sup>14</sup>C-3 or <sup>14</sup>C-4] glucose lead to no incorporation of <sup>14</sup>C into AEP.

Warren also demonstrated the conversion of [<sup>32</sup>P] PEP to [<sup>32</sup>P] AEP with a 0.0007% yield in a system of a cell-free homogenate of *Tetrahymena pyriformis* W.<sup>51</sup> Accompanying [<sup>32</sup>P] AEP was the formation of [<sup>32</sup>P] phosphonoalanine (P-ala) **5**. P-ala could be subsequently converted to AEP in a 0.04% yield, implicating it as a possible intermediate between PEP and AEP. (Scheme 13, pathway **b**).

An alternative mechanism for AEP formation, employing PEP as a precursor, was proposed by Horiguchi and coworkers<sup>52</sup>. They proposed, contrary to Warren's mechanism, that P-pyr was first decarboxylated to phosphonoacetaldehyde (P-ald) **6** and subsequently transaminated to form AEP (Scheme 13, pathway **a**).

**Scheme 13.** Proposed Pathways for the Biosynthesis of AEP in *T. pyriformis*.



Evidence supporting pathway **a**, decarboxylation followed by transamination, was provided by Horiguchi and coworkers.<sup>52</sup> A radiolabel dilution study examined the ability of unlabeled P-ala or P-ald to dilute the incorporation of [<sup>32</sup>P] from PEP into AEP. Under optimal conditions Horiguchi could incorporate 0.34% of [<sup>32</sup>P] from 150 nmol [<sup>32</sup>P] PEP into AEP. However, if three equivalents of unlabeled P-ald (750 nmol) were added, incorporation of radiolabel diminished to 0.021%. Conversely, three equivalents of unlabeled P-ala decreased incorporation only to 0.29%. Therefore, the authors concluded on the basis of those results that P-ald was the direct precursor to AEP and P-ala decarboxylation was, at most, only a minor pathway to AEP.

The intermediates in the pathway, P-pyr and P-ald, were never directly observed but Horiguchi did claim to trap them as hydrazone derivatives. [<sup>32</sup>P] PEP (0.017 mmol) was incubated with cell-free extracts

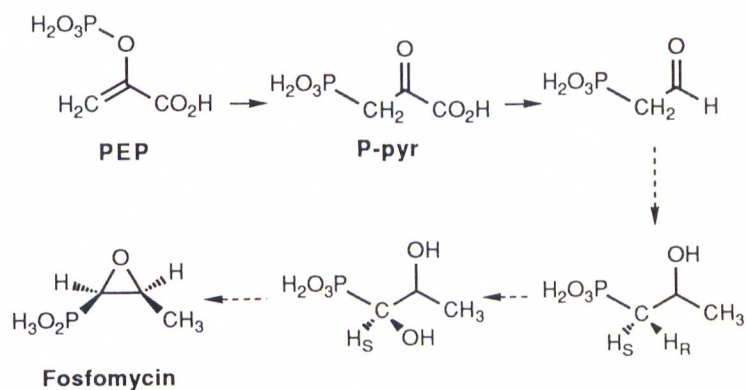
of *T. pyriformis* which were subsequently treated with 2,4-dinitrophenylhydrazine and subjected to hydrogenolysis. The hydrazone derivative of P-pyr and P-ald should yield P-Ala and AEP, respectively, upon catalytic hydrogenation. Chromatography of the reaction mixture resulted in radiolabeled material coincident with authentic P-ala and AEP.<sup>53</sup> However, these derivatives were not further characterized. In a more recent report Takada and Horiguchi claimed to have trapped P-pyr as a hydrazone derivative using non-radiolabeled PEP. Phosphoenolpyruvate was incubated with 24 gm of a cell-free homogenate of *T. pyriformis* which was subsequently treated with 2,4-dinitrophenylhydrazine. Chromatography of the reaction mixture yielded two compounds which were coincident with authentic P-pyr and P-pyr-2,4-dinitrophenylhydrazone. Catalytic hydrogenolysis produced a ninhydrin-positive substance which was indistinguishable from P-Ala on cellulose TLC analysis.<sup>54</sup>

The mechanism of the presumed PEP to P-pyr conversion was probed by Horiguchi and Rosenberg.<sup>53</sup> By using doubly-labelled PEP they set out to test whether or not P-pyr formation occurred via an intra- or intermolecular reaction of PEP. They observed that doubly-labelled [<sup>32</sup>P], [<sup>14</sup>C-3] PEP (consisting of 991 nmol of phosphoenol-[<sup>14</sup>C-3]pyruvate and 48 nmol [<sup>32</sup>P] PEP) was converted to AEP (0.013%) and P-ala (0.0022%) having the same <sup>14</sup>C/<sup>32</sup>P ratio of the starting material. These results were consistent with an intramolecular rearrangement.

## B. Phosphonate Antibiotic Biosynthetic Pathways

The biosynthetic pathways of two phosphonate antibiotics have been the focus of intense research. Fosfomycin is an antibiotic produced by various strains of *Streptomyces* at the end of their log phase growth. Fosfomycin works by inhibiting bacterial cell wall biosynthesis by alkylating a thiol group in the active site of phosphoenolpyruvate: UDP-Glc-NAC-enolpyruvyl transferase.<sup>55</sup> Current knowledge of the biosynthetic pathway of fosfomycin is presented in Scheme 14. The C-P bond in fosfomycin is believed to be derived from the same pathway responsible for AEP synthesis. Glucose labelled in the 1- or 6- position with <sup>13</sup>C produced [<sup>13</sup>C-1]fosfomycin and [<sup>13</sup>C- 2]glucose produced [<sup>13</sup>C-2]fosfomycin.<sup>56</sup> The C-3 methyl group of fosfomycin was derived from S-adenosyl-L-methionine.<sup>57</sup> These results indicate the P-C<sub>2</sub> unit most likely comes from a rearrangement of PEP to phosphonopyruvate followed by decarboxylation to P-Ald.

**Scheme 14.** Biosynthesis of Fosfomycin.



The steps elaborating P-Ald to fosfomycin, specifically methylation and oxirane formation, are still not well understood. The methylation of the C-2 of P-Ald with a 'CH<sub>3</sub><sup>+</sup>' donor, S-adenosyl methionine, is precluded due to the electrophilic nature of the C-2 of P-Ald. Unless the carbonyl polarity is reversed or a different functionality exists at C-2, it is hard to imagine the involvement of an electrophilic methyl donor. To date no information has been published on the P-C<sub>2</sub> methylation event.

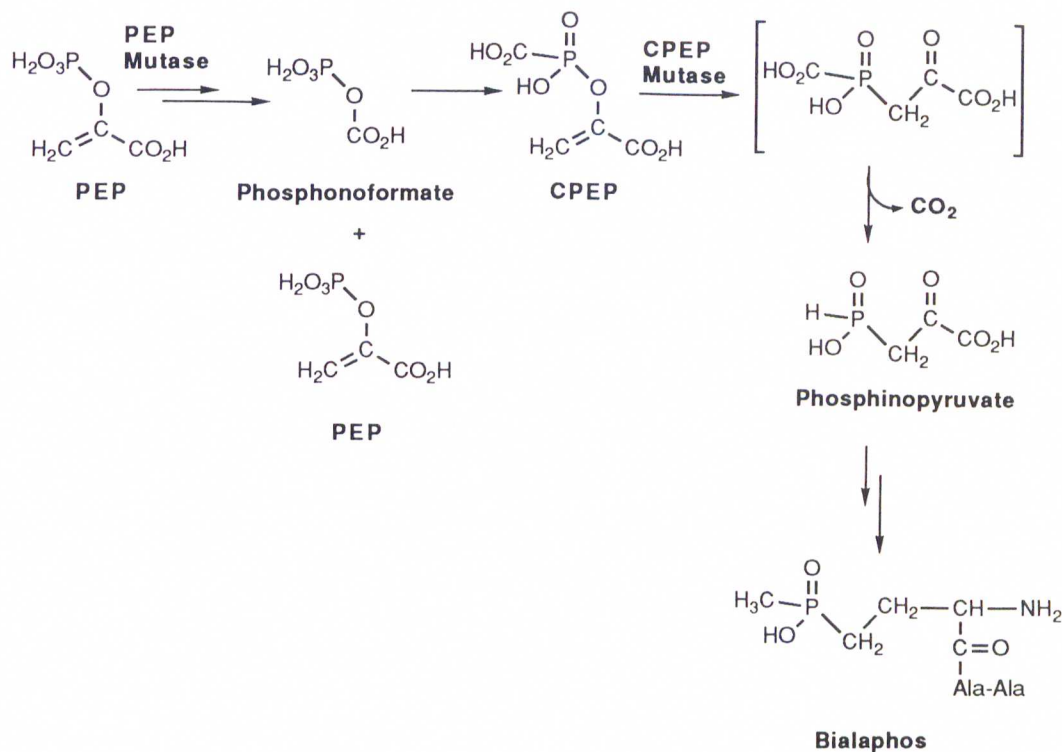
The oxirane ring could derive from oxidation of cis-1-propenyl phosphonate (**8**) (Scheme 15), since several species of *Penicillium* can carry out this reaction to form fosfomycin.<sup>58</sup> However, this is not the approach used in the actual biosynthesis. If the oxirane oxygen is derived from an oxidation step then the bacteria would incorporate label from <sup>18</sup>O<sub>2</sub> into the oxirane ring of fosfomycin. *Streptomyces* do not produce <sup>18</sup>O-labeled fosfomycin in the presence of <sup>18</sup>O<sub>2</sub> and therefore, the oxirane oxygen of fosfomycin is most likely derived from water.<sup>59</sup> Hammerschmidt and coworkers<sup>60</sup> discovered that 2-hydroxypropylphosphonate (HPP) is a precursor to fosfomycin. To probe the mode of functionalization of C-1 during the oxirane formation, these workers incubated (R)-1-deutero(HPP) and (S)-1-deutero(HEP) with growing cell cultures of *S. fradiae*. The bacteria replaced the pro-R hydrogen on C-1 with a C-O bond. This result is consistent with hydroxylation of C-1 with retention of configuration, followed by displacement of the C-1 hydroxyl group by the C-2 hydroxyl group with inversion of configuration.

**Scheme 15.** Epoxidation of cis-1-Propenyl-1-Phosphonate



The biosynthesis of Bialaphos has also been studied. This biosynthetic pathway is comparatively more complicated since bialaphos contains a phosphorus with two carbons attached to it (a phosphinate). The multistep synthesis can be broken down into two basic processes. First is the synthesis of phosphinothricine, the phosphinate portion, which is an L-glutamic acid analog. Second, two alanine residues are added to the carboxyl group of phosphinothricine. Bialaphos contains a unique C-P-C moiety. The first P-C bond comes from the PEP mutase rearrangement of PEP to P-pyr.<sup>61</sup> The second P-C bond is formed by the enzyme carboxyphosphoenolpyruvate (CPEP) mutase.<sup>62-63</sup> The biosynthetic pathway to bialaphos is shown in Scheme 16. The pathway was determined by analyzing the intermediates which accumulated in the growth media of mutants which were blocked at different steps in the pathway.<sup>64</sup> The sequence of the steps was determined by the conversion of intermediates to bialaphos by mutants which were blocked at earlier steps in the pathway. The enzymes responsible for the formation of the two C-P bonds will be discussed later.

### Scheme 16. The Biosynthetic Pathway of Bialphos



### C. Enzymology of P-C Bond formation

Typical laboratory syntheses of P-C bonds employ a nucleophilic phosphorus in a reduced oxidation state (+3 or +1) and an electrophilic carbon. Alternatively, and much less commonly, the electronic demands may be reversed, employing an electrophilic phosphorus (+5) and a nucleophilic carbon. Since biological systems overwhelmingly utilize phosphorus in its (electrophilic) +5 oxidation state, one anticipates the later carbon nucleophile mechanism to be employed in biological P-C synthesis. However, some bacteria are able to oxidize phosphite

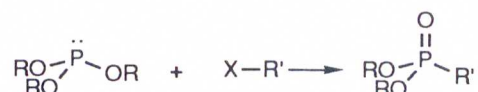
(nucleophilic, +3 phosphorus) to phosphate.<sup>65-67</sup> It is therefore conceivable that the reverse of this process could be a source of nucleophilic phosphorus species in bacteria. Therefore, the typical mode of P-C synthesis involving a +3 phosphorus nucleophile may be possible in biological systems. Since both approaches to P-C bond formation are possible in biological systems, both modes of laboratory syntheses of P-C bond will be described.

### **1. Chemical Models for P-C Bond formation via Nucleophilic Phosphorus**

Examples of P-C bond formation reactions employing a nucleophilic phosphorus are illustrated in Scheme 17 and exemplified by the classical Michaelis-Arbuzov reaction employing a trialkylphosphite and an alkyl halide. A variation of the reaction is the Perkow reaction which is the reaction of a trialkyl phosphite and an  $\alpha$ -halocarbonyl compound. The course of this reaction can produce either a vinylphosphate and/or a  $\beta$ -ketophosphonate.<sup>68</sup> Interestingly, these are the two species involved in the putative rearrangement of PEP to P-pyr. The product distribution of the Perkow reaction is dependent upon the type of halogen, the temperature and the polarity of the reaction solvent. In general, the vinyl phosphate product formation is enhanced by lower temperature and increased electronegativity of the halogen. The mechanism is not entirely understood. The  $\beta$ -ketophosphonate product is believed to arise from direct displacement of the halogen. The intermediate salt produced does not rearrange to the vinyl phosphate. Thus, the vinyl phosphate product is

believed to arise from nucleophilic attack at the carbonyl carbon, followed by phosphoryl migration to the oxygen and loss of an alkylhalide.

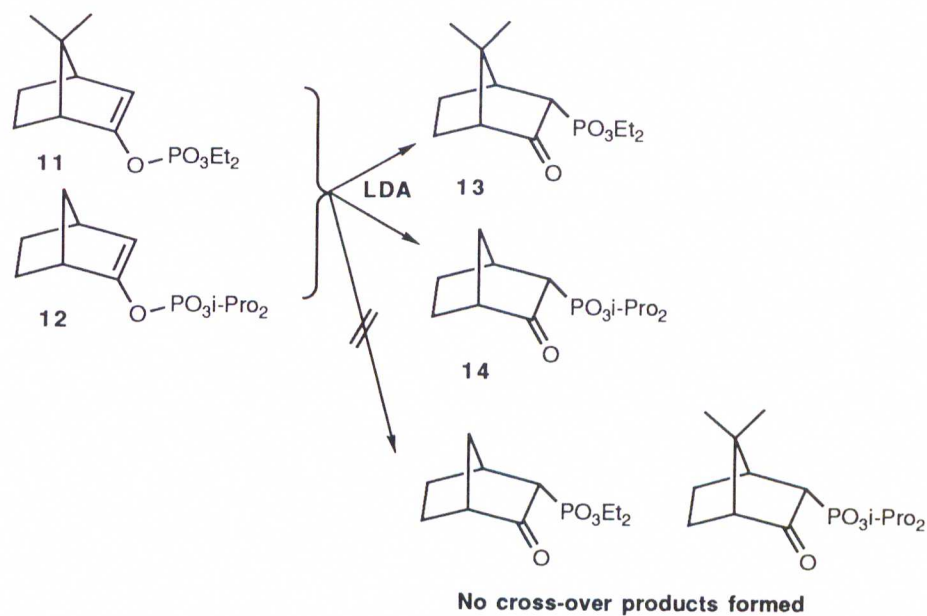
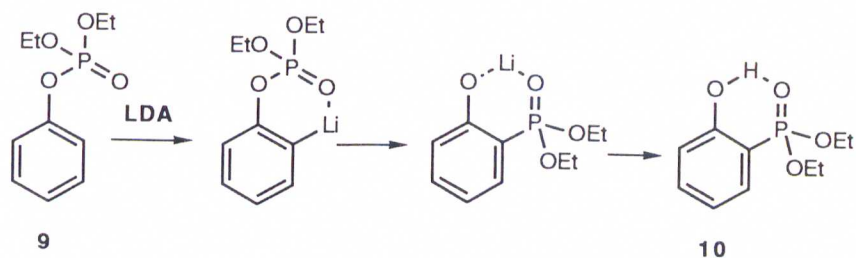
**Scheme 17.** C-P Bond Formation via a Nucleophilic Phosphorus



## 2. Chemical Models of P-C Bond Formation via Electrophilic Phosphorus

Routes to P-C bond syntheses via a nucleophilic carbon and an electrophilic phosphorus are known. These syntheses are base catalyzed intramolecular rearrangements of vinyl phosphates to  $\beta$ -ketophosphonates. In 1981 Melvin<sup>69</sup> reported phenylphosphate (**9**) rearranged to *o*-hydroxyphenylphosphonate (**10**) in the presence of *n*-butyl lithium or lithium diisopropylamide (LDA). Weimer and coworkers<sup>70,71</sup> reported similar rearrangements of numerous cyclic vinyl phosphates to  $\beta$ -ketophosphonates illustrated in Scheme 18. The rearrangement of a mixture of (**11**) and (**12**) produced only (**13**) and (**14**) and therefore the rearrangement was an intramolecular process. The rearrangement was initiated by the abstraction of an allylic or (in the absence of an allylic) a vinyl proton by strong base.

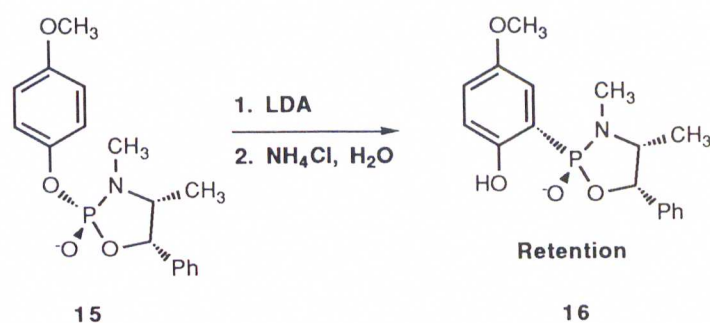
**Scheme 18.** P-C Bond Formation via a Nucleophilic Carbon.



The stereochemical course of the base catalyzed rearrangement of an arylphosphate ester to an *o*-hydroxy phosphonate recently has been reported. Welch and coworkers<sup>72</sup> reacted pseudoephedrine or ephedrine (aryloxy) phospholidine derivatives with lithium diisopropylamide in tetrahydrofuran and discovered they undergo P-O (**15**) to P-C (**16**) rearrangement with retention of configuration. Although the investigators

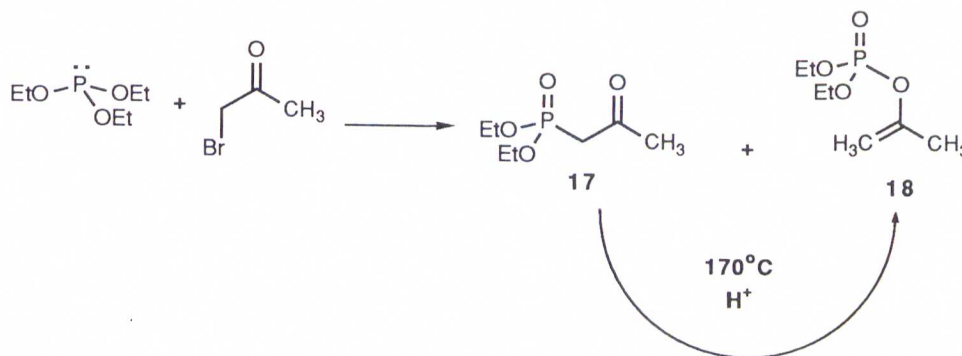
did not speculate on the mechanistic implications, these results are consistent with a mechanism which proceeds through a four membered ring, pentavalent intermediate that must pseudorotate to form product.

**Scheme 19.** Stereochemical Analysis of P-C Bond Formation via Nucleophilic Phosphorus



The rearrangement of a vinyl phosphate to a beta keto phosphonate by acid catalysis has also been reported. Machleidt et. al.<sup>73</sup> reported that the thermal rearrangement of O,O-diethyl phosphonoacetone (**17**) to the O,O-diethyl enolphosphate (**18**) occurred to a larger extent in the presence of acid. The addition of 2-butanone had no influence on the products formed and therefore, the reaction appeared to be an intramolecular process (Scheme 20).

**Scheme 20.** Acid Catalyzed Rearrangement of a Vinylphosphate to a  $\beta$ -Keto Phosphonate



Understanding the way in which nature creates a P-C bond is important for both scientific and practical reasons. From a scientific point of view the P-C bond formation in nature is challenging to our present understanding of enzyme catalysis. The rearrangement could employ either a nucleophilic carbon or a nucleophilic phosphorus, however either possibility is somewhat problematic. The general view that PEP directly rearranges to P-pyr requires a nucleophilic carbon acid, analogous to the carbanions produced in the LDA catalyzed rearrangements of cyclic vinylphosphates to  $\beta$ -oxophosphonates. Formation of such a carbon anion in PEP seems out of reach for an enzyme. The reported acid catalyzed thermal rearrangement may be a better model. Alternatively, the phosphorus in PEP could act as the nucleophile if it were first reduced to the phosphite. However, there is no evidence for such a reductive step. Therefore, the enzyme catalyzed rearrangement of PEP to P-pyr is of great chemical interest.

From a practical viewpoint the P-C bond formation in nature may serve as an attractive target for the design of anti-parasite compounds. It is believed that some parasitic organisms rely on phosphonolipids to be able to live inside other organisms. Since only a select few organisms can synthesize a P-C bond, the P-C bond synthetic machinery is a good target for the design of inhibitors to control these parasitic organisms. By understanding the P-C bond formation involved in AEP (and phosphonolipid) biosynthesis, scientists may be able to rationally design a molecule to inhibit it, thus killing the parasite.

The understanding of P-C bond formation in nature and the possible development of a phosphonate-dependent antiparasitic reagent were lofty goals in 1986. Before 1986 all of the studies of AEP biosynthesis were characterized by low yields of AEP, and no phosphonate precursors to AEP were ever directly observed, thus making characterization of the pathway very difficult. Additionally, attempts by scientists to isolate the P-C bond forming enzyme from *T. pyriformis* or *S. hygroscopicus* for mechanistic studies had not been successful. Our goal was to establish the mode of AEP biosynthesis in *T. pyriformis* and discover the origin of the P-C bond. This dissertation describes the progress made in understanding the detailed pathway of AEP biosynthesis. Additionally, this dissertation describes the discovery, purification, and initial characterization of the mechanism of the enzyme responsible for P-C bond formation, phosphoenolpyruvate mutase.

## RESEARCH PROPOSAL

Our strategy was to first firmly establish the pathway of AEP formation in *Tetrahymena pyriformis* W. by demonstrating the intermediacy of P-pyr and P-ald as a result of their ability to be converted to AEP in cell-free homogenate. This would be facilitated if we could increase the AEP forming activity in the cell-free homogenate. If P-pyr and P-ald prove to be intermediates, a direct method for assaying PEP mutase activity would then be developed for its isolation. Purified enzyme would then be used to characterize the mechanism of the phosphoryl transfer. First the rearrangement would be characterized as either intermolecular or intramolecular. If the reaction is an intramolecular rearrangement then the determination a stepwise or concerted process will be ascertained by analyzing the stereochemical consequence of the rearrangement.

### I. Verification of the $PEP \leftrightarrow P\text{-pyr}$ Mode of P-C Bond Formation

Since the conversion of  $PEP \leftrightarrow P\text{-pyr}$  is common to both pathways in Scheme 13, we wanted to demonstrate the precursor role of P-pyr, thereby strengthening the putative  $PEP \leftrightarrow P\text{-pyr}$  mode of P-C bond formation. To distinguish between the two pathways in Scheme 14 we would examine the intermediates and the differing cofactor requirements for each pathway. Pathway **b** requires P-ala as an intermediate, and pyridoxal phosphate (PLP) could serve as a cofactor for both the transamination and decarboxylation. However, pathway **a** requires P-ald

as an intermediate and would require an  $\alpha$ -keto decarboxylase cofactor, thiamine pyrophosphate (TPP), as well as PLP for transamination. Therefore, the two pathways can be distinguished by testing the cofactor-dependent conversion of P-pyr, P-ald, and P-ala to AEP.

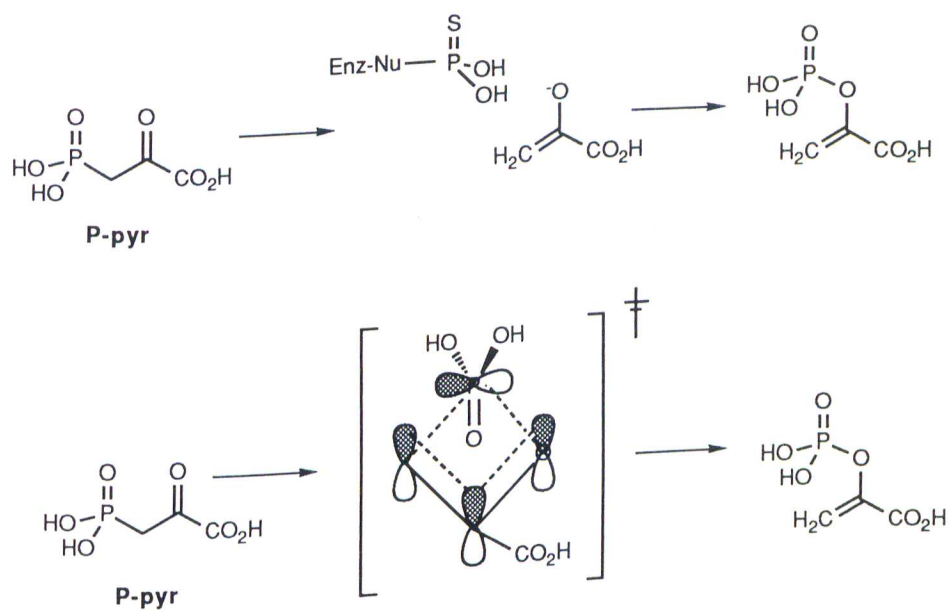
## II. Examination of the Catalytic Mechanism of the PEP $\leftrightarrow$ P-pyr Rearrangement.

If the rearrangement catalyzed by PEP mutase is analogous to other phosphomutases it could proceed either by an intramolecular or intermolecular rearrangement. This will be determined by reacting PEP mutase with an equimolar mixture of isotopically double-labeled substrate and unlabeled substrate. The absence of a single labeled crossover product would be evidence for an intramolecular rearrangement.

Assuming the mechanism is an intramolecular process, it could be considered as occurring via a stepwise or concerted mechanism (Scheme 21). The most likely stepwise mechanism involves an enzyme nucleophile displacing the phosphoryl group, forming an enolate and a phosphorylated enzyme intermediate. The enolate could then be phosphorylated on C-3 forming P-pyr. We reasoned the operating mechanism could, in part, be elucidated by knowing the stereochemical consequence of the reaction at phosphorus. The stepwise mechanism should result in retention of configuration at phosphorus.<sup>74</sup> The concerted mechanism should result in overall inversion of configuration at phosphorus. Orbital topology dictates that  $[2\pi + 2\sigma]$  migrations in the ground state have a Mobius transition state and the absolute configuration of the migrating center undergoes

inversion.<sup>75</sup> If the rearrangement is a stepwise process, the intermediate might be trapped by rapid quench techniques.

**Scheme 21.** Possible Intramolecular Mechanisms for the PEP ⇌ P-pyr Rearrangement



## RESULTS AND DISCUSSION

The results and discussion section consists of the two major phases of my research on PEP mutase. The first section describes (I) The verification of the  $\text{PEP} \leftrightarrow \text{P-pyr}$  mode of P-C bond formation in *T. pyriformis* AEP biosynthetic pathway. This section is further divided into the determination of the (A)  $\text{PEP} \Rightarrow \text{AEP}$ , (B)  $\text{P-pyr} \Rightarrow \text{AEP}$ , (C)  $\text{P-ald} \Rightarrow \text{AEP}$  conversions (D) the discovery of PEP mutase and, (E) the purification and characterization of PEP mutase. The second section describes (II) Studies of the catalytic mechanism of PEP mutase. This section is divided into three parts (A) Is the  $\text{PEP} \Rightarrow \text{P-pyr}$  rearrangement an intramolecular process?, (B) The stereochemical course of the PEP mutase reaction, and (C) The search for the intermediate in the  $\text{PEP} \leftrightarrow \text{P-pyr}$  rearrangement.

### I. Verification of the $\text{PEP} \leftrightarrow \text{P-pyr}$ Mode of P-C Bond Formation

The goal of these studies was to locate and purify the enzyme responsible for the putative  $\text{PEP} \leftrightarrow \text{P-pyr}$  rearrangement. Initial pathway studies were directed at gaining convincing evidence for the  $\text{PEP} \Rightarrow \text{AEP}$  conversion, and examining whether the pathway involved the intermediacy of P-ald or P-ala. Results from these studies lead to the purification and characterization of the enzyme responsible for the  $\text{PEP} \leftrightarrow \text{P-pyr}$  rearrangement, PEP phosphomutase (hereafter called 'PEP mutase' [EC 5.4.2.9] as recommended by the International Union of Biochemists).<sup>76</sup>

**A. Evidence for the PEP⇒AEP Conversion in *T. pyriformis***

A cell-free homogenate of *T. pyriformis* was obtained from a 6 L culture which was grown to a cell density of OD<sub>530</sub>=0.9. Centrifugation of the culture media yielded about 20 mL of cell paste which was homogenized in 80 mL of buffer. Reactions containing 20 mL of cellular homogenate of *Tetrahymena pyriformis* W. and an equal volume of a basal solution containing 10 mM MgCl<sub>2</sub>, 20 mM L-alanine, 2.5 mM PLP and 20 mM PEP (0.6 mmol) were incubated on a gyratory shaker (110 rpm) for 18 h at 27°C. A control reaction consisting of 20 mL of cell-free homogenate and 20 mL of basal solution not containing PEP was run in parallel to quantitate endogenous AEP.

The workup procedure is the same as described by Barry.<sup>77</sup> Reactions were quenched with 20% (w/v) trichloroacetic acid (TCA). The protein precipitate was removed by centrifugation (2500g for 10 min). The TCA was removed by extraction with ether, and the aqueous portion was concentrated to 2 mL, and the solution was acidified. The reaction products were separated by ion exchange chromatography. Phosphoenolpyruvate (as well as P-pyr, P-ald, and P-ala) was found in the water eluate of the Dowex-50 (H<sup>+</sup>) column, whereas AEP was eluted from the Dowex-50 (H<sup>+</sup>) by 3 M NH<sub>4</sub>OH. After concentration, the NH<sub>4</sub>OH fraction was loaded on a Dowex-1 (acetate) column and the AEP removed by elution with 5% acetic acid. The eluates were concentrated *in vacuo*, and redissolved in a 50% D<sub>2</sub>O buffer containing 50 mM K<sup>+</sup>HEPES at pH 8 for <sup>31</sup>P NMR analysis.

We assayed the products of the pathway enzymes by <sup>31</sup>P NMR. The <sup>31</sup>P NMR chemical shifts of phosphonate (10 to 25 ppm) are well separated

from those of phosphates (5 to -25 ppm). The relative amounts of reaction product were quantitated by comparing their integrals with the integral of a known internal standard.

### **1. Cell-free Homogenate Conversion of PEP to AEP**

We expected the conversion of PEP to AEP would be low since PEP is an intermediate in glycolysis, which will be converted by enolase to 2-phosphoglyceric acid, and hence to 3-phosphoglycerate by 3-phosphoglucomutase, or be hydrolyzed by phosphatases to inorganic phosphate. Both of these side reaction products should be found in the Dowex-50 (H<sup>+</sup>) water fraction. The reaction of PEP with the cell free homogenate, as described above, produced a product mixture consisting of AEP (0.4%), phosphate (40%), and 2-phosphoglyceric acid and 3-phosphoglyceric acid (55%). The small but significant conversion of PEP to AEP was encouraging. The large amounts of glyceric acids indicated glycolytic processes were more effective than those of the AEP pathway.

### **2. TPP-Enhanced Conversion of PEP to AEP**

We attempted to increase the activity of the AEP pathway by adding thiamine pyrophosphate (TPP) to the reaction mixtures. The choice of TPP was based on the following rationale. Pathway **a** was the most likely of the two proposed pathways in Scheme 13 and it requires P-ald to be derived from a decarboxylation of P-pyr. Enzymatically, such a  $\beta$ -keto decarboxylation reaction typically requires a TPP cofactor.<sup>78</sup> Therefore, we expected the conversion of PEP to AEP would be enhanced in the cell free homogenate if TPP were added to the reactions. Two reactions were run

as previously described. A reaction of the same cell-free homogenate with PEP which did not contain TPP converted PEP to AEP in only a 3% yield, but an identical reaction in which 2.5 mM TPP was included, produced AEP in a 27% yield. These results provided indirect evidence that the AEP pathway involved a rearrangement of PEP to P-pyr which underwent a TPP-dependent decarboxylation to P-ald which was converted to AEP. Both pathways in Scheme 13 involve P-pyr as an intermediate. We therefore sought direct evidence for the involvement of P-pyr in the AEP pathway.

#### **B. Cell-free Homogenate Conversion of P-pyr to AEP**

Having demonstrated efficient TPP-dependent conversions of PEP to AEP we felt we could test directly the precursor role of P-pyr. The reaction conditions were the same as those described for the conversion of PEP to AEP except 9.5 mM P-pyr was used in place of PEP. P-pyr and PEP were found in the Dowex-50 water fraction. The cell free homogenate containing PLP, L-alanine, and  $Mg^{2+}$  could convert P-pyr to AEP in a 4% yield. The same reaction mixture when supplied with 2.5 mM TPP produced 8% AEP from P-pyr. The conversion of both PEP and P-pyr to AEP and the fact that both conversions are dependent on TPP provided convincing evidence that the  $PEP \leftrightarrow P\text{-pyr}$  rearrangement was indeed the source of the P-C bond in the AEP biosynthetic pathway. Although these results strongly suggested the operation of pathway **a** in Scheme 13, we wanted direct evidence that P-ald (pathway **a**) and not P-ala (pathway **b**) was the immediate precursor to AEP.

### **C. Cell-free Homogenate Conversion of P-ald to AEP**

The ability of the cell free homogenate to convert P-ald to AEP was examined. The reaction contained a cell-free homogenate of *T. pyriformis* and  $Mg^{2+}$ , PLP, D,L-alanine with 0.60 mmol P-ald. Unreacted P-ald would be found in the Dowex-50 water fraction.  $^{31}P$  NMR analysis revealed that the reaction produced 43% inorganic phosphate, and 27% AEP. These data give strong evidence that P-pyr is decarboxylated to P-ald and P-ald is transaminated to AEP. Thus pathway **a** in Scheme 13 is the major pathway to AEP.

### **D. Discovery of PEP Mutase**

#### **1. Relative Conversions of PEP, P-pyr, and P-ald to AEP**

The relatively low yield of AEP (8%) from P-pyr with respect to PEP (27%) and P-ald (27%) was disconcerting. The unexpected lower yield of AEP from P-pyr may have been due the fact that the PEP, P-ald, and P-pyr reactions were carried out separately, using different batches of cell-free homogenate. We decided to further detail the pathway by determining the relative conversions of PEP, P-pyr and P-ald to AEP using the same cell free homogenate. Four trial were run with different cell batches. We expected the highest conversion from P-ald since it lies closest to AEP in the pathway and requires only one enzymic transformation. The lowest conversion should be observed from PEP since its conversion to AEP requires three enzyme transformations. The results of these four trials are shown in Table 1.<sup>3</sup>

**Table I:**<sup>3</sup> Conversion of proposed intermediates to AEP.

Reactant	AEP Isolated			
	Trial 1	Trial 2	Trial 3	Trial 4
None <sup>a</sup>	4 $\mu$ mol	6 $\mu$ mol	5 $\mu$ mol	0 $\mu$ mol
PEP [200 $\mu$ mol]	12 $\mu$ mol/6%	25 $\mu$ mol/13%	75 $\mu$ mol/37%	36 $\mu$ mol/18%
P-pyr [130-200 $\mu$ mol] <sup>b</sup>	11 $\mu$ mol/8%	10 $\mu$ mol/11%	10 $\mu$ mol/8%	22 $\mu$ mol/16%
P-ald [200 $\mu$ mol]	19 $\mu$ mol/9%	133 $\mu$ mol/66%	166 $\mu$ mol/83%	80 $\mu$ mol/40%

<sup>a</sup>These are control reactions to which the addition of the PEP, P-pyr and P-ald had been omitted.

<sup>b</sup>The trial 1 reaction mixture contained 130 mmol, trial 2 and trial 3 reaction mixtures contained 136 mmol and trial 4 reaction mixture contained 200 mmol.

In every case P-ald gave the highest conversion to AEP. Similar to the original observations, the conversion of PEP was consistently higher than P-pyr. These results indicate that there are other pathways which compete for P-pyr, and that these pathways must be more predominant than the pathways which compete for PEP. These results also seem to indicate that P-pyr formed from PEP does not readily dissociate from the AEP pathway enzymes. Therefore, the decarboxylase may not readily bind free P-pyr, thus making it susceptible to degradation before it can be converted to AEP. The possibility that the pathway enzymes are coupled is consistent with our failure to observe P-pyr and P-ald as products from the reaction of PEP. These low conversions of P-pyr to AEP prompted us to investigate the other pathways responsible for the fate of P-pyr in the cell-free homogenate.

## 2. Determining the *In Vitro* Fate of P-pyr in the Cell-Free Homogenate.

It was necessary to determine the degradation products of P-pyr in the cellular homogenate so that enzymes competing for P-pyr might be removed or inhibited. In order to determine the degradation products of P-pyr in the cellular homogenate short-term reactions were carried out as previously described except the AEP pathway cofactors, TPP and PLP were omitted and the reaction time was 10 min. The crude product mixture was worked up as before, with the exception that the products were not separated by chromatography. Identification and quantitation of phosphorus species were carried out using  $^{31}\text{P}$  NMR techniques. Within 10 minutes P-pyr had been totally degraded into inorganic phosphate (3.2 ppm), and minor amounts of other phosphonates (17 ppm and 15 ppm), possibly P-ala and phosphonoacetic acid, respectively. Also formed was an organophosphate at -0.17 ppm, possibly PEP from the reverse reaction of the phosphomutase. The phosphorus recovered accounted for all the P-pyr added to the reaction within 5% (Figure 1).

The identity of the phosphorus species having a  $^{31}\text{P}$  NMR resonance at -0.17 ppm was determined to be PEP by demonstrating its conversion to ATP with ADP and pyruvate kinase. Phosphonopyruvate (136  $\mu\text{mol}$ ) was incubated with the cell-free homogenate and  $\text{Mg}^{2+}$  in the absence of the pathway cofactors for 20 minutes and the reaction was quenched with trichloroacetic acid. The products were chromatographed and the  $^{31}\text{P}$  NMR analysis of the Dowex-1 ( $\text{H}^+$ ) water fraction indicated P-pyr had been converted to  $\text{P}_i$  (60%) plus pyruvate and to PEP (ca. 47  $\mu\text{mol}$ , 35%). To one half of the NMR sample was added  $\text{MgCl}_2$  (20  $\mu\text{mol}$ ), ADP

(23.5  $\mu\text{mol}$ ), and 54 units of pyruvate kinase (Figure 1a). After 20 minutes the  $^{31}\text{P}$  NMR spectrum was obtained and nearly quantitative formation ATP was observed with concomitant loss of PEP at -0.17 ppm and ADP (Figure 1b). These results<sup>79</sup> show that PEP mutase *in vitro* catalyzes the reverse reaction, forming PEP from P-pyr. The implication of this result was that the PEP mutase activity should be assayed by measuring PEP formation upon the addition of P-pyr. This quickly lead to the purification of PEP mutase.

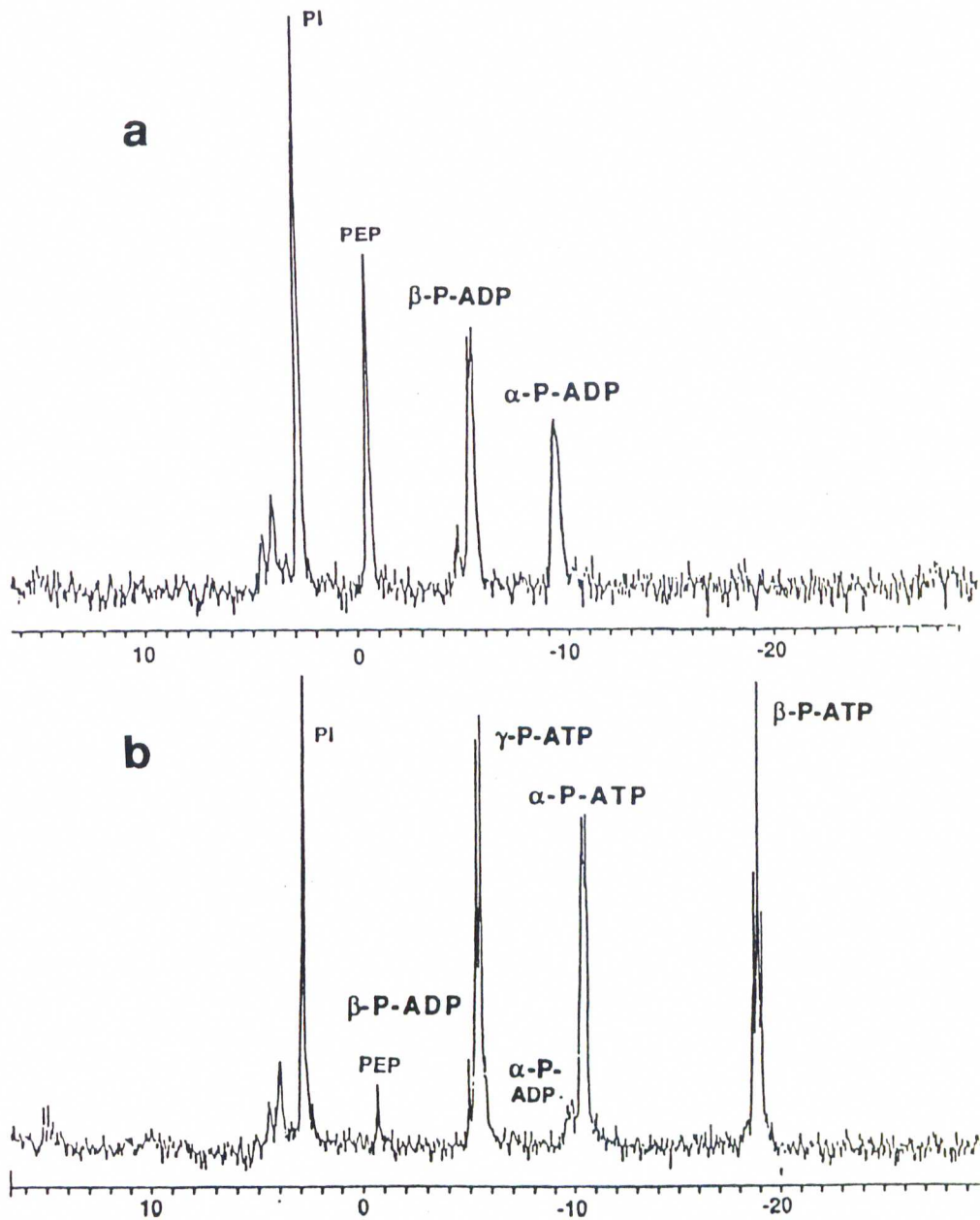


**Figure 1.**  $^{31}\text{P}$  NMR of the products formed from 47  $\mu\text{mol}$  of P-pyr in the cell-free homogenate, and 23.5  $\mu\text{mol}$  of added ADP. b) The same reaction mixture 20 min after the addition of 54 units of pyruvate kinase.

## E. Purification and Characterization of PEP Mutase

Since the equilibrium position of the PEP mutase catalyzed reaction favors PEP formation we used a pyruvate kinase-ADP/ lactate dehydrogenase-NADH coupled enzyme system to assay the enzyme in cellular fractions. This convenient assay greatly facilitated the purification of PEP mutase. Studies of the kinetic and catalytic mechanisms were carried out in the P-pyr $\Rightarrow$ PEP direction.

### 1. Purification of PEP Mutase

The original purification procedure for PEP mutase was developed in our laboratory by Elise Bowman and Dr. Jeffrey Scholten.<sup>4</sup> The procedure was modified slightly since its publication. The modified procedure is presented here. *T. pyriformis* cells were harvested near the end of log phase growth and frozen at -80°C. The 250 g of frozen cells were lysed in the presence of BSA and protease inhibitors by thawing followed by blending for 5 min. The cell-free homogenate was centrifuged at 17000g to remove cellular debris. Nucleic acids were precipitated from the supernatant using streptomycin sulfate and removed by centrifugation at 17000g. PEP mutase was precipitated from the cellular extract in 70% ammonium sulfate. Purification by chromatography took advantage of the enzyme's hydrophobicity. The precipitated enzyme was subjected to a DEAE-cellulose column to remove anionic proteins. PEP mutase was fractionated on a phenyl-Sepharose column to which it bound very tightly. The proteins which coeluted with mutase were removed by gel filtration on

Biogel P-200. The purification process was followed by SDS-PAGE (Figure 2) and is summarized in Table 2. PEP mutase purified in this manner typically had a specific activity of 20-30 Units/mg protein.

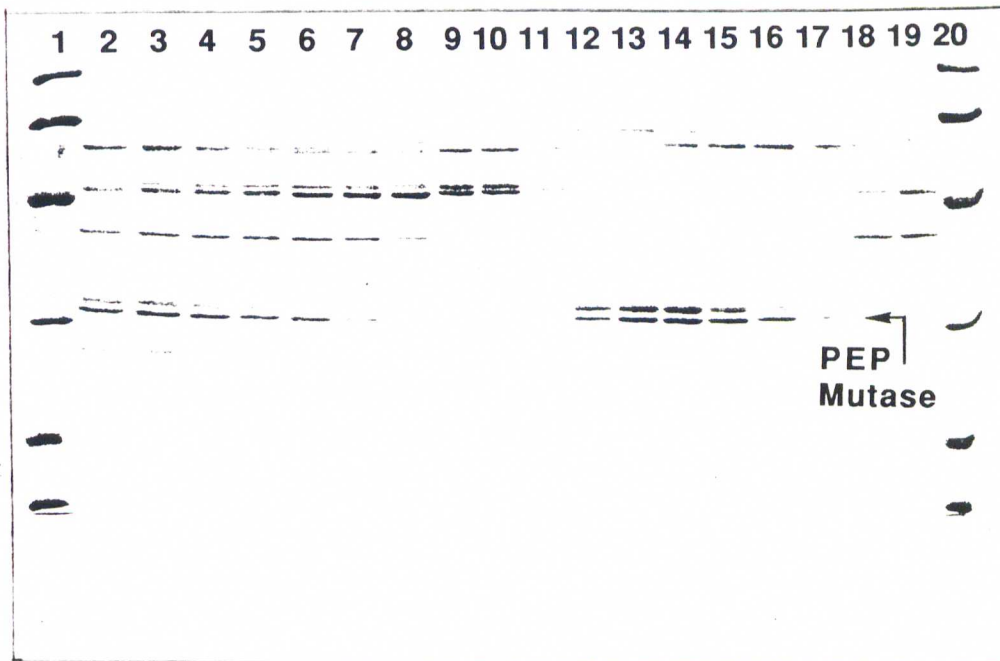


**Figure 2.** SDS-PAGE of the column chromatographic purification of PEP mutase. Lanes 2-8 are tubes 90 to 96 from the phenyl Sepharose column and lanes 9 -19 are tubes 31-41 from the Biogel. column. Columns 1 and 20 display molecular weight markers.

The molecular weight of the denatured PEP mutase obtained from SDS-PAGE is about 38000 daltons. Elise Bowman determined the molecular weight of the native enzyme was 81000 daltons using gel filtration techniques, thus concluding PEP mutase was an  $\alpha_2$  dimer. Seidel et al. reported the PEP mutase isolated from *T. pyriformis* was determined to be an  $\alpha_2$  dimer using SDS-PAGE and nondenaturing gel filtration

techniques.<sup>5</sup> However, in every purification of PEP mutase that I performed, the purified PEP mutase consisted of two closely-migrating protein bands of equal intensity on SDS-PAGE. This may have been due to the action of proteases although we took the extra precautions of having protease inhibitors in the dialysis solution, and subsequently, performed all three column chromatographies within 30 h. Alternatively, the PEP mutase may be an  $\alpha\beta$  dimer, consisting of subunits of similar but not equal size. However, the N-terminal sequence analysis reported by Seidel et al. would suggest otherwise.<sup>5</sup> Thus either my preparations contained a contaminating protein or one subunit was unstable to partial proteolysis.

The kinetic mechanism, metal ion cofactor specificity, and pH dependence of purified PEP mutase were determined by Jeff Scholten.<sup>4</sup> The kinetic mechanism is a rapid equilibrium ordered reaction, with P-pyr binding both following and tightening metal cofactor binding. PEP mutase was found to be activated by several metals. The activations relative to magnesium were  $Mg^{2+}$  (1.0),  $Co^{2+}$  (0.5),  $Zn^{2+}$  (0.4), and  $Mn^{2+}$  (0.3). The pH effects on the  $V_m$  showed no ionizable groups in the range of pH 5 to 9, which might act as acid-base catalysts. The plot of  $V_m/K_m$  vs pH showed that catalysis is slowed at acid and alkaline pH. The researchers thus concluded that substrate binding is inhibited by the protonation of a group with an apparent  $pK_a$  of about 6.4 and deprotonation of a second group  $pK_a$  8.4. or, the ionizing groups are acting as acid-base catalysts but are not apparent in the  $V_m$  vs pH profile due to subsequent rate-limiting step such as product release.

Table 2: Purification of Phosphoenolpyruvate Mutase

Step	Total protein (mgT)	total units (mol/min)	specific activity [mol/min-mg of protein]	% yield	purification (x-fold)
250g cell extract	32000	1320	0.041	100	
15%(w/v) streptomycine sulfate	-	1200	-	91	
(NH <sub>4</sub> ) <sub>2</sub> SO <sub>4</sub> fraction (45-70%)	-	1020	-	77	
DEAE-cellulose	1227	743	0.61	41	14.8
phenyl-Sepharose	12.9	188	14.6	11	356
Bio-Gel P-200	3.8	78	20.5	4	500

## 2. Determination of the External Equilibrium of PEP

### Mutase

The <sup>31</sup>P NMR data of the conversion of P-pyr to PEP in the cell-free homogenate indicated the equilibrium of PEP mutase heavily favored PEP formation. We attempted to accurately measure the equilibrium of PEP and P-pyr in the presence of partially purified PEP mutase. The approximate equilibrium constant for PEP mutase was determined by HPLC separation and quantitation of PEP and P-pyr after equilibration with partially purified PEP mutase.<sup>79</sup> A reaction containing 10 mM P-pyr and 10 mM PEP, 10 mM MgCl<sub>2</sub> in 160 μl of 50 mM K<sup>+</sup>HEPES buffer (pH 7.8) was incubated with PEP mutase at 25°C. Within thirty minutes the P-pyr absorbance had diminished to near baseline, see Figure 3. The ratio of the absorbance for PEP (ε=2600) and P-pyr (ε=1100) was >500:1. The diminutive amount of P-pyr was very difficult to measure. A more accurate value for the equilibrium constant has yet to be determined.

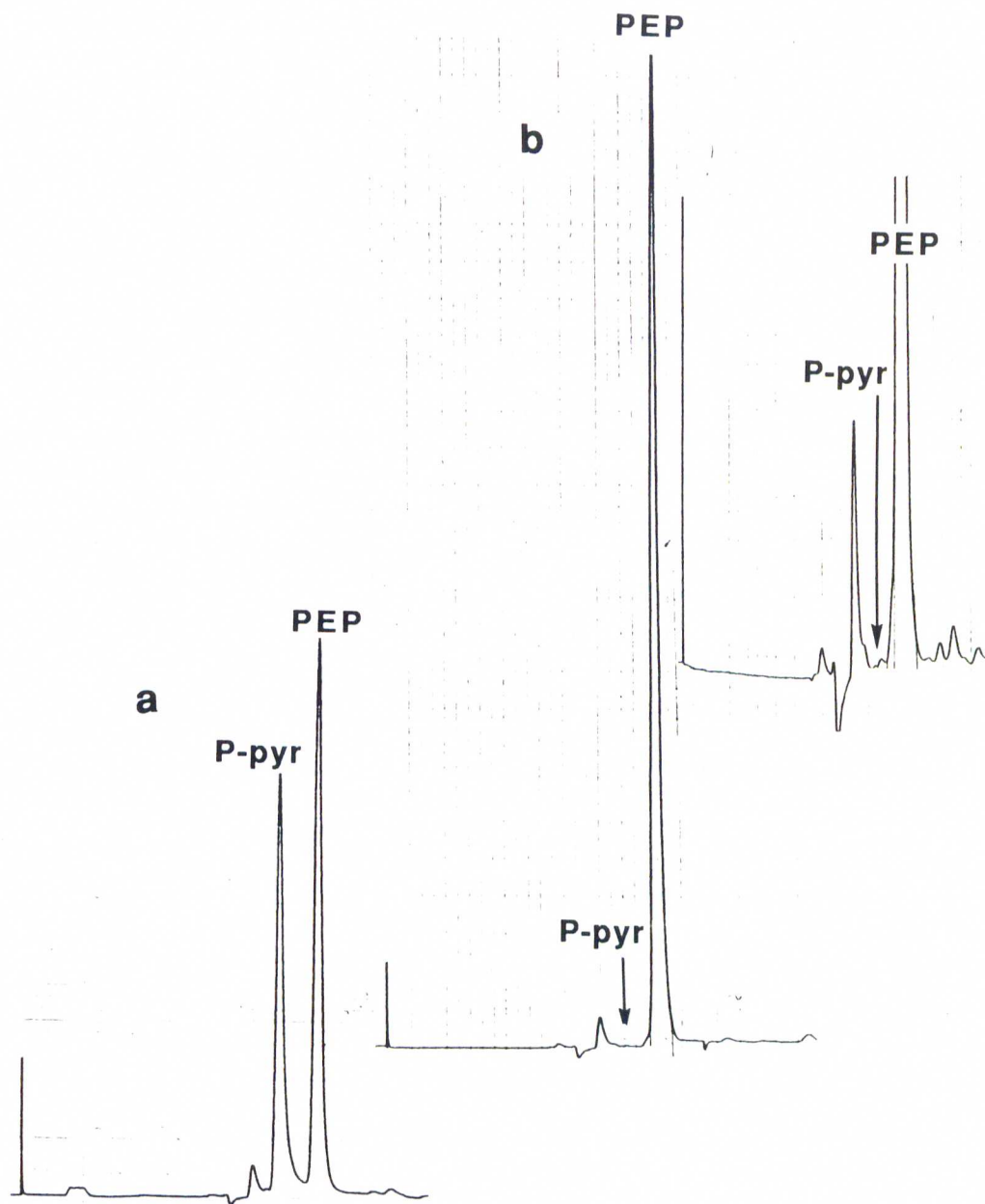


**Figure 3.** HPLC elution profile of a reaction of 10mM PEP and 10mM P-pyr in 50 mM  $K^+$ HEPES buffer containing 10 mM  $MgCl_2$  **a)** before addition of PEP mutase and **b)** after a 30 min reaction with PEP mutase. Inset is magnified 10-fold.

PEP is one of the highest energy organophosphate in biological systems.<sup>80</sup> Approximately 13 kcal/mole of energy is released upon hydrolysis owing to the energetically favorable keto formation and separation of closely disposed negative charges upon hydrolysis.<sup>79</sup> Therefore, the equilibrium of the phosphomutase was not expected to favor PEP. It seemed reasonable to assume the phosphoenol moiety rearrangement to the  $\beta$ -keto phosphonate would behave in an analogous fashion to phosphoenol hydrolysis. However, the bond strength of the P-C bond in the resulting  $\beta$ -keto phosphonate was not taken into consideration. Published values suggest P-C BDEs are *ca.* 10-17 kcal/mol higher in energy than P-O bond dissociation energies.<sup>81</sup> The energy obtained from the hydrolysis of PEP is only 10-12 kcal/mol more than the 2-3 kcal/mol for the hydrolysis of phosphate esters.<sup>82</sup> Using these data we can estimate that  $\Delta G$  for the conversion of phosphonopyruvate to phosphoenolpyruvate to be -5 to -7 kcal/mol. Therefore, considering the relative weakness of the P-C bond in phosphonopyruvate one can rationalize the intrinsic thermodynamic instability of phosphonopyruvate and the observed equilibrium.

Recently Swalbe et. al.<sup>83</sup> reported the equilibrium constant for the rearrangement of phosphonopyruvate to phosphoenolpyruvate based on theoretical calculations. Energies of optimized structures of the tris(cyclohexylammonium) salt of phosphonopyruvate were compared to known optimized structures of PEP based upon the PEP monoanion crystal structure. Gas phase  $\Delta G$  energies calculated using the MNDO, STO-3G, and 3-21G basis sets were -6.7, -4.6, and -9.9 Kcal/mol, respectively, which imply the equilibrium constant is at least 2500 in favor of PEP. The authors

noted these gas phase energies should correspond to the solvated species since calculated solvation energies for PEP and P-pyr are very similar.

PEP mutase was also purified from the bialphos-producing *Streptomyces hygroscopicus* by Seto and coworkers. The same external equilibrium heavily favoring PEP was noted by these researchers. Additionally, Seto demonstrated that phosphonopyruvate formed from phosphoenolpyruvate by PEP mutase could be trapped *in situ* by reduction to phosphonolactate using malate dehydrogenase and NADH. This result would suggest that the equilibrium constant probably does not favor PEP vs P-pyr by more than a factor of 1000 otherwise coupling could not occur.

### 3. Discussion of the Internal and External Equilibria of PEP Mutase

The unfavorable rearrangement of PEP to P-pyr catalyzed by PEP mutase *in vitro* may somehow be offset *in vivo* so that AEP biosynthesis can occur more readily. The external equilibrium is >500 to 1 in favor of PEP. The internal equilibrium was measured to be >25 to 1 in favor of PEP by single turnover experiments which are described later in the last section of the Results and Discussion. The more favorable equilibrium of bound P-pyr and PEP should allow the AEP pathway to produce AEP if the bound P-pyr could be presented to the decarboxylase by a channelling process. The decarboxylase carries out an irreversible reaction which would pull the intermediate forward in the pathway to AEP.

Direct transfer of metabolites from the active site of one enzyme to another is termed "channeling." A recent review article by Srere<sup>84</sup> provides evidence for channeling in many biosynthetic processes.

Channeling is proposed to be operating in pathways to provide efficient processing of intermediates which have no other metabolic use other than to form the pathway product, for example, antibiotic or protein synthesis. Considering the potential toxic nature of some phosphonates and the apparent instability of P-pyr, channeling in the AEP biosynthetic pathway seems reasonable. Further research into channeling of P-pyr is currently being conducted in our laboratory.

There were two other reports of the purification of PEP mutase. Another research group reported purification of PEP Mutase From *T. pyriformis*. Seidel et al.<sup>5</sup> reported on purification of PEP mutase by chromatography first on DEAE-cellulose then through hydroxylapatite. The enzyme was purified 470-fold and had a specific activity of 74 U/mg. The kinetic constants obtained were  $K_{cat} = 41 \text{ s}^{-1}$ ,  $K_m = 67 \text{ }\mu\text{M}$ , and  $K_{cat}/K_m = 6 \times 10^5 \text{ M}^{-1}\text{s}^{-1}$ . Seto and coworkers<sup>61</sup> isolated PEP mutase from a bialaphos-producing strain of *Streptomyces hygrosopicus*. PEP mutase obtained from this bacteria was reported to be extremely unstable and hence the purification by DEAE-cellulose, hydroxylapatite, and FPLC (Mono Q) resulted only in a partially purified enzyme which had a specific activity of 15.5 U/mg.

## **I. Studies of the Catalytic Mechanism of the PEP $\leftrightarrow$ P-pyr Rearrangement Catalyzed by PEP Mutase**

The focus of our research turned to defining the catalytic mechanism of PEP mutase. We intended to carry out experiments to determine if the rearrangement catalyzed by PEP mutase was an intra- or intermolecular process. Additionally, we wished to determine the stereochemical course of phosphoryl transfer during the P-pyr $\Rightarrow$ PEP rearrangement. Both of these experiments would be carried out in the thermodynamically favored P-pyr  $\Rightarrow$  PEP direction rather than the physiological PEP  $\Rightarrow$  P-pyr direction. We envisioned both of these studies to involve  $^{31}\text{P}$  NMR analysis of  $^{18}\text{O}$ -induced shift perturbations of the phosphorus nuclei in phosphonopyruvate and phosphoenolpyruvate. It is well known that a sulfur attached to such phosphorus monoesters facilitates such NMR analyses by enhancing the shift perturbations caused by an  $^{18}\text{O}$  in a nonbridge position on phosphorus.<sup>85-87</sup> Therefore, we pursued a synthesis of thiophosphonopyruvate (SP-pyr).

### **1. Synthesis of Thiophosphonopyruvate**

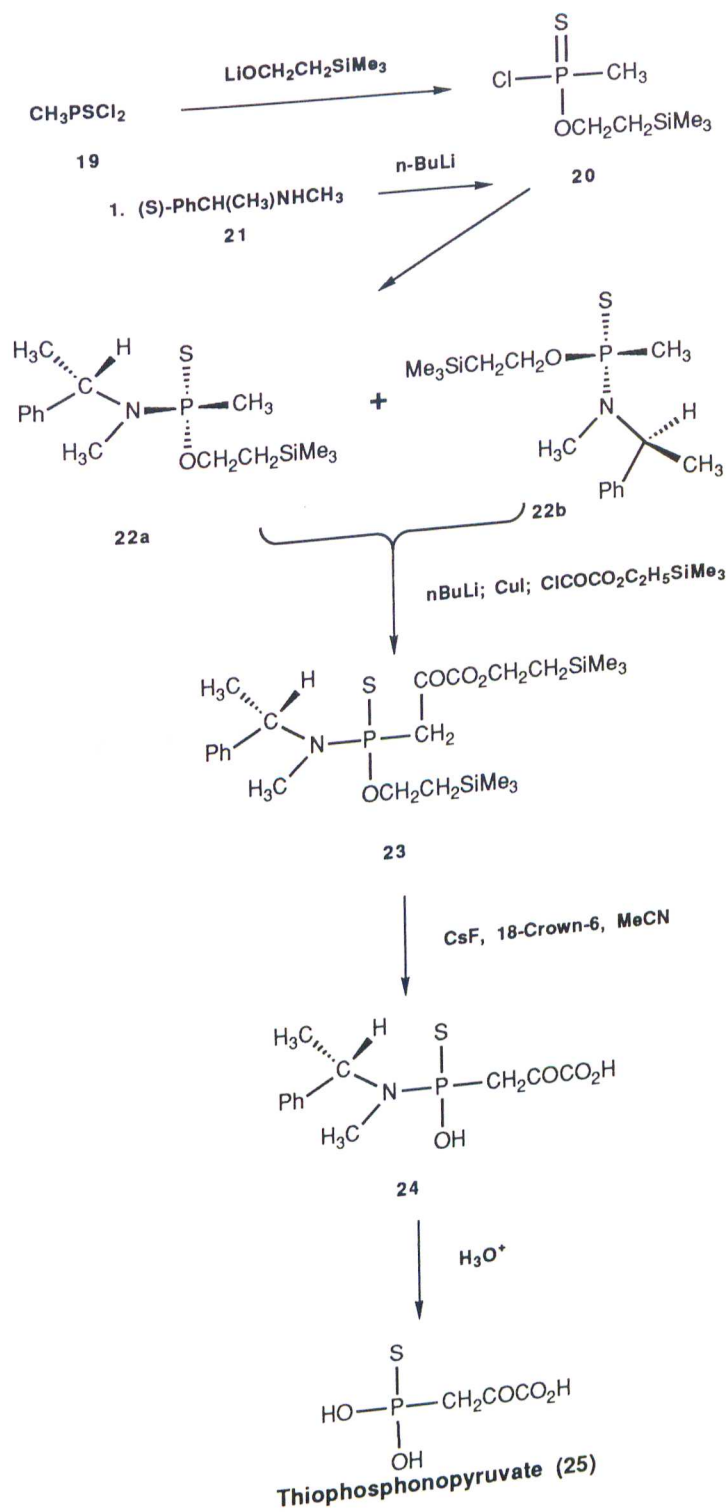
The synthesis of thiophosphonopyruvate is based upon the methodology developed by Tim Hepburn and Sheng-lian Lee in our laboratory for the synthesis of chiral thiophosphonates.<sup>44</sup> The methodology requires a reduced form of phosphate which is derivatized with oxyester and amide substituents. If the amide is asymmetric it can serve as a chiral auxiliary for the synthesis of a chiral thiophosphonate.

The synthesis of thiophosphonopyruvate is shown in Scheme 22. Methyl phosphonodichloridothioate (**19**) is reacted with one equivalent of the lithium alkoxide of trimethylsilylethanol followed by one equivalent of lithium (*S*)-*N*-methyl methylbenzylamine to form diastereometric *N,P*-dimethyl-*N*-(phenylethyl)-*O*-[2-(trimethylsilyl)ethyl] phosphonamidothioate (**22**). The *P*-methyl group then had to be elaborated into the pyruvoyl moiety. This was accomplished by a known methodology<sup>88</sup> which involved forming the copper enolate of the diastereomers and reacting it with the 2-trimethylsilylethyl half ester of oxalylchloride, forming (**23**). Bisdtrimethylsilylethylation was accomplished using two equivalents of cesium fluoride. The phosphonamide was then hydrolyzed under acidic conditions, thus producing thiophosphonopyruvate (**25**).

## **2. Substrate Activity of Thiophosphonopyruvate with PEP Mutase**

The initial velocities of PEP mutase catalyzed conversion of thiophosphonopyruvate to thiophosphoenolpyruvate or phosphonopyruvate to phosphoenolpyruvate were measured at pH 8.0 as a function of the concentration of pure thiophosphonopyruvate or phosphonopyruvate. The thiophosphonopyruvate gave  $K_m = 5 \mu\text{M}$  and  $V_m = 16 \text{ s}^{-1}$  values and phosphonopyruvate gave  $K_m = 20 \mu\text{M}$  and  $V_m = 24 \text{ s}^{-1}$  values. The lower  $K_m$  and nearly equal  $V_m$  values for thiophosphonopyruvate vs phosphonopyruvate justify its use as a substrate for mechanistic studies. The mechanistic implications of these kinetic constants will be discussed later.

**Scheme 22. Synthesis of Thiophosphonopyruvate.**



## **A. Determination of the Intramolecularity of the PEP Mutase Rearrangement of PEP**

We wanted to unambiguously determine if the P-Pyr to PEP rearrangement catalyzed by PEP mutase was an inter- or intramolecular process. An intramolecular process involves the transfer of the phosphorus from carbon to oxygen (and vice versa) in the same substrate molecule. An intermolecular process involve the transfer of the phosphoryl group from one molecule of P-pyr to the pyruvoyl moiety of another substrate molecule. Both intra- and intermolecular processes are documented for phosphomutases.

### **1. Precedence for Intra- and Intermolecular Mechanisms in Phosphomutases**

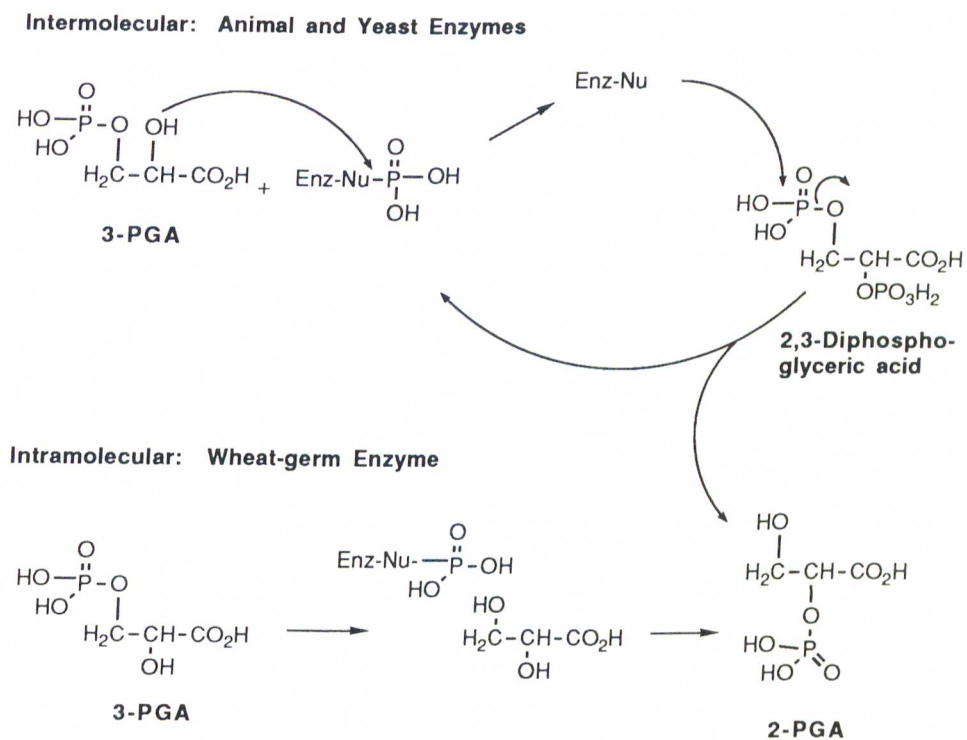
Intermolecular reactions are documented for both phosphoglucomutase and phosphoglycerate mutase. Of these two examples phosphoglucomutase is more interesting since its reaction can also follow an intramolecular pathway. The reaction for both of the 2-phosphoglycerate enzymes are shown in Scheme 23.

The rearrangement of 2-phosphoglyceric acid (2-PGA) to 3-phosphoglyceric acid (3-PGA) can occur in either an intramolecular<sup>89</sup> or an intermolecular<sup>90</sup> process depending upon the source of the phosphoglucomutase. Phosphoglycerate isolated from animals or from yeast carries out an intermolecular shuttling of the phosphoryl group between two molecules of phosphoglyceric acid. The active form the the enzyme has a phosphorylated histidine which phosphorylates the C-3 hydroxyl of 2-phosphoglyceric acid to form the 2,3-diphosphoglycerate.

Then, the phosphoryl group from C-2 is removed, thus reforming the active phosphorylated form to the phosphomutase and 3-phosphoglyceric acid.

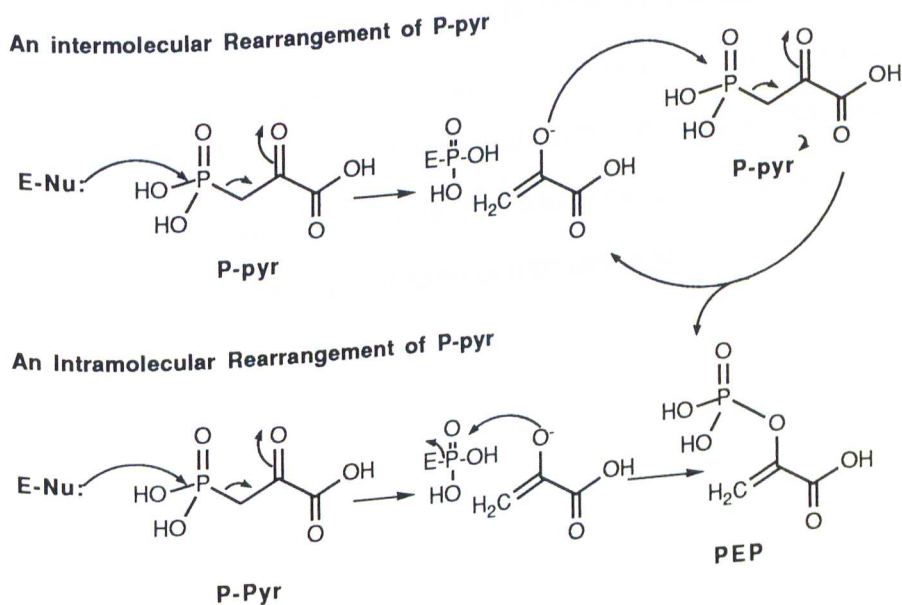
Phosphoglycerate isolated from wheat germ carries out an intermolecular rearrangement in which the phosphoryl group in the substrate, 2-phosphoglycerate, is the same phosphoryl group in the 3-phosphoglycerate product. It is believed that the intramolecular rearrangement is assisted by an active site nucleophile.

**Scheme 23.** Intermolecular and Intramolecular Mechanism for 2-Phosphoglucomutase



Analogous intra- and intermolecular processes for the PEP mutase-catalyzed rearrangement of phosphonopyruvate to phosphoenolpyruvate are drawn in Scheme 24. The intramolecular process involves a molecule of P-pyr rearranging to a molecule of PEP. One can imagine the intermolecular process occurring by a reaction involving two molecules of phosphonopyruvate in which there is an exchange of phosphoryl and pyruvoyl moieties.

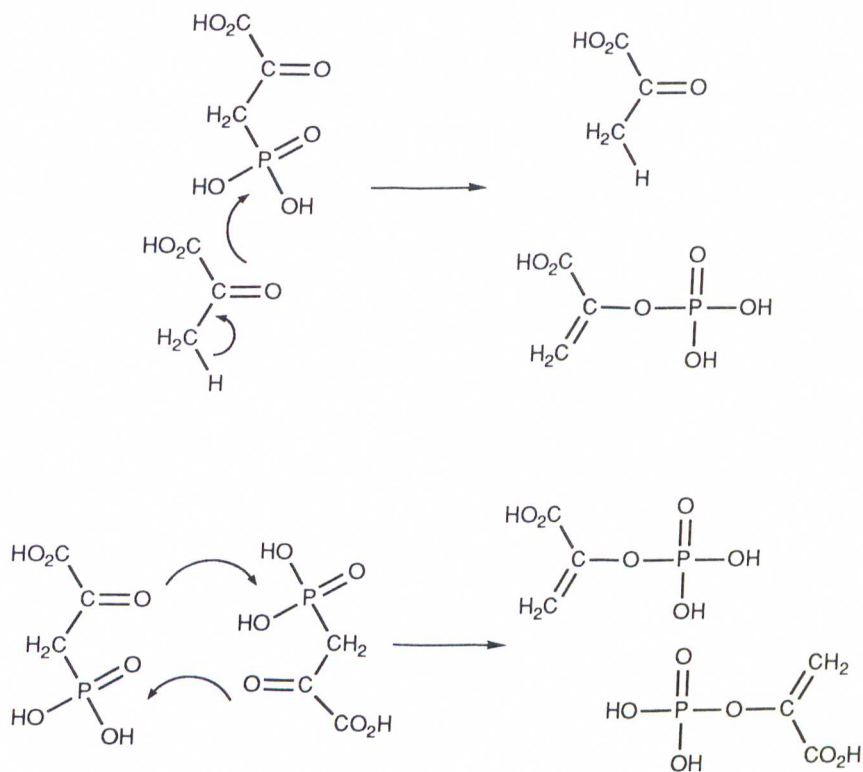
**Scheme 24.** Intra- and intermolecular Reaction Mechanisms for PEP Mutase



## 2. Does the PEP Mutase Reaction Proceed Intramolecularly?

We set out to determine whether the reaction proceeded intramolecularly or intermolecularly. The two intermolecular mechanisms considered are illustrated in Scheme 25. One involves phosphoryl transfer from phosphonopyruvate to enzyme bound pyruvate while the second requires phosphoryl exchange between two phosphonopyruvate molecules bound in a head-to-tail arrangement. Both pathways involve transfer of a phosphoryl group from phosphonopyruvate to the pyruvate unit of a second reactant molecule. We hoped to distinguish this process from the intramolecular phosphoryl transfer reaction by  $^{18}\text{O}$ -labelling both the phosphoryl group and the C<sub>2</sub>-carbonyl in one reactant and reacting it with a second, unlabelled reactant. Product  $^{18}\text{O}$ -labelled at the phosphoryl moiety but not at the C<sub>2</sub>-carbonyl (*or vice versa*) would signify an intermolecular reaction while the absence of cross labelled product would give evidence for an intramolecular process.

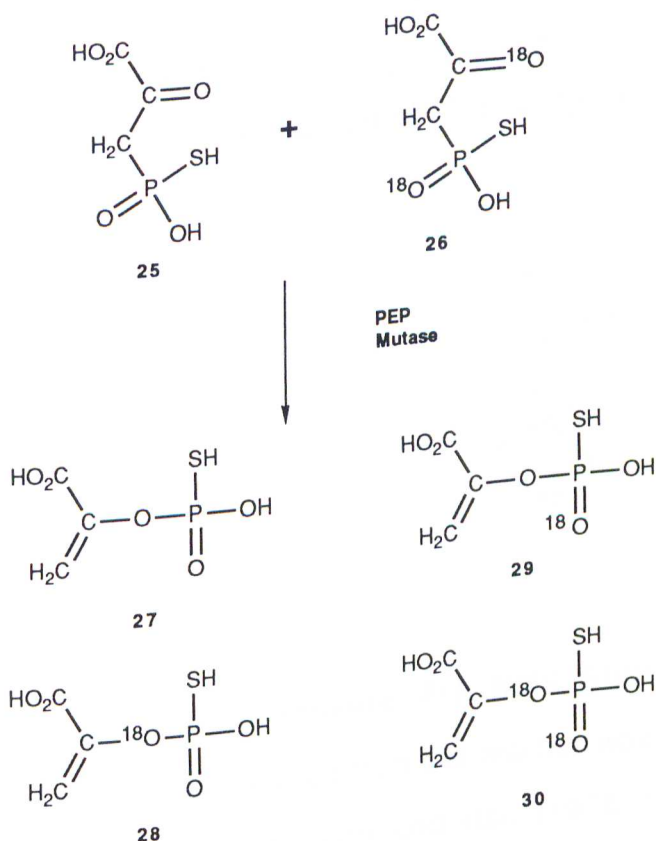
**Scheme 25.** Possible Intermolecular Mechanisms of PEP Mutase Catalysis



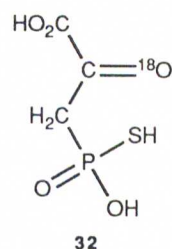
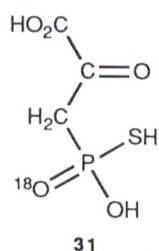
The actual experiment was, as illustrated in Scheme 26, carried-out with an equimolar mixture of all  $^{16}\text{O}$ -thiophosphonopyruvate (**25**) and thiophosphonopyruvate (**26**) labelled with one  $^{18}\text{O}$  at the thiophosphoryl center and one  $^{18}\text{O}$  at the  $\text{C}_2$  carbonyl center. Thiophosphonopyruvate was used in place of phosphonopyruvate to simplify analysis of the  $^{18}\text{O}$ -labelled product by  $^{31}\text{P}$ -NMR. We anticipated that we would be able to resolve the  $^{31}\text{P}$  NMR resonances for the thiophosphoenolpyruvate isotopomers. Our prediction was based upon studies of electron distributions in thiophosphates which have demonstrated that the nonbridging oxygen atoms have at the expense of the sulfur atom, more

double bond character than do the oxygen atoms of their phosphate counterparts. Initial velocity studies of the substrate activity of thiophosphonopyruvate demonstrated that it is turned over at 75% the rate of phosphonopyruvate and that it has a  $K_m$  ( $5 \mu\text{M}$ ) which is 4-fold smaller than that of the phosphonopyruvate ( $20 \mu\text{M}$ ). Thus, its use as an alternate substrate is well justified.

**Scheme 26.** Test For Intramolecular vs. Intermolecular PEP Mutase Catalysis



The criterion for an intermolecular process through this experimental design is the formation of the cross labelled product [P- $^{18}\text{O}$ -(C-2)]thiophosphoenolpyruvate (**28**) which could only derive from the transfer of the thiophosphoryl group of [ $^{16}\text{O}_2$ ]thiophosphonopyruvate to the [ $^{18}\text{O}$ -(C-2)]pyruvate unit originating from [P= $^{18}\text{O}$ ,C(2)- $^{18}\text{O}$ ]thiophosphonopyruvate (**26**). Likewise, the formation of [P= $^{18}\text{O}$ ]thiophosphoenolpyruvate (**29**) in the product mixture would, in principal, also demonstrate the operation of the intermolecular mechanism. However, as described below, this product can also derive from an intramolecular rearrangement of [P= $^{18}\text{O}$ ]thiophosphonopyruvate (**31**) generated *in situ* from [P= $^{18}\text{O}$ , C(2)- $^{18}\text{O}$ ]thiophosphonopyruvate (**26**) by a competitive solution exchange reaction ( $\text{C}=\text{}^{18}\text{O} + \text{H}_2\text{}^{16}\text{O} \rightleftharpoons \text{C}=\text{}^{16}\text{O} + \text{H}_2\text{}^{18}\text{O}$ ).



#### a. [ $^{18}\text{O}$ ]Thiophosphonopyruvate $^{31}\text{P}$ NMR Shift Standards

Analysis of the mixture obtained from this reaction was performed by using the  $^{31}\text{P}$  NMR method of Cohn and Hsu (1978) to distinguish between and quantitate the four possible products differing in their  $^{18}\text{O}$  labelling patterns at phosphorus, *i. e.*, thiophosphoenolpyruvate containing: (1) zero  $^{18}\text{O}$  atoms at phosphorus (**27**), (2) one  $^{18}\text{O}$  at the C<sub>2</sub>-O-P bridge

position (**28**), (3) one  $^{18}\text{O}$  at the nonbridge position of phosphorus (**29**), , and (4) one  $^{18}\text{O}$  at the bridge position and one  $^{18}\text{O}$  at the nonbridge position of phosphorus (**30**). In order to assess the resolution of the NMR analysis and also test for competing solution  $^{18}\text{O}$  exchange at the ketone carbonyl position of the  $\text{C}_2$   $^{18}\text{O}$ -labelled reactant **26**,  $^{31}\text{P}$  NMR analyses were conducted on product mixtures obtained from separate PEP mutase catalyzed reactions of  $[\text{C}(2)\text{-}^{18}\text{O}]$ thiophosphonopyruvate (**32**) and  $[\text{P}=\text{}^{18}\text{O}, \text{C}(2)\text{-}^{18}\text{O}]$ thiophosphonopyruvate (**26**) in  $\text{H}_2\text{}^{16}\text{O}$ . In the time frame required to complete the phosphomutase reactions of **32** and **26** 60% of the  $^{18}\text{O}$  label at the  $\text{C}_2$  carbonyl was lost. This level of wash-out could be easily accounted for in the test experiment and thus posed no problem. Equally important was the finding that the  $^{31}\text{P}$  NMR resonances of each product, *viz* (all- $^{16}\text{O}$ )thiophosphoenol pyruvate (**27**) and  $[\text{C}(2)\text{-}^{18}\text{O}]$ thiophosphoenolpyruvate (**28**) formed from **32**, and  $[\text{P}=\text{}^{18}\text{O}]$ thiophosphoenolpyruvate (**29**) and  $[\text{P}=\text{}^{18}\text{O}, \text{C}(2)\text{-}^{18}\text{O}]$ thiophosphoenolpyruvate (**30**) formed from **26**, were well resolved (0.026 ppm upfield shift for  $^{18}\text{O}$  in the bridge position **28** and 0.046 ppm for  $^{18}\text{O}$  in the nonbridge position **29** on the phosphorus).

#### **b. PEP Mutase Crossover Experiment**

The PEP mutase crossover reaction was carried out with an equimolar ratio of 52  $\mu\text{mol}$  (all- $^{16}\text{O}$ )thiophosphonopyruvate and 52  $\mu\text{mol}$   $[\text{P}=\text{}^{18}\text{O}, \text{C}(2)\text{-}^{18}\text{O}]$ thiophosphonopyruvate with 10 units of PEP mutase at 25°C for 10 min. For a purely intramolecular reaction pathway, we expected (based on a 60%  $^{18}\text{O}$  wash-out at the  $\text{C}_2$  carbonyl) that (all- $^{16}\text{O}$ )thiophosphoenolpyruvate (**27**),  $[\text{C}(2)\text{-}^{18}\text{O}]$ thiophosphoenolpyruvate

(**28**), [P= $^{18}\text{O}$ ]thiophosphonopyruvate (**29**) and [P= $^{18}\text{O}$ , C<sub>2</sub>- $^{18}\text{O}$ ]thiophosphonopyruvate (**30**) would be formed in a 1 : 0 : 0.6 : 0.4 ratio. For an intermolecular process, on the other hand, the **27** : **28** : **29** : **30** ratio should be 1 : 0.25 : 1 : 0.25.  $^{31}\text{P}$  NMR analysis of the product mixture (Figure 4) gives a 1 : 0 : 0.6 : 0.4 ratio of these substances, thus, demonstrating that the PEP mutase catalyzed rearrangement of phosphonopyruvate to phosphoenolpyruvate occurs via an intramolecular mechanism.

Thus, we have demonstrated that PEP mutase rearranges a single substrate molecule to a single product molecule. However, there are numerous possible intramolecular mechanisms one can envision for the PEP mutase reaction, therefore, we needed to further define the intramolecular reaction mechanism. The next logical question to ask was how many steps are involved in this intramolecular rearrangement. At an elementary level, this process could occur in either a single, concerted step or in two consecutive steps.

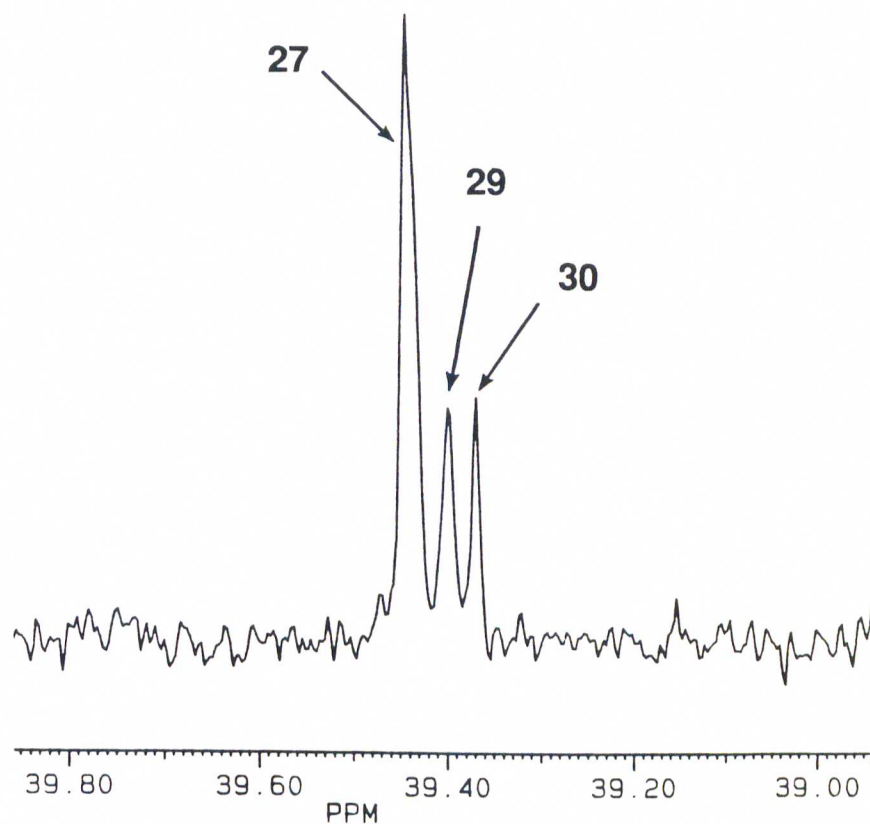


**Figure 4.** The  $^{31}\text{P}$  NMR spectrum of the mixture of isotopically labelled thiophosphoenolpyruvates obtained by PEP mutase catalyzed reaction of a mixture of  $[\text{P}=\text{}^{18}\text{O}, \text{C}(2)\text{-}^{18}\text{O}]$ thiophosphonopyruvate (**26**) and  $[\text{all-}^{16}\text{O}]$ thiophosphonopyruvate (Scheme 2). The observed resonances correspond to the thiophosphoenolpyruvate isotopomers **27**, **29**, and **30** as labelled.

## **B. Is the PEP Mutase-Catalyzed Intramolecular Rearrangement Concerted or Stepwise?**

The enzyme catalyzed intramolecular rearrangement of phosphonopyruvate to PEP could occur in either a concerted or a stepwise fashion (Scheme 21). The experimental technique we employed to distinguish between these two possibilities was a phosphorus stereochemical analysis of the enzyme reaction. Although the results contained herein may be somewhat complicated the conclusion to which they point is unambiguous: PEP mutase catalyzes a stepwise rearrangement of P-pyr to PEP.

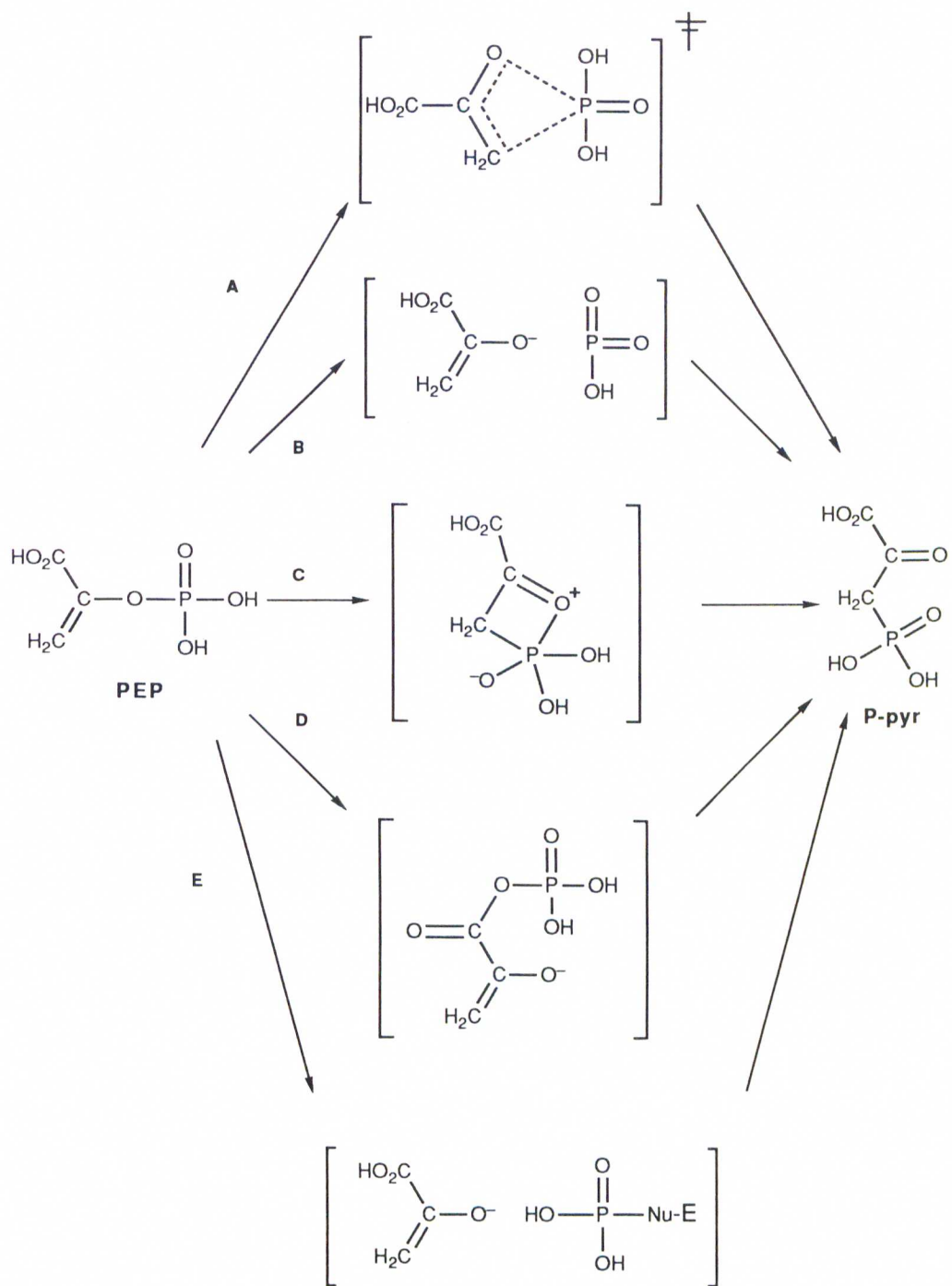
### **1. Analysis of Possible Mechanisms**

Examples of the two general reaction types are shown in Scheme 27. The single step process corresponds to a sigmatropic rearrangement and, as such, should proceed *via* a Möbius transition state<sup>75</sup> (pathway A, Scheme 27). There are several possible stepwise mechanisms. By definition, the stepwise process must possess, between each step, a discrete intermediate. The form of this intermediate can be widely variable. The first of these (pathway B, Scheme 27) involves heterolytic dissociation of the phosphorus from the bridge oxygen to form a paired monomeric metaphosphate-enolate anion intermediate. Addition of the phosphorus of metaphosphate to the C<sub>3</sub> of pyruvate enolate would then form phosphonopyruvate. The second possible nonconcerted mechanism (pathway C, Scheme 27) would proceed *via* formation of an oxaphosphetane intermediate, formed by bonding of the carbonyl oxygen

in the pyruvate moiety to the phosphonate phosphorus followed by rupture of the O-P bond. involves covalent participation by the enzyme through use of a nucleophilic active site amino acid residue to accept to the phosphoryl group from C<sub>2</sub> of phosphonopyruvate and transfer it to the oxygen atom of the resulting pyruvate enolate. The third mechanism, described by Seidel et. al.<sup>91</sup> in 1990 and shown as pathway D in Scheme 27, proceeds through strain free 5-membered transition states associated with transfer of the phosphoryl group from C<sub>2</sub> to form an acylphosphate intermediate and with subsequent nucleophilic attack by the charged oxygen atom of the enolate moiety. A fourth (pathway E in Scheme 27) involves covalent participation by the enzyme through use of a nucleophilic active site amino acid residue to accept to the phosphoryl group from C<sub>2</sub> of phosphonopyruvate and transfer it to the oxygen atom of the resulting pyruvate enolate.

REPRODUCED FROM: J. Biol. Chem. 265:11111-11115 (1990)  
Copyright © 1990 American Chemical Society  
DOI: 10.1021/bi00300a011

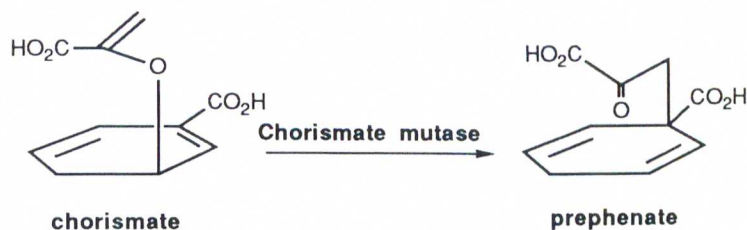
**Scheme 27.** Possible Mechanisms for PEP Phosphomutase Catalysis.



### a. Precedence for a Concerted Mechanism

Although no precedence for concerted phosphoryl shifts could be found in the literature, one example of a pericyclic process in an enzyme reaction has been found, namely chorismate mutase. The rearrangement of prephenate to chorismate shown in Scheme 28 is a Claisen rearrangement. It has been suggested that chorismate mutase assists the rearrangement of chorismate to prephenate by holding the substrate in the correct alignment thereby allowing the sigmatropic shift to occur readily.<sup>92</sup> The concerted mechanism proposed for the PEP mutase is justified in light of the lack of information surrounding the mechanisms of enzyme-catalyzed phosphoryl transfers involving phosphonates.

**Scheme 28.** Chorismate Mutase Catalyzed Rearrangement of Chorismate to Prephenate



### b. Precedence for Stepwise Mechanisms

Of the four stepwise mechanisms proposed only two have precedence in phosphoryl transfer enzymes. The most likely stepwise mechanism involves the formation of a phosphorylated enzyme intermediate in which the enolate of pyruvate is also stabilized. There are

many examples of phosphoryl enzyme intermediates in the reactions catalyzed by phosphatases,<sup>93</sup> phosphomutases,<sup>94</sup> and adenosine triphosphatases.<sup>95</sup> The other intermediate in the enzyme phosphoryl mechanism is the enolate of pyruvate, which is known to be stabilized in pyruvate kinase<sup>96</sup> and pyruvate phosphate dikinase.<sup>97</sup> Some enzymes which are believed to catalyze phosphoryl transfers in a dissociative fashion. Evidence supporting such dissociative mechanisms has been gained through <sup>18</sup>O primary and secondary isotope studies.

## **2. Stereochemical Analysis to Probe the Concerted vs Stepwise Mechanisms**

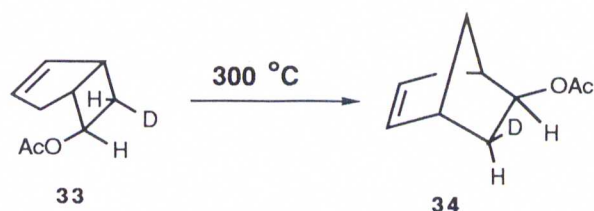
The second goal in our investigations of PEP phosphomutase catalysis was to determine whether the intramolecular rearrangement of phosphonopyruvate occurs by a concerted or stepwise pathway. We felt that this determination could be made by elucidation of the stereochemical course of the catalyzed reaction. The concerted reaction is expected to invert the phosphorus stereochemistry while any stepwise process should retain the phosphorus stereochemistry.

### **a. Stereochemical Course of the Concerted Reaction**

Orbital topology considerations<sup>75</sup> suggest that a concerted route (pathway A in Scheme 27) for suprafacial C to O 1, 3-phosphoryl migration should proceed through a Möbius transition state with inversion of configuration at phosphorus. This prediction is based on the analogy

gained from studies of 1,3 sigmatropic rearrangements of a carbon systems carried out by Berson.<sup>98</sup> Scheme 30 illustrates the rearrangement of endo-bicycl[3.2.0]-hept-2-en-6-yl acetate (**33**) to exo-norbornyl acetate (**34**) was shown to take place with inversion of configuration at the migrating carbon.

**Scheme 29.** 1,3-Sigmatropic Carbon Shift Occurs with Inversion



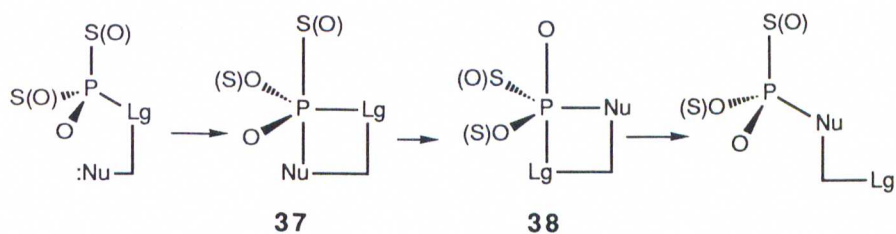
### b. Stereochemical Course of the Stepwise Pathways

All of the possible stepwise process should retain the original phosphorus stereochemistry. The four stepwise mechanisms are shown in Scheme 27. The metaphosphate formed in the dissociative pathway (pathway B, Scheme 27) should rebond to the pyruvate unit at C3 using the same face of the phosphorus from which the pyruvate unit dissociated. Thus, retention of stereochemistry at phosphorus is predicted. The double displacement pathway (pathway E, Scheme 27) should also display net retention of the phosphorus configuration owing to the fact that two sequential, in line displacements are involved and each should invert the configuration at phosphorus.<sup>74</sup>

The mechanism involving the four-membered ring, oxaphosphetane intermediate, (pathway C) is also predicted to proceed with retention of

phosphorus stereochemistry based upon information gained from studies of the Wittig reaction and other reactions which occur through analogous carba- and azaphosphetane intermediates. The prediction that this mechanism should retain the absolute configuration at phosphorus is based upon the assumption that the pentavalent phosphorus is formed by apical attack opposite the more electronegative sulfur or oxygens.<sup>99</sup> Pseudorotation is then required to place the leaving group in an apical position for departure. (Scheme 30)

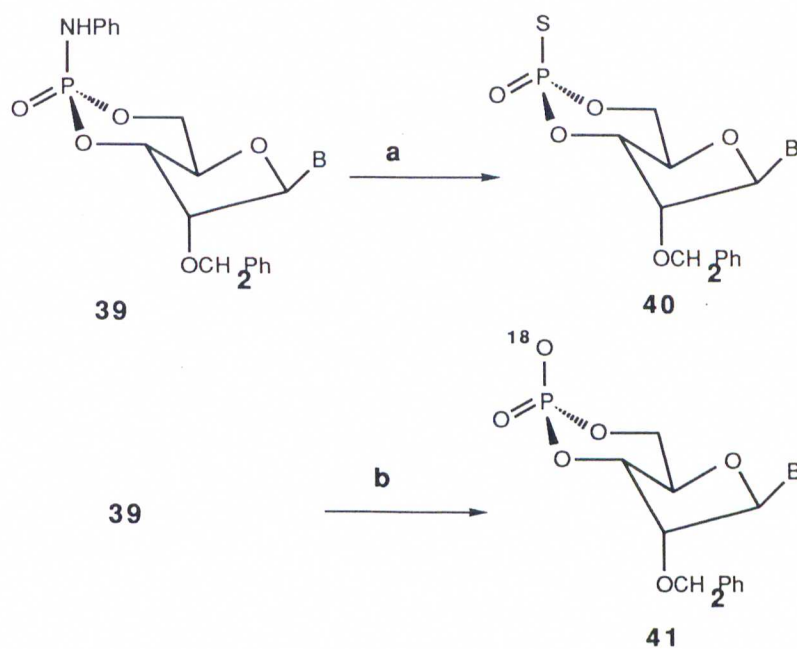
**Scheme 30.** Reactions Proceeding Through a Phosphetane Intermediate Should Proceed with Retention of Configuration



In the Wittig reaction oxaphosphetane intermediates analogous to **35** and **36** (Nu = O, Lg = C) undergo pseudorotation at a rate  $10^8$  faster than the rate of decomposition.<sup>100</sup> However, pseudorotation within the 4-membered ring to place the leaving group in the apical position always leads to retention of configuration of the phosphorus atom. Corroborative evidence for retention of configuration via this mechanism can be found in the results of Stec<sup>101</sup> and Gerlt.<sup>102</sup> Stec showed that treatment of

phosphoroanilidate **37** with potassium and carbon disulfide produced the thiophosphate **38** with retention of configuration (Scheme 31).

**Scheme 31.** Conversion of Phosphoroanilidates to Thiophosphates Proceed with Retention of Configuration



Gerlt demonstrated a similar conversion of phosphoroanilidate **37** with [<sup>18</sup>O]<sub>2</sub> carbon dioxide to form **39** to proceed with retention of configuration (Scheme 31). These reactions presumably go through an azaphosphetane intermediate which should be analogous to the possible oxaphosphetane intermediate in the PEP mutase reaction.

We anticipate that pathway D involving initial transfer of the phosphoryl grouping to the internal carboxyl group should also proceed with overall retention of configuration at phosphorus since it is comprised of two individual steps, each of which should preserve the original phosphorus configuration. Each step would require pseudorotation in a cyclic pentavalent phosphorus intermediate, as opposed to concerted back side displacement, since critical steric constraints are placed on the entering nucleophile and leaving group.

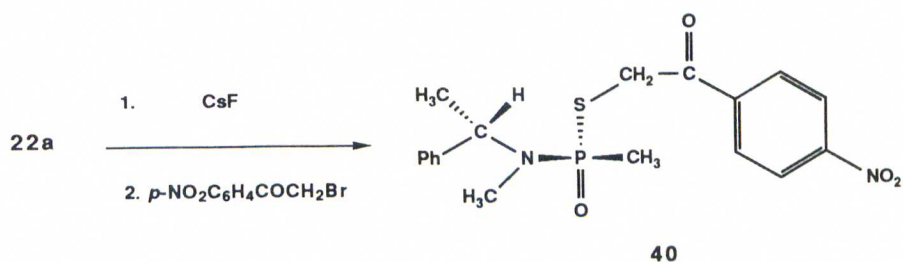
### **3. Design of the Phosphorus Stereochemical Analysis**

In order to gain information about these mechanistic alternatives, the stereochemical course of the PEP phosphomutase rearrangement was explored. For this purpose, enantiomerically pure samples of the antipodes of a chiral phosphonopyruvate with known stereochemistry were needed as was a method of determining the absolute configuration of the chiral PEP product formed. One option was to use the enantiomers of chiral [ $^{18}\text{O}$ ,  $^{17}\text{O}$ ,  $^{16}\text{O}$ -P]phosphonopyruvate as stereochemical probes and to analyze the corresponding enantiomers of [ $^{18}\text{O}$ ,  $^{17}\text{O}$ ,  $^{16}\text{O}_2$ -P]phosphoenolpyruvate, the product of enzymatic rearrangement. Another involved the use of the enantiomers of [ $\text{P}=\text{}^{18}\text{O}$ ]thiophosphopyruvate as chiral probes and required the stereochemical analysis of the corresponding [ $\text{P}=\text{}^{18}\text{O}$ ]thiophosphoenolpyruvate enantiomers. We elected to use the latter approach based on an initial evaluation that the sulfur rather than the  $^{17}\text{O}$  replacement to create a chiral center at phosphorus would represent an easier synthetic challenge and at the

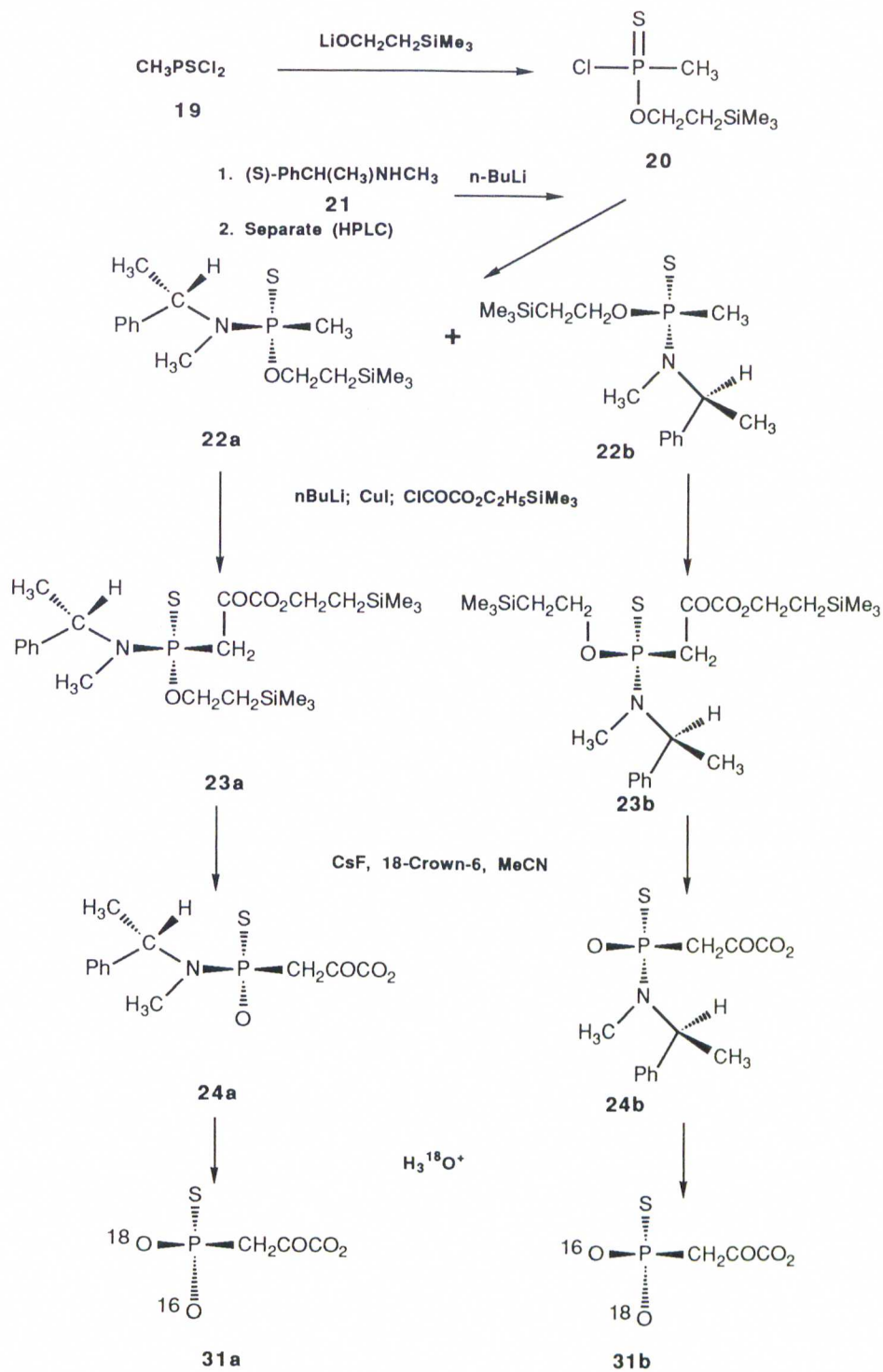
same time would take advantage of the published procedure<sup>101</sup> for the configurational analysis of the chiral product, [<sup>18</sup>O,<sup>13</sup>C]thiophosphoenolpyruvate.

### a. Synthesis of Chiral Thiophosphonopyruvate

The synthetic route to the individual enantiomers of chiral [<sup>18</sup>O]thiophosphonopyruvate (**31a** and **31b**) that was developed is outlined in Scheme 32. It involves the elaboration of methylphosphonothioic dichloride to the (Sp,Sc) and (Rp,Sc) diastereomers of the N, P-dimethyl-N-(1-phenylethyl)-O-[2-(trimethylsilylethyl)] phosphonamidothioate (**22a** and **22b**). Reaction of dichloride **19** with the lithium amide of (S)-N-methyl-N-(1-phenylethyl)amine to give a mixture of **22a** and **22b**. Separation of these diastereomers was accomplished by HPLC. In order to determine the configuration of the phosphorus atom in each of the diastereoisomers, the crystalline *p*-nitrophenacyl derivative was prepared from **22a** by removal of the trimethylsilylethyl protecting group by  $\beta$ -elimination using cesium fluoride followed by S-alkylation. X-ray analysis<sup>103</sup> of **40** provided the structure shown in Figure 5 and the absolute stereochemistry at phosphorus in **22a** is (Sp).



**Scheme 32.** Synthesis of the (*S<sub>P</sub>*) and (*R<sub>P</sub>*) Enantiomers of [<sup>18</sup>O]Thiophosphonopyruvate



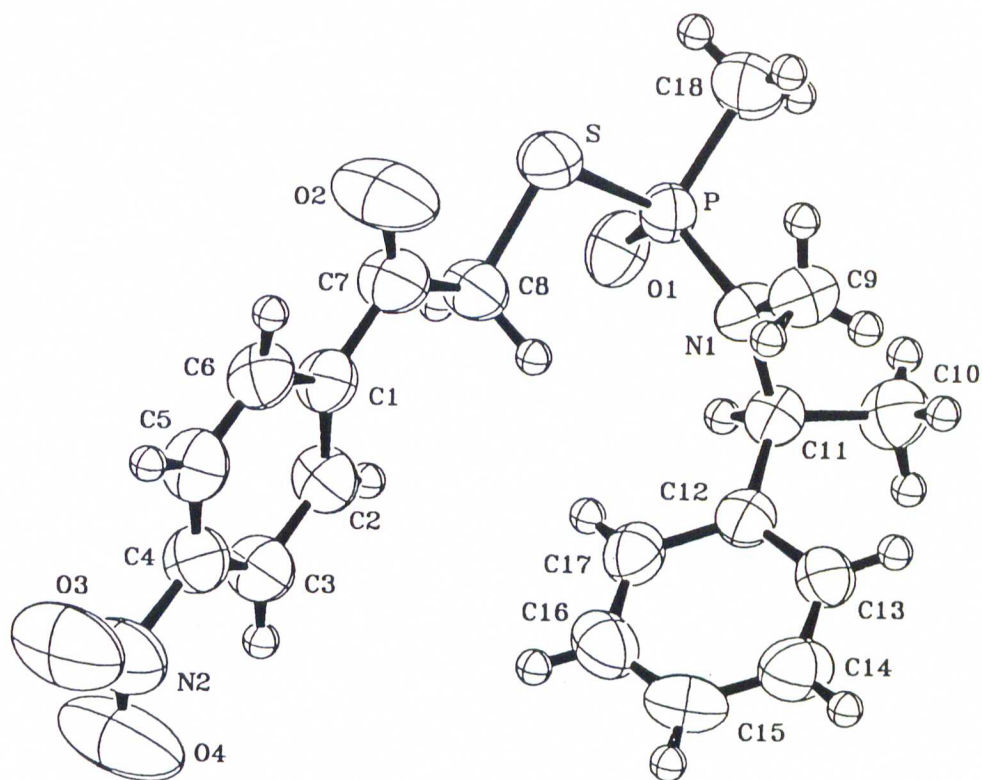


**Figure 5.** X-Ray Structure of the Crystalline Derivative of **40** Derived from the Methylphosphonamidate **22a**.

Conversion of the ( $S_P, S_C$ ) and ( $R_P, S_C$ ) diastereomers (**22a** and **22b**) of N,P-Dimethyl-N-(1-phenylethyl)-O-[2-(trimethylsilyl)ethyl] phosphonamidothioate to the respective ( $R_P$ ) and ( $S_P$ ) enantiomers (**31a** and **31b**) of  $[P=^{18}O]$ thiophosphonopyruvate was accomplished by

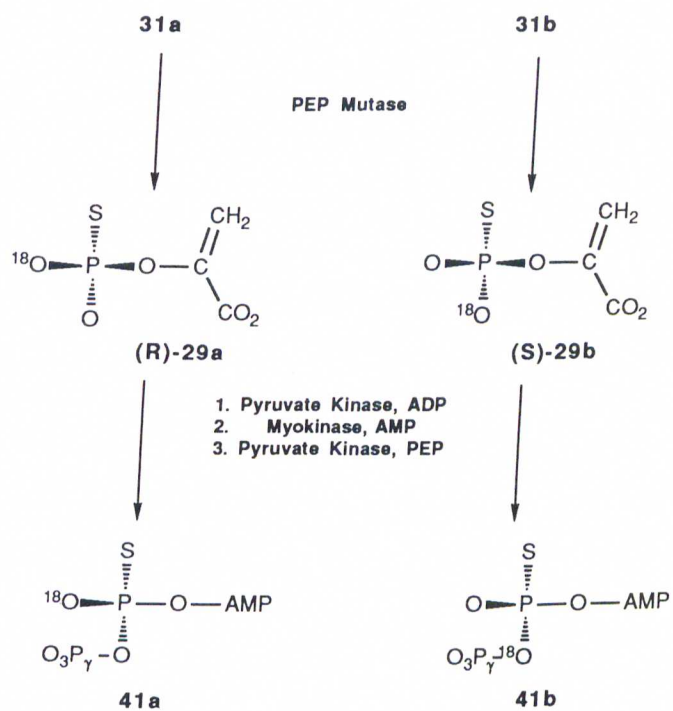
coupling the individual lithium cuprate derived from **22a** and **22b** with the trimethylsilylethyl half ester of oxalyl chloride to introduce the pyruvyl moiety in **23a** and **23b**. This step was followed by deprotection to both of the silylethyl ester functionalities using two equivalents of cesium fluoride with 18 crown 6 serving as a phase transfer catalyst, to form **24a** and **24b**, respectively. The final step was removal of the amine substituent of **24a** or **24b** in acidic  $H_2^{18}O$ . This final step, leading to **31a** and **31b** proceeds with retention of the phosphorus configuration. Evidence supporting this assessment is outlined later in this report.

### b. Stereochemical Analysis

The (Rp) and (Sp) enantiomers (**31a** and **31b**) of chiral  $[P=^{18}O]$ thiophosphonopyruvate were reacted separately with PEP mutase giving the individual antipodes of chiral  $[P=^{18}O]$ thiophosphoenolpyruvate for which the absolute configurations at phosphorus were not known. The method used to determine the absolute configurations of these products (Scheme 33) is modeled after that reported by Frey and coworkers.<sup>104</sup> The chiral  $[^{18}O]$ thiophosphoryl moiety in each was transferred to ADP (with inversion of configuration) by the catalytic action of pyruvate kinase and then from the resulting  $ATP\gamma S$  to AMP (with inversion of configuration) by myokinase catalysis. The  $ADP\beta S$  samples generated in this fashion were reacted with PEP in the presence of pyruvate kinase in order to effect phosphorylation of the pro-S oxygen atom of the  $\beta$ -P group.<sup>105</sup>  $^{31}P$  NMR analysis was then performed on the resulting (Sp)- $ATP\beta S$  samples in order to determine whether the  $^{18}O$  at  $\beta$ -P was located in the bridge or nonbridge position. The molar equivalent of the (Sp)- $[^{16}O_3-P]ATP\beta S$

present in the sample served as a chemical shift standard thus allowing determination of the magnitude of the  $^{18}\text{O}$  induced chemical shift of the  $\beta$ -P resonance. The 0.037 ppm isotopic shift observed (Figure 6) for the (Sp)-[ $^{18}\text{O}$ -P]ATP $\beta$ S (**41a**) sample produced from the [P= $^{18}\text{O}$ ]thiophosphoenolpyruvate enantiomer **29a** derived from (Rp)-[P= $^{18}\text{O}$ ]thiophosphonopyruvate **31a** demonstrates that the  $^{18}\text{O}$  is located in a nonbridge position. Thus, [P= $^{18}\text{O}$ ]thiophosphoenolpyruvate **29a** generated in this way has the Rp configuration. The 0.021 ppm isotopic shift observed for the (Sp)-[ $^{18}\text{O}$ -P]ATP $\beta$ S sample (**41b**, Figure 7) produced from the [P= $^{18}\text{O}$ ]thiophosphoenolpyruvate enantiomer **29b** derived from (Sp)-[P= $^{18}\text{O}$ ]thiophosphonopyruvate **41b** demonstrates that the  $^{18}\text{O}$  is located in the bridge position and, that this [P= $^{18}\text{O}$ ]thiophosphoenolpyruvate precursor **29b** has the Sp configuration. In summary, PEP phosphomutase catalyzes the conversion of (Rp)-[P= $^{18}\text{O}$ ]thiophosphonopyruvate to (Rp)-[P= $^{18}\text{O}$ ]thiophosphoenolpyruvate and of (Sp)-[P= $^{18}\text{O}$ ]thiophosphonopyruvate to (Sp)-[P= $^{18}\text{O}$ ]thiophosphoenolpyruvate (Scheme 33). Thus, we conclude that the PEP phosphomutase reaction proceeds with retention of configuration at phosphorus.

**Scheme 33.** Stereochemical Analysis of the Thiophosphonopyruvate to Thiophosphoenolpyruvate Reaction Catalyzed by PEP Mutase.



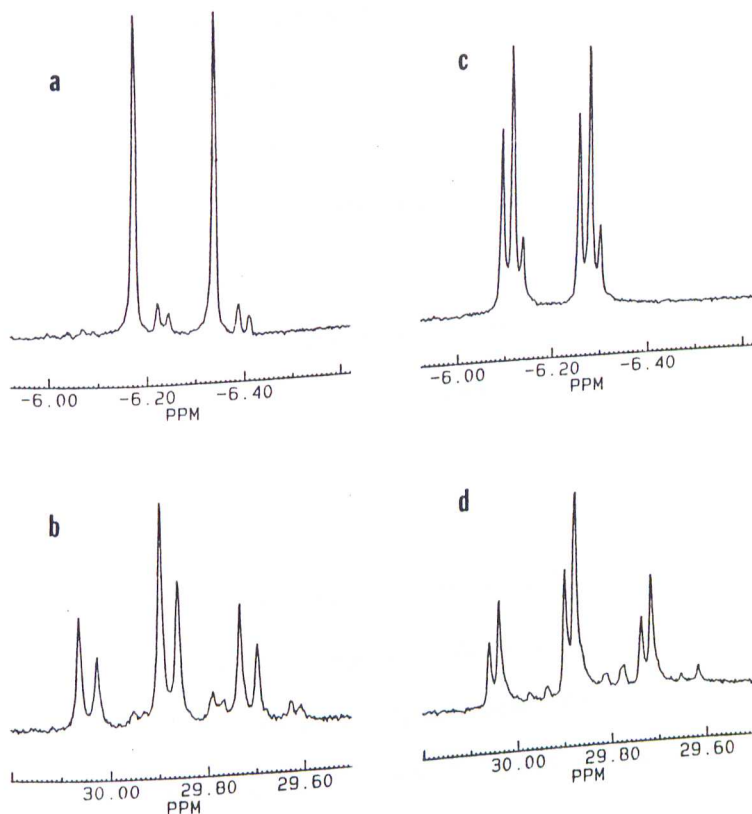


**Figure 6.** The  $\gamma$ -P region(a) and  $\beta$ -P region (b) of the  $^{31}\text{P}$  NMR spectra of a mixture of (SP)-(all- $^{16}\text{O}$ )ATP $\beta$ S and (SP)-[P( $\beta$ )= $^{18}\text{O}$ ]ATP $\beta$ S (**41a**) isotopomers derived from (RP)-[P= $^{18}\text{O}$ ]thiophosphoenolpyruvate enantiomer **29a** formed *via* PEP phosphomutase reaction of the (RP)-thiophosphonopyruvate enantiomer **31a**; the  $\gamma$ -P region(c) and  $\beta$ -P region (d) of the  $^{31}\text{P}$  NMR spectra of a mixture of (SP)-[ $^{16}\text{O}_3$ -P]ATP $\beta$ S and (SP)-[P( $\beta$ )= $^{18}\text{O}$ ]ATP $\beta$ S (**41b**) isotopomers derived from (SP)-[P= $^{18}\text{O}$ ]thiophosphoenolpyruvate enantiomer **29b** formed *via* PEP phosphomutase reaction of the (SP)-thiophosphonopyruvate enantiomer **31b**.

#### **4. Direct Evidence for Carboxyl-Assisted P-N Bond Hydrolysis with Retention of Phosphorus Stereochemistry.**

The stereochemical assignments of the  $[P=^{18}O]$ thiophosphonopyruvate enantiomers **31a** and **31b** (Scheme 32) are based on two considerations: (1) the phosphorus stereochemistry of the (Sp,Sc)- and (Rp,Sc)-3[[methyl(1-phenylethyl)amino]phosphinothioyl]-2-oxo-2-propanoate diastereomers **24a** and **24b** derived from the X-ray crystallographic determination of the phosphorus stereochemistry in the *p*-nitrophenacyl derivative **40** of the (Sp,Sc)-N,P-dimethyl-N-(1-phenylethyl)-O-[2-(trimethylsilyl)ethyl]phosphonamidothioate diastereomer **22a**, and (2) the assumption that acid catalyzed hydrolyses of the diastereoisomers of the 3[[methyl(1-phenylethyl)amino]phosphinothioyl]-2-oxo-2-propanoate diastereomers **24a** and **24b** in  $H_2^{18}O$  take place with retention of the phosphorus configuration. Below, we provide evidence to support the proposal that hydrolyses of the thiophosphonamidate diastereomers do in fact follow this stereochemical course.

##### **a. Kinetic Evidence for Carboxyl-Assisted P-N Bond Hydrolysis**

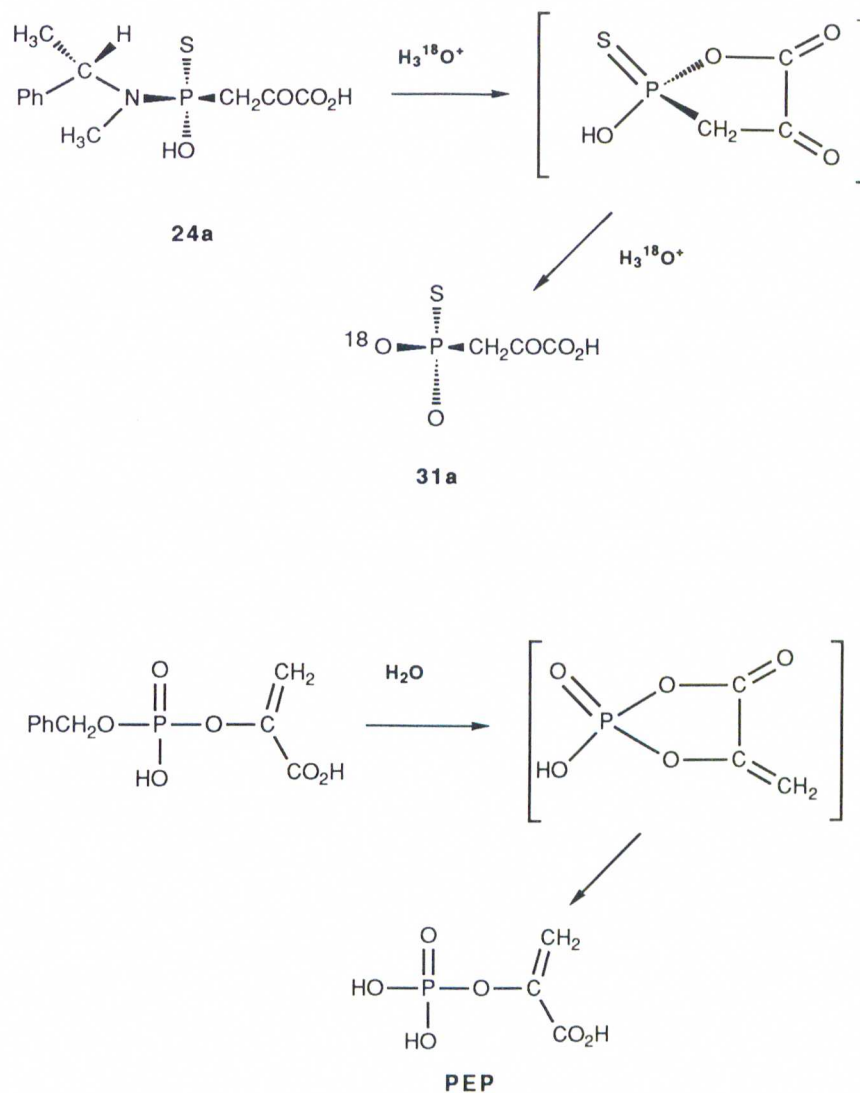
Acid catalyzed hydrolyses of phosphoroamidates and phosphonamidates have been previously reported<sup>106,107</sup> to occur with net inversion of phosphorus stereochemistry. Our original,<sup>108</sup> and since revised,<sup>109</sup> assumption was that hydrolyses of the diastereoisomers **24a** and **24b** would follow this same stereochemical course. Two features of the thiophosphonamidate hydrolysis reactions however, suggested to us

that these 3-[[methyl(1-phenylethyl)amino]phosphinothioyl]-2-oxo-2-propanoate diastereomers were not behaving as "typical" thiophosphonamidates. For example, while the hydrolysis of the diastereoisomers of the close structural analog, N-(1-phenyleth-1-yl)-[ $^{17}\text{O}$ ,  $^{18}\text{O}$ -P]-1-ethoxylvinylthiophosphonamidate, studied earlier in our laboratory<sup>44</sup> required 3.5 h at 25 °C in 1.0 M *p*-TsOH/THF- $\text{H}_2^{16}\text{O}$  for completion, hydrolyses of the related diastereomers of **24a** and **24b** were complete within 10 sec under much less vigorous conditions (2 equivalents of HCl in  $\text{H}_2^{18}\text{O}$ , 25° C). In addition, we<sup>44</sup> have observed that hydrolysis of each of the diastereoisomers of N-(1-phenyleth-1-yl)-[ $^{17}\text{O}$ ,  $^{18}\text{O}$ -P]-1-ethoxylvinylthiophosphonamidate consistently gave *ca.* 60% inversion of configuration at phosphorus and *ca.* 40% racemization. In contrast, **24a** and **24b** were each found to undergo acid catalyzed hydrolysis in  $\text{H}_2^{18}\text{O}$  to produce single [P= $^{18}\text{O}$ ]thiophosphonopyruvate enantiomers. This was demonstrated by the formation in each case of a single (Sp)-[P( $\beta$ )= $^{18}\text{O}$ ]ATP $\beta$ S product (Figure 7) *via* the reaction sequence displayed in Scheme 35.

Both the larger than expected hydrolysis rates for **24a** and **24b** and the atypically "clean" stereochemistry indicated that neighboring group assistance by the carboxyl substituent was likely occurring in these reactions (Scheme 34). In fact, precedence for carboxyl group participation in hydrolysis reactions of this type can be found in the work of Schray and Benkovic.<sup>110</sup> These investigators have demonstrated that hydrolysis of the O-benzyl phosphate ester of phosphoenolpyruvate is assisted through initial intramolecular displacement of the alcohol leaving group by the

internal carboxyl moiety (Scheme 36) followed by ring opening of the resulting phospholactone.

**Scheme 34.** Carboxylate Participation in Thiophosphonamidate and O-Benzyl Phosphate Ester Hydrolysis



The occurrence of carboxyl group participation in amine displacement in the aqueous acid reactions of the 3[[methyl(1-phenylethyl)amino]phosphinothioyl]-2-oxo-2-propanoates (**24**) could in principle be demonstrated by comparing the stereochemical course of hydrolyses of carboxylate ester derivatives of **24a** and **24b**. The presence of carboxylate ester functionality in these substances would prevent neighboring group participation and, thus, allow for direct displacement of the protonated amine by water with inversion rather than retention of configuration at the phosphorus. A plan designed for this purpose would include preparation of an appropriate carboxylate ester derivative of the 3-[[methyl(1-phenethyl)amino]phosphinothioyl]-2-oxo-2-propanoates, removal of the amine functionality by hydrolysis in  $\text{H}_3^{18}\text{O}^+$ , and deesterification of the carboxyl group. Although conceptually simple, execution of this sequence turned out to be complicated by some of the unique chemical properties of thiophosphonates. However, the result obtained from studies of "blocked carboxyl" systems, while intricate, do demonstrate unambiguously the role of *carboxyl group assistance* in governing the stereochemical course of the hydrolyses of 3-[[methyl(1-phenethyl)amino]phosphinothioyl]-2-oxo-2-propanoates and support the conclusion that these processes proceed with *retention of configuration at phosphorus*.

## b. Stereochemical Evidence for Carboxyl-Assisted P-N Bond Hydrolysis

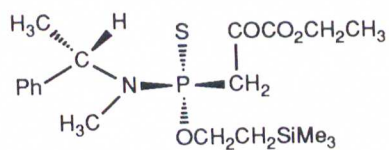
At the outset, it appeared that the most expedient way to introduce the  $^{18}\text{O}$ -label by  $\text{H}_2^{18}\text{O}$  displacement of the amine functionality in the 3-[[methyl(1-phenethyl)amino]phosphinothioyl]-2-oxo-2-propanoates without the assistance by the carboxyl group would be to subject the bis-trimethylsilylethyl esters **23a** and **23b** (Scheme 32) to mild acid hydrolysis in  $\text{H}_2^{18}\text{O}$  and then to remove both the carboxylate and phosphonate silylethyl ester groups. However, this approach was not feasible owing to the fact that the product of the hydrolysis reaction, [[2-(trimethylsilyl)ethoxy]phosphinothioyl]-2-oxo-2-(trimethylsilyl)ethyl propanoate, does not undergo desilylethylation at the thiophosphonate center when treated under the standard deblocking conditions (*eg.* CsF).<sup>111</sup> Likewise, classical ester C-O bond cleaving reagents like TMSBr and TMSI, which work well with phosphonate monoesters,<sup>111</sup> fail to deesterify thiophosphonate monoesters. The results clearly point out the necessity for 2-trimethylsilylethyl deprotection of the thiophosphonamidate prior to hydrolytic displacement of the amine moiety. To accomplish this, selective thiophosphonamidate monodesilylethylation of **23a** by treatment with CsF was attempted. Indeed, the monoester **42a** (Scheme 35) could be prepared in this way (contaminated with starting material and phosphinothioyl-2-oxo-2-[(trimethylsilyl)ethyl] propanoate (**43a**) by treating **23a** with one equivalent of CsF.



Hydrolysis of **42a** under mild conditions (*viz* 1.2 equivalents of *p*-TsOH, 25°C, 20 min) led to the replacement of the amine substituent with OH as desired but also resulted in the hydrolysis of the (2-trimethylsilyl)ethyl carboxyester substituent. Given the mild reaction conditions employed, this secondary hydrolysis reaction was unexpected. Because the relative timing of the two hydrolysis events was unknown, the issue of carboxyl group participation in the hydrolysis at phosphorus remained. To resolve this problem we took steps to identify the cause of the abnormally rapid deesterification in **42a** and to subsequently eliminate it.

Consideration of alternatives to the classical addition-elimination mechanism for ester hydrolysis led us to consider solvolysis of **42a** by nucleophilic attack at silicon. Consequently, the non-silyl analog, 3-[[methyl(1-phenylethyl)amino][2-trimethylsilyl)ethoxy]phosphinothioyl]-2-oxo-ethyl propanoate (**44a**) was prepared and then subjected to the same hydrolysis conditions used for **42a**. The hydrolysis of **44a** took place with the same efficiency as that of **42a** ruling out the suspected reaction pathway. By the process of elimination, ester hydrolysis by neighboring group (*viz.* thiophosphono moiety) assistance was adopted as a working model for the deesterification reaction of **42a**. As illustrated in Scheme 36, the participation of the thiophosphono moiety in the deesterification of the carboxy ester group in **42a** could occur before the hydrolytic displacement of the N-methyl-N-(phenethyl)amine from the phosphorus (pathway I) or, preferably, after it (pathway II). We reasoned that if deesterification occurred first, **42a** would be converted to **24a** and hence (in H<sub>2</sub><sup>18</sup>O) to the same [P=<sup>18</sup>O]thiophosphonopyruvate enantiomer (**31a**) generated by

the hydrolysis of **24a** (Scheme 32). On the other hand, if hydrolysis at phosphorus in **42a** preceded deesterification, the stereochemistry at phosphorus would be inverted and the  $[P=^{18}O]$ thiophosphonate enantiomer (**31b**) having the opposite configuration would be generated.<sup>4</sup>



**44a**



To distinguish between the two pathways of Scheme 36, the configuration at phosphorus in the  $[P=^{18}O]$ thiophosphonate product obtained from the hydrolysis of **42a** in acidic  $H_2^{18}O$  was determined (relative to the  $[P=^{18}O]$ thiophosphonate product from **24a**) by using PEP phosphomutase to convert the  $[P=^{18}O]$ thiophosphonopyruvate to  $[P=^{18}O]$ thiophosphoenolpyruvate and the combined actions of pyruvate kinase and myokinase (Scheme 33) to convert the  $[P=^{18}O]$ thiophosphoenolpyruvate to  $^{18}O$ -labelled ATP $\beta$ S for analysis. Figure 7 shows that the  $[P=^{18}O]$ thiophosphonopyruvate generated from **42a** consisted of a 87:13 mixture of the enantiomers **31a** and **31b**, respectively. For comparison, the hydrolysis of **24a** had produced only enantiomer **31a**. These results were interpreted to mean that both of the reaction pathways shown in Scheme 36 were operative in the hydrolysis of **42a** and that the pathway leading to **31a** by deesterification followed by aminolysis was the more efficient of the two pathways.

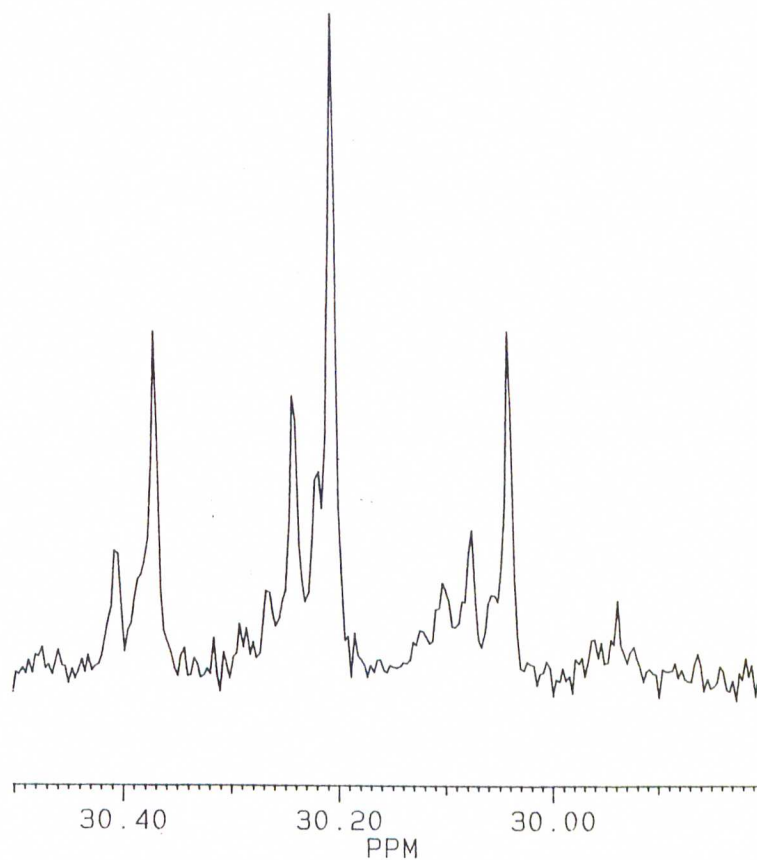
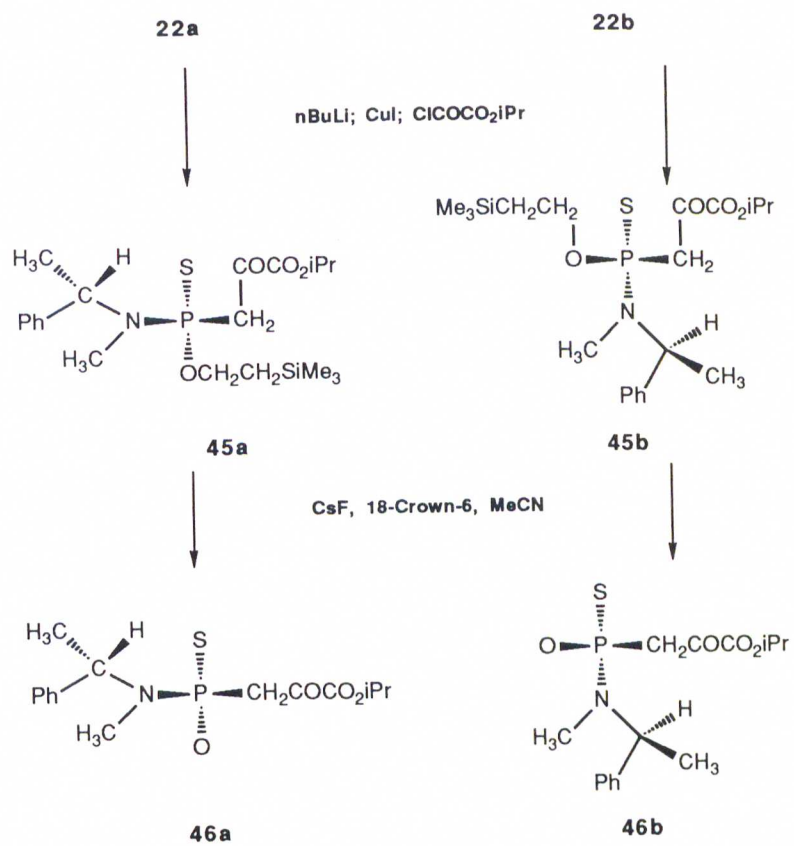


**Figure 7.** The  $\beta$ -P region of the  $^{31}\text{P}$  NMR spectra of a mixture of (S<sub>P</sub>)-(all- $^{16}\text{O}$ )ATP $\beta$ S and (S<sub>P</sub>)-[P( $\beta$ )= $^{18}\text{O}$ ]ATP $\beta$ S (**41a** and **41b**) isotopomers derived from (S<sub>P</sub>)- and (R<sub>P</sub>)-[P= $^{18}\text{O}$ ]thiophosphoenolpyruvate enantiomers **29a** and **29b** formed *via* PEP mutase reaction of a mixture of (S<sub>P</sub>)-and (R<sub>P</sub>)-thiophosphonopyruvate enantiomers **31a** and **31b**. produced from the hydrolysis of **42a**.

Given this finding and our original goal which was to demonstrate that hydrolysis of **24a** and **24b** in acidic H<sub>2</sub><sup>18</sup>O proceeds with carboxyl group assistance (and hence with retention of configuration), the focus of the final phase of this work became the design and synthesis of carboxyester derivatives of **24a** and **24b** which would hydrolyze to [P=<sup>18</sup>O]thiophosphonate enantiomers **31b** and **31a**, respectively by following pathway II of Scheme 36 and avoiding pathway I. The approach taken to reduce the rate of thiophosphonamidate assisted carboxylate ester cleavage relative to amine hydrolysis was to increase the steric bulk of the alkyl group at the carboxyl center by using an isopropyl protecting group in place of the 2-trimethylsilylethyl protecting group. The isopropyl derivatives **46a** and **46b** were thus prepared (Scheme 37) and independently subjected to hydrolysis in acidified H<sub>2</sub><sup>18</sup>O. This led to removal of both N-methyl-N-phenylethylamine and isopropanol. Stereochemical analysis by the procedure described above revealed that near equal amounts of [P=<sup>18</sup>O]thiophosphonate enantiomers **31a** and **31b** had formed in reaction of the individual isopropyl ester diastereomers, **46a** and **46b**. Specifically, the thiophosphonamidate **46a** having the (Sp) configuration at phosphorus gave rise to 55% of the same (Rp)-[P=<sup>18</sup>O]thiophosphonate enantiomer (**31a**) which is formed exclusively by hydrolysis of the the "unblocked" (Sp,Sc)-3-[[methyl(phenylethyl)amino]phosphinothioyl]-2-oxo-propanoate (**24a**) and 45% of the enantiomer (**31b**) with the opposite (Sp) configuration. Likewise, hydrolysis of the isopropyl (Rp,Sc)-thiophosphonamidate **46b** produced 57% of (Sp) (**31b**) and 43% (Rp)-

[P=<sup>18</sup>O]thiophosphonopyruvate (**31a**). The <sup>31</sup>P NMR result is shown in Figure 8.

**Scheme 37.** Synthesis of the *iso*-propyl protected carboxyl derivative.



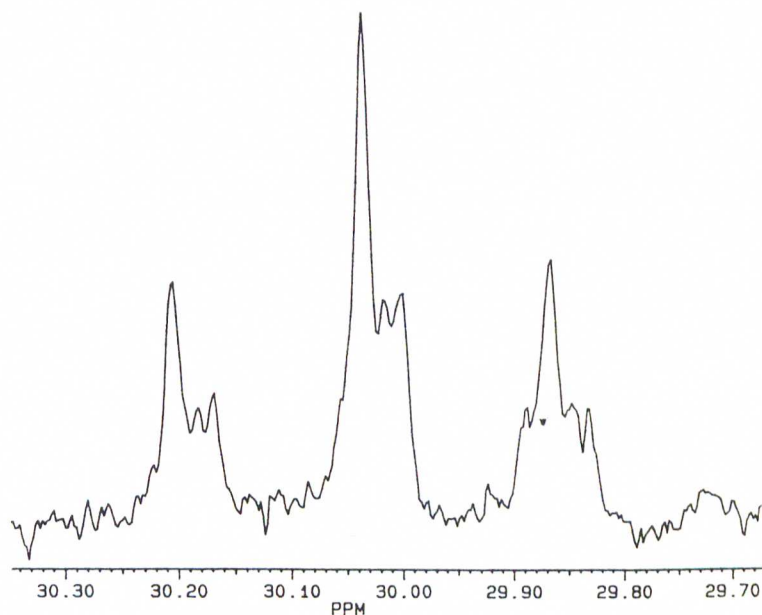


**Figure 8.** The  $\beta$ -P region of the  $^{31}\text{P}$  NMR spectra of a mixture of (SP)- $(\text{all-}^{16}\text{O})\text{ATP}\beta\text{S}$  and (SP)- $[\text{P}(\beta)=^{18}\text{O}]\text{ATP}\beta\text{S}$  (**41a** and **41b**) isotopomers derived from (SP)- and (RP)- $[\text{P}=^{18}\text{O}]\text{thiophosphoenolpyruvate}$  enantiomers **29a** and **29b** formed *via* PEP mutase reaction of a mixture of (SP)- and (RP)-thiophosphonopyruvate enantiomers **31a** and **31b**, produced from the hydrolysis of **46a**.

These results indicate that utilization of the isopropyl ester leads to retardation of the rate of carboxylate deesterification as compared to thiophosphonamidate hydrolysis thus resulting in near equal rates for the two pathways. In an attempt to obtain a more selective stereochemical result, hydrolysis of the *Oc-tert*-butyl derivative was explored. Unfortunately, as a result of the limited solubility of this substance in water, the acid catalyzed hydrolysis required the use of a mixed aqueous-organic solvent system. Under these conditions, dethiophosphonylation of the product, thiophosphonopyruvate, to form thiophosphate occurs rapidly. Thus, our conclusion regarding the neighboring group participation by the carboxyl group in the hydrolytic displacement of the *N*-methyl-*N*-phenylethylamine from the (Sp,Sc)-3-[[methyl(phenylethyl)amino]phosphinothioyl]-2-oxo-propanoate (**24a**) rests upon the stereochemical trends observed in the enantiomeric compositions of the [P=<sup>18</sup>O]thiophosphonopyruvate products generated by hydrolysis of single diastereomers of (Sp,Sc)-and (Rp,Sc)3-[[methyl(phenylethyl)amino]phosphinothioyl]-2-oxo-propanoate (**24a** and **24b**), and its *Oc*-2-trimethylsilylethyl (**42a**) and *Oc*-isopropyl analogs (**45a** and **45b**). The combined results suggest that the configuration at phosphorus is retained in hydrolysis of the (Sp,Sc)-and (Rp,Sc)3-[[methyl(phenylethyl)amino]phosphinothioyl]-2-oxo-propanoate diastereoisomers **24a** and **24b** as a result of the carboxyl group assistance depicted in Scheme 34. Furthermore, esterification of the assisting carboxyl group does not fully reverse this stereochemical outcome because hydrolysis of the carboxyl ester is competitive with displacement of the amine function (Scheme 36). However, the relatively

high level (*ca.* 50%) of inversion of phosphorus configuration observed for reaction of the isopropyl ester nicely correlates with an expected decrease in the rate of deesterification of this substance.

We conclude that the stereochemistry of the hydrolysis of the key [P =  $^{18}\text{O}$ ]thiophosphonate precursor, -3-[[methyl(phenylethyl)amino]phosphinothioyl]-2-oxo-propanoate (**24**) in acidic  $\text{H}_2^{18}\text{O}$ , proceeds with retention of configuration and, therefore, that the PEP phosphomutase catalyzed rearrangement of this substance to [P =  $^{18}\text{O}$ ]thiophosphoenolpyruvate also proceeds with retention of configuration. These conclusions are consistent with those recently made by Knowles and his coworkers in their follow-up<sup>91,112</sup> to our original communication<sup>108</sup> on the stereochemistry of the PEP phosphomutase reaction.

The observed intramolecular nature and retention of phosphorus stereochemistry for the PEP phosphomutase catalyzed rearrangement of phosphonopyruvate to phosphoenolpyruvate has important mechanistic implications. Clearly, the two intermolecular pathways in which reaction occurs between either pyruvate and phosphonopyruvate or two molecules of phosphonopyruvate can be eliminated from consideration on the basis of  $^{18}\text{O}$ -labelling results (Figure 4) which show that phosphoryl group transfer occurs between carbon and oxygen of the same substrate molecule. Also, our stereochemical findings preclude the operation of a concerted, pericyclic mechanism since inversion of the phosphorus configuration is predicted for this process on the basis of orbital topology control. This leaves the four nonconcerted mechanisms (B through E in Scheme 27) as being possible for the PEP phosphomutase reaction.

Finally, the similar reactivity of the oxo- and thio-substituted substrates suggests that, independent of mechanism, nucleophilic attack at the phosphorus is not involved in the rate limiting step for this rearrangement reaction.<sup>113</sup>

### C. The Search for the Intermediate in the $\text{PEP} \rightleftharpoons \text{P-pyr}$

#### Rearrangement.

Since the stereochemical course of the PEP mutase reaction involves retention of the phosphorus configuration a stepwise mechanism is operative. The stepwise mechanism can be identified by its intermediate. The intermediates in the four stepwise mechanisms are shown in Scheme 28. We sought to determine which stepwise mechanism was operative by attempting to trap an intermediate by performing rapid-quench experiments with radiolabeled phosphonopyruvate.

The most likely intermediate most susceptible to trapping is the pyruvate which is formed in the phosphorylated-enzyme mechanism (Pathway E in Scheme 28). The enolate of pyruvate is formed in the dissociative mechanism but is expected to be too short lived to be trapped.  $[^3\text{H}]\text{P-pyr}$  was used as a radiolabeled probe to monitor the disappearance of P-pyr, the transient formation of pyruvate and PEP formation in single turnover reactions. The turnover number for PEP mutase is  $30 \text{ s}^{-1}$ , and hence a single turnover in the active site should require 33 msec if product release is not rate limiting. In theory we should be able to see an intermediate using the KinTek rapid quench instrument since it can produce reaction times as short as 5 msec. Radiolabeled PEP would appear to be a more obvious choice as a probe since it is commercially available. However the equilibrium of  $\text{PEP} \rightleftharpoons \text{P-pyr}$  is  $> 500:1$ . Although the  $K_m$  of PEP is not known, we anticipated that it would be difficult to accumulate enzyme-bound species in the thermodynamically unfavored  $\text{PEP} \Rightarrow \text{P-pyr}$  direction.

An idealized time course for the reaction of P-pyr to PEP via a single intermediate is shown in Figure 9.

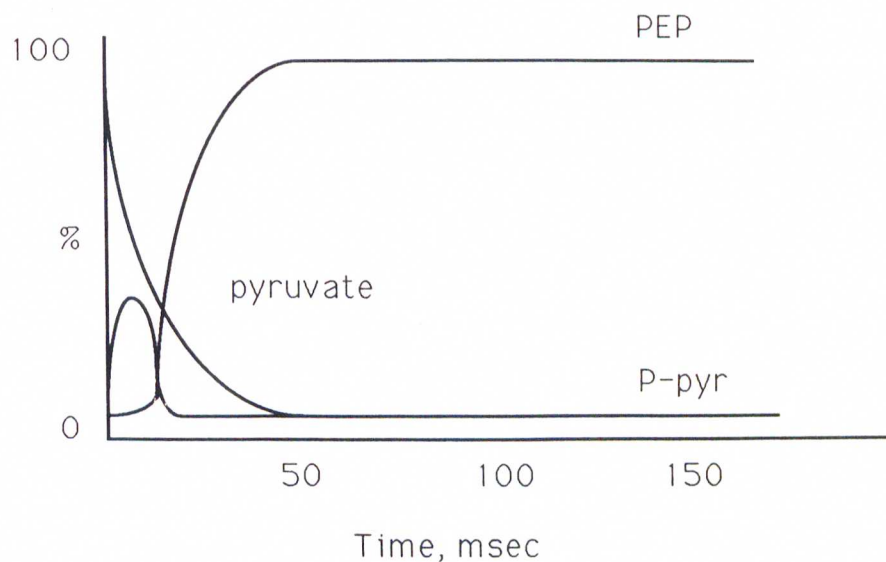


**Figure 9.** Idealized hypothetical time course of the PEP mutase reaction with [ $^3\text{H}$ ]P-pyr under single turnover conditions.

Our ability to trap the intermediate in rapid quench experiments would depend on its lifetime. As can be seen in Figure 10 the intermediate can be trapped only if the rate of breakdown of the intermediate,  $k_5$  is slow with respect to its rate of formation,  $k_3$ . The following pages describe the rapid quench experiments we performed to test the intermediacy of pyruvate in the PEP mutase reaction.

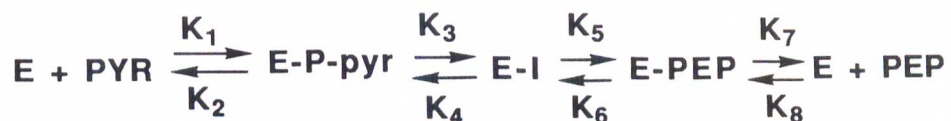


**Figure 10.** Kinetic equation of the PEP mutase-catalyzed rearrangement of P-pyr

### 1. Rapid Quench Experiments with PEP Mutase Reaction

The experimental design is illustrated in Figure 11. Forty-three microliters of 10  $\mu\text{M}$  [ $^3\text{H}$ ]P-pyr and 43  $\mu\text{L}$  of 100  $\mu\text{M}$  PEP mutase were mixed in a rapid quench apparatus and quenched with 164  $\mu\text{L}$  of 20 mM HEPES adjusted to pH 1.6 with HCl, at varying conversions (5 to 1000 ms). The reaction products, [ $^3\text{H}$ ]P-pyr and [ $^3\text{H}$ ]pyruvate were reduced with NaCNBH<sub>3</sub> in order to prevent the loss of the tritium by solvent exchange. After 15 min the pH of reaction solution was adjusted to 7. The reaction mixture was subjected to chromatographic separation by using an HPLC equipped with an anion exchange column. A mixture of 0.1 M KH<sub>2</sub>PO<sub>4</sub> and 0.4 M KCl (pH 2.75) was used as eluent.  $^3\text{H}_2\text{O}$  and [ $^3\text{H}$ ]lactate eluted at the solvent front and [ $^3\text{H}$ ]P-lactate at 4 min and [ $^3\text{H}$ ]PEP at 12 min. A separate chromatography using a mixture of 3 mM KH<sub>2</sub>PO<sub>4</sub> and 10 mM KCl (pH 5.5) as eluent was employed to resolve [ $^3\text{H}$ ]lactate (10 min) from  $^3\text{H}_2\text{O}$  (solvent front)

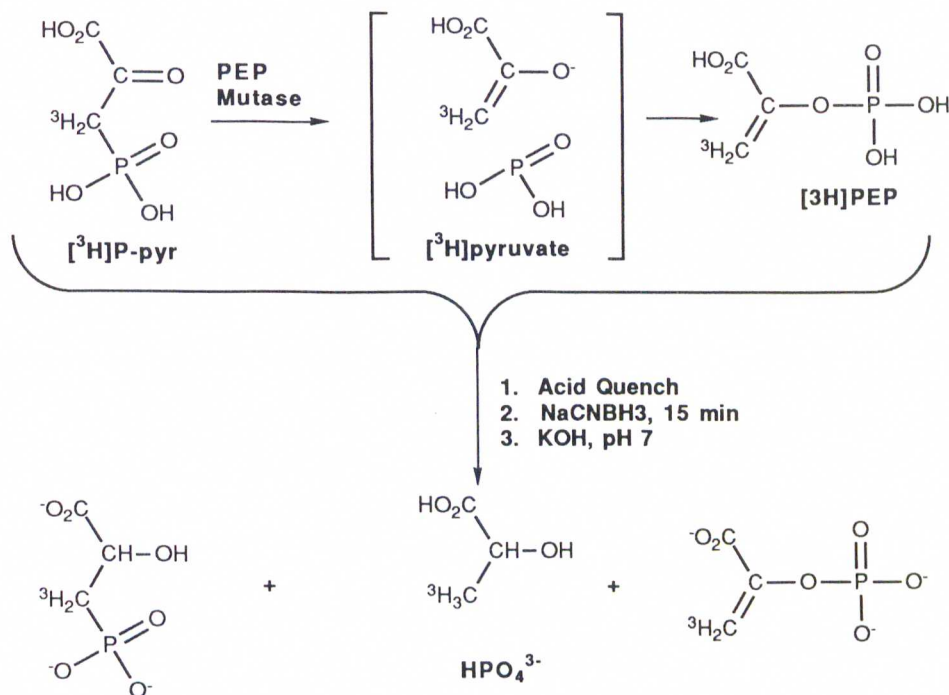


**Figure 11.** Flowchart of the rapid quench experiments.

Control studies were carried out to test the efficiency of NaCNBH<sub>3</sub> reduction of P-pyr to P-lac, pyruvate to lactate and to determine whether or not lactate is not formed from either P-pyr or PEP under the quench or reduction conditions. Phosphonopyruvate (75 mM) and phosphoenolpyruvate (75 mM) were reacted separately with 75 mM NaCNBH<sub>3</sub> at 25°C for 15 min at pH 2. <sup>31</sup>P NMR analysis indicated P-pyr ( $\delta=10$  ppm) was quantitatively converted to phosphonolactate ( $\delta=19$  ppm)

with no observed phosphate (lactate) formation. The  $^{31}\text{P}$ -NMR analysis of PEP/  $\text{NaCNBH}_3$  reaction indicated the formation of 3% phosphate and hence 3% lactate. The 3% lactate formation was confirmed by  $^1\text{H}$  NMR analysis of the same sample. A reaction containing pyruvate (75 mM) and  $\text{NaCNBH}_3$  (75 mM) quantitatively produced lactate as judged by  $^1\text{H}$  NMR analysis. The quantitative conversions of P-pyr to P-lac, pyruvate to lactate and the minimal formation of lactate from either P-pyr or PEP under these quench and reduction conditions allowed for the use of this methodology in the rapid quench analysis.

#### **a. Synthesis of $^3\text{H}$ P-pyr**

The phosphonopyruvate was labeled with tritium by exchange of the C-2 protons in 110 Ci/mol  $^3\text{H}$ water at 25°C at pH 9 (the pH of a solution of  $\text{Li}_3\text{P-pyr}$ ). After 24 h the  $^3\text{H}$ P-pyr was precipitated with ethanol and dried *in vacuo*, thus producing  $^3\text{H}$ P-pyr with a specific activity of 40 Ci/mol. A 10  $\mu\text{M}$  solution of  $^3\text{H}$ P-pyr in 50 mM  $\text{K}^+$ HEPES (pH 7.5) was prepared immediately before use in the rapid quench experiments.

Because of the tendency of the tritium to exchange from the  $^3\text{H}$ P-pyr to solvent the purity of the synthetic  $^3\text{H}$ P-pyr could not be determined by chromatographic separation of the  $^3\text{H}$ P-pyr. Instead the purity of the  $^3\text{H}$ P-pyr was examined by converting it to  $^3\text{H}$ PEP by reaction with a catalytic amount of PEP mutase and in a separate experiment, by converting it to  $^3\text{H}$ P-lac by reduction with  $\text{NaCNBH}_3$ . Elution profiles obtained from HPLC anion exchange chromatographic analysis of the  $^3\text{H}$ PEP derived from the  $^3\text{H}$ P-pyr is shown in Figure 12 as is the elution profile obtained from the HPLC analysis of  $^3\text{H}$ P-lac derived by reduction

of the  $[^3\text{H}]\text{P-pyr}$ . These results indicate the synthetic  $[^3\text{H}]\text{P-pyr}$  is a mixture of 14%  $^3\text{H}_2\text{O}$ , 8% of an unidentified contaminant, 78%  $[^3\text{H}]\text{P-pyr}$ .

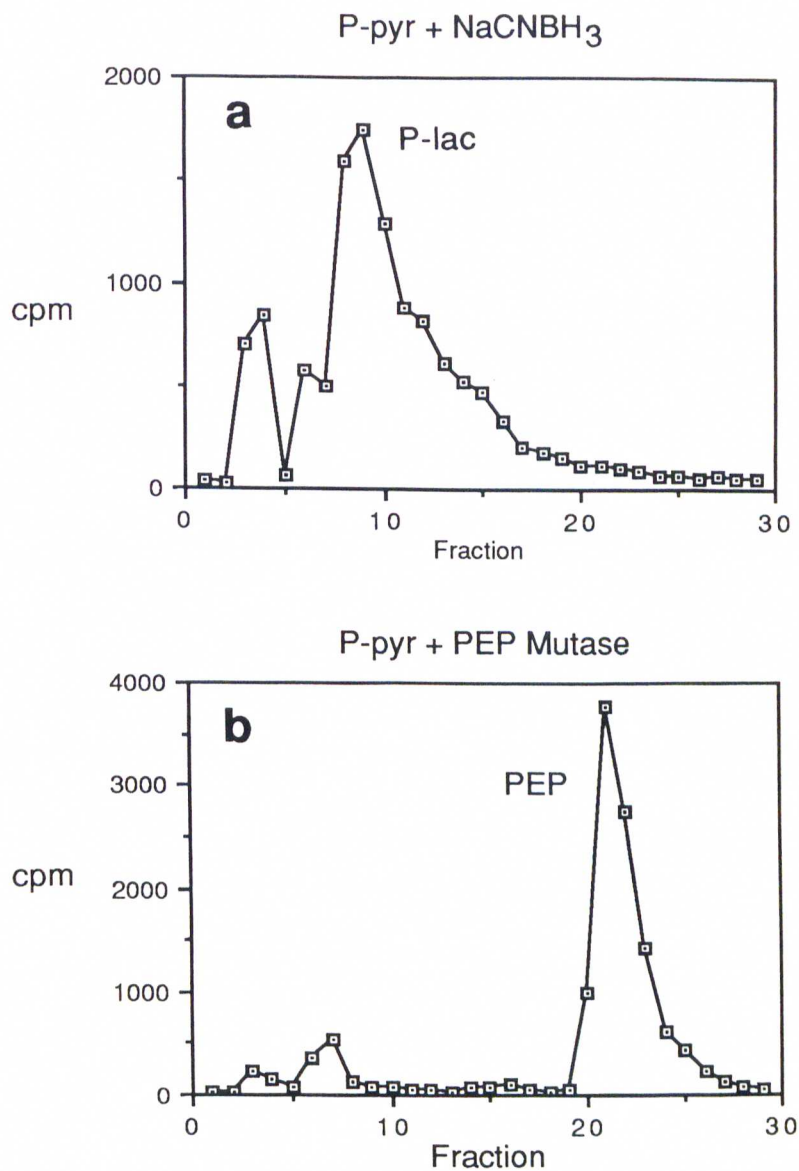


**Figure 12.** HPLC elution profiles of **a**)  $[^3\text{H}]\text{P-lac}$  derived from a reaction of  $[^3\text{H}]\text{P-pyr}$  and **b**)  $[^3\text{H}]\text{PEP}$  derived from a reaction of  $[^3\text{H}]\text{P-pyr}$  with a catalytic amount of PEP mutase

**b. Single Turnover Experiment with [<sup>3</sup>H]P-pyr and Mg<sup>2+</sup>  
Activated PEP Mutase**

An initial experiment was carried to determine whether the rapid quench experiments could accurately measure the formation of PEP, the disappearance of P-pyr and detect a pyruvate intermediate by observing lactate formation. The concentration of each reactant in this initial experiment after mixing was [<sup>3</sup>H]P-pyr (ca. 13 μM), PEP mutase (46 μM) and MgCl<sub>2</sub> (5 mM). The timecourse of the single turnover is shown in figure 13.

The results in figure 13 indicated that we could follow the formation of PEP and the disappearance of P-pyr. Approximately 1% of the P-pyr substrate was converted to lactate which corresponded to only 100 cpm, hence the measurement was very inaccurate. Because the P-pyr concentration was not accurately quantitated the reaction may have been more than one turnover of PEP mutase. The next experiment was performed to tighten up the conditions so as to obtain an accurate measurement of the time required for a single turnover.

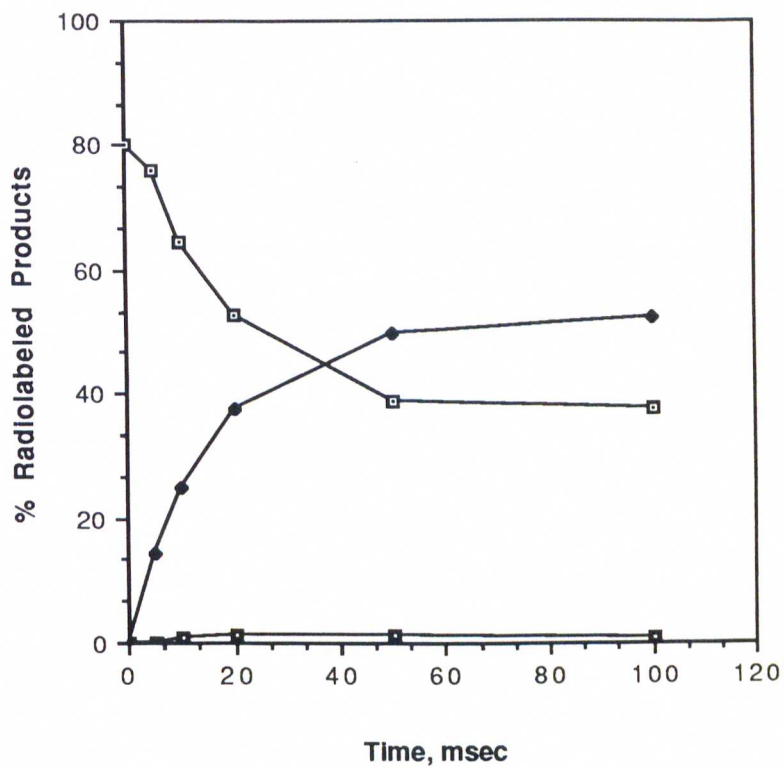


**Figure 13.** Time course for a single turnover of P-pyr in the active site of  $Mg^{2+}$ -activated PEP mutase at 25°C. The reaction contained ca. 13  $\mu M$  [ $^3H$ ]P-pyr, 46  $\mu M$  PEP mutase (subunit Mol. Wt. 39000 Daltons), 5 mM  $MgCl_2$  and 50 mM  $K^+$ HEPES (pH 7.5): ( $\blacklozenge$ ) PEP, ( $\square$ ) P-Lac, ( $\blacksquare$ ) lactate.

The single turnover experiment to determine the time required for a single turnover of PEP mutase was carried out using a buffered solution (43  $\mu$ L) containing 100  $\mu$ M PEP mutase, 10 mM  $MgCl_2$  which was mixed using the rapid quench instrument with a buffered solution (43  $\mu$ l) containing 10  $\mu$ M [ $^3H$ ]P-pyr to give final concentrations after mixing of PEP mutase (40-50  $\mu$ M, Mol. Wt. 39,000),  $MgCl_2$  (5 mM), [ $^3H$ ]P-pyr (5  $\mu$ M). After a specified time (5-200 msec) the solutions was quenched with 164  $\mu$ L of 20mM HEPES adjusted to pH 1.6 with HCl and reacted with  $NaCNBH_3$  (final concentration 4 mM). After 15 min the reaction mixtures were neutralized with 12  $\mu$ L of 1 M KOH. The reaction products were then separated on HPLC. The results from this experiment are shown in Figure 14. The single turnover was complete in about 20 msec. There was no evidence of a lag in the formation of PEP. No attempt was made to detect lactate.

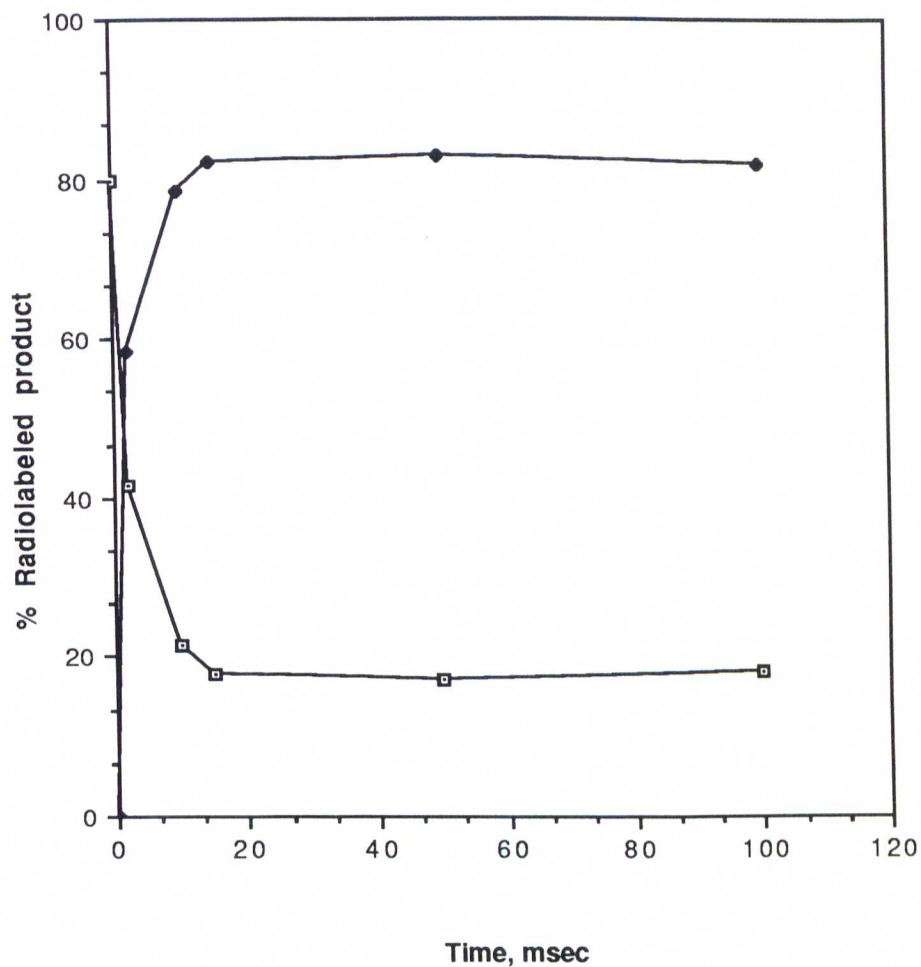


**Figure 14.** Time course for a single turnover of P-pyr in the active site of  $Mg^{2+}$ -activated PEP mutase at 25°C. The reaction contained 5  $\mu M$  [ $^3H$ ]P-pyr, 50  $\mu M$  PEP mutase (subunit Mol. Wt. 39000 Daltons), 5 mM  $MgCl_2$  and 50 mM  $K^+$ HEPES (pH 7.5): (●) PEP, (□) P-Lac.

These results indicated that the rate of turnover at 25°C is too fast to observe formation and reaction of a intermediate along the reaction pathway. Therefore, we attempted to change the reaction conditions (pH, metal cofactor, temperature) so that the turnover rate might be slow enough to evaluate intermediate formation during the initial phases of the reaction. From  $V_m$  pH profile, which is flat in the pH 6-9 range, we suspected that adjusting the reaction pH would have little impact on the turnover rate. The metal cofactor was found to have a small influence the rate of catalysis.<sup>4</sup> The  $V_m$  of the PEP mutase reaction with other divalent metals replacing magnesium were  $\text{Co}^{2+}$  (0.5),  $\text{Zn}^{2+}$ (0.4), and  $\text{Mn}^{2+}$ (0.3), relative to the  $V_m$  for  $\text{Mg}^{2+}$ . Although the reduction in  $V_m$  for these metals are somewhat small, the effect may be masked by a rate limiting product release step. The results in figure 14 indicate that product release may indeed be rate limiting, since the single turnover reaction was complete in 15 msec which was less than the 33 msec predicted, based upon the turnover number of  $30 \text{ s}^{-1}$  obtained from initial velocity studies. In the hope that the reduced of  $V_m$  with these metals could result in the observation of an intermediate in a single turnover, we pursued a rapid quench experiment in which the magnesium cofactor was replaced with manganese. We chose to use manganese since it produced the largest reduction in  $V_m$ .

## **2. Single Turnover Experiment with [<sup>3</sup>H]P-pyr and $\text{Mn}^{2+}$ -Activated PEP Mutase**

PEP mutase (0.3mg/mL, 20 mL) was dialyzed against 50 mM  $\text{K}^+$ HEPES(pH 7.5) containing 1mM EDTA. The enzyme was then

reconstituted with 5 mM manganese chloride and concentrated to 50  $\mu$ M. The time course of a single turnover of the  $Mn^{2+}$ -activated PEP mutase is shown in Figure 15. Equilibration of PEP and P-pyr in the active site took only 40 to 50 ms. Pyruvate was formed in about a 17% yield. This large amount of pyruvate may be due to either an  $Mn^{2+}$ -catalyzed solution hydrolysis of [ $^3H$ ]P-pyr or by a manganese-induced enhancement of a dephosphorylase side reaction catalyzed by PEP mutase. The time course showed that pyruvate formation did not precede PEP formation, therefore these data do not implicate pyruvate as an intermediate.

The rate of transformation of P-pyr could not be followed in this time course. The P-pyr precipitated during the quench and could be found associated with the enzyme pellet. Presumably the unreacted P-pyr formed a complex with the manganese cofactor at low pH which was not soluble. This complication and the large amounts of pyruvate formed in this  $Mn^{2+}$ -activated PEP mutase reaction discouraged us from further pursuing the use of manganese under other condition, such as altered pH or at a lower temperature. Thus having failed to significantly slow the PEP mutase reaction and trap pyruvate by using the manganese cofactor we opted to try reducing the temperature of the  $Mg^{2+}$ -activated PEP mutase single turnover reaction.

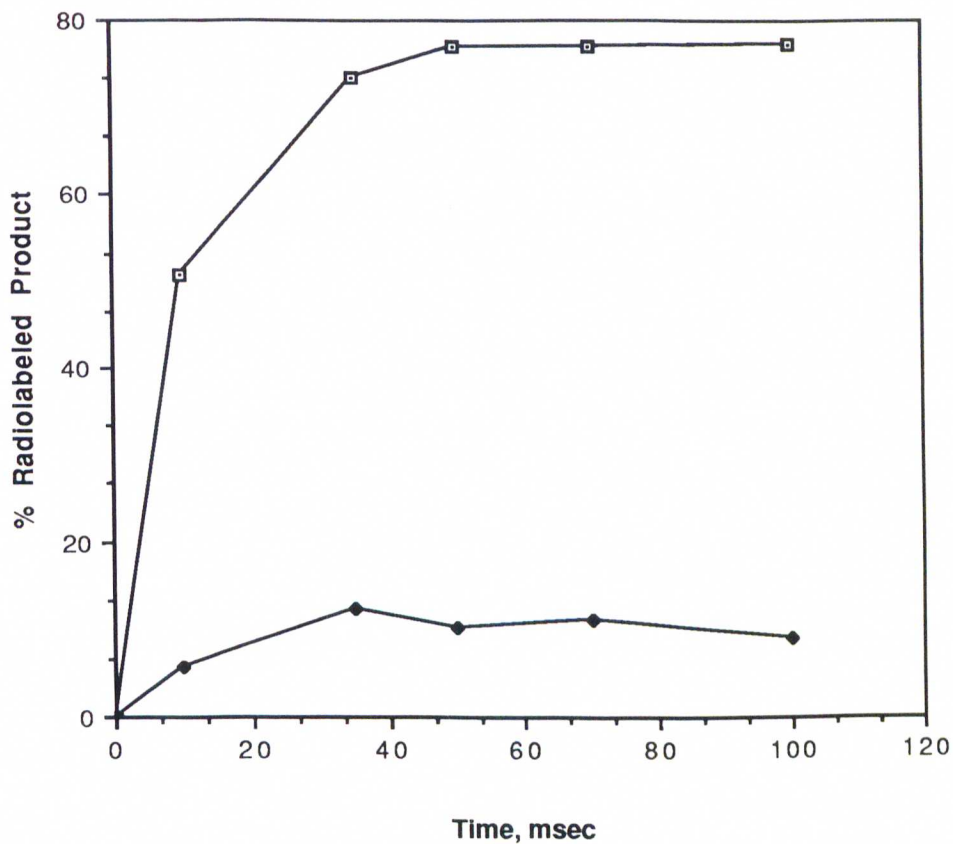


**Figure 15.** Time course for a single turnover of P-pyr in the active site of  $Mn^{2+}$ -activated PEP mutase at 25°C. The reaction contained 5  $\mu M$  [ $^3H$ ]P-pyr, 50  $\mu M$  PEP mutase (subunit Mol. Wt. 39000 Daltons), 5 mM  $MgCl_2$  and 50 mM  $K^+$ HEPES (pH 7.5): (□) PEP, (●) lactate.

### 3. Rapid Quench of the $Mg^{2+}$ -Activated PEP Mutase

#### Reaction at 4°C.

A more sensitive assay for pyruvate was developed for this experiment. Recall the amount of pyruvate formed at 25°C in the  $Mg^{2+}$ -activated PEP mutase rapid quench experiment at 25°C was 1%, and its quantification was unreliable due to the low specific activity of the  $[^3H]P$ -pyr starting material. We reasoned we could trap and label the pyruvate intermediate with  $[^3H]NADH$  using lactate dehydrogenase.  $[^3H]NAD^+$  could be purchased having a specific activity of 1610 Ci/mol which was 40 times that of the  $[^3H]P$ -pyr (40 Ci/mol). Radiolabeled  $[^3H]NADH$  having tritium in the  $H_R$  position at C-4 was synthesized by reacting  $[^3H]NAD^+$  (31  $\mu M$ ), glyceraldehyde-3-phosphate (625  $\mu M$ ), and  $Na_3AsO_4$  (3.1 mM), with glyceraldehyde -3-phosphate dehydrogenase (57 U) in a 160  $\mu L$  solution containing 50 mM  $K^+$ HEPES, pH 7.5 for 30 min at 25°C. The  $[^3H]NADH$  was produced in an 82% yield and purified using an HPLC equipped with a C-18 reverse phase column. Elution with 5 mM  $K_2HPO_4$ , 5% (v/v) triethylamine, 10% (v/v) MeOH pH 7.5 eluted  $NAD^+$  at 13 min and  $NADH$  at 19 min. The  $[^3H]NADH$  product obtained directly from the column was determined to be 1.65  $\mu M$  based upon a specific activity of 1610 Ci/mol.  $[^3H]NADH$  which proved to be unstable at room temperature and partially unstable in solution below pH 7 was stored at -80°C and used immediately after thawing.

The single turnover reaction was carried out using 43  $\mu L$  of a buffered solution of 100  $\mu M$  of PEP mutase mixed using a rapid quench apparatus with 43  $\mu L$  of 10  $\mu M$   $[^3H]P$ -pyr at 4°C to produce a final concentration of 5  $\mu M$   $[^3H]P$ -pyr, 50  $\mu M$  PEP mutase, 5 mM  $MgCl_2$ . The

time course of this reaction is shown in Figure 16. A single turnover required about 50 msec to complete. This is approximately three fold slower than the  $Mg^{2+}$ -activated PEP mutase reaction at 25°C. An identical single turnover experiment was carried out using 43  $\mu$ L of 100  $\mu$ M PEP mutase with 43  $\mu$ M 50  $\mu$ M unlabeled-P-pyr at 4°C so that pyruvate could be trapped and labeled with the  $[^3H]NADH$ / lactate dehydrogenase system. The reactions were quenched and immediately neutralized to pH 7 with 12  $\mu$ l 1M KOH. One fourth of the quenched reaction mixture (63  $\mu$ L) containing P-pyr, PEP and pyruvate (corresponding to 0.11 nmol of  $[^3H]P$ -pyr substrate) was reacted with  $[^3H]NADH$  (44  $\mu$ L, 0.072 nmol) and lactate dehydrogenase (100 U) for 2 min at 25°C. After removing the lactate dehydrogenase by precipitation with  $CCl_4$ , the reaction solution was separated on an HPLC equipped with a C-18 reverse phase column. The column was eluted with 5 mM  $K_2HPO_4$ , 5% (v/v) triethylamine, and 10% MeOH at pH 7.5.  $[^3H]$ Lactate eluted with the solvent front while  $NAD^+$  and  $[^3H]NADH$  had retention times of 13 and 19 min, respectively. The results are shown in Figure 16. The amount of lactate produced was about 10% of the total P-pyr starting material. Lactate formation did not precede PEP formation. Two possible explanations for this observed 10% lactate was that the  $[^3H]NADH$  decomposed during the reaction producing  $^3H_2O$  which coeluted with lactate under these HPLC conditions, or the PEP mutase preparation contained a dephosphorylase side reactivity.

The single turnover experiments described above indicate that the putative pyruvate intermediate in the  $PEP \rightleftharpoons P$ -pyr catalyzed rearrangement has a very short lifetime. A possible way to enhance the lifetime of the pyruvate intermediate would be to carry out single turnover experiments

using the thiophosphonopyruvate as a substrate. However a methodology for either labeling the thiophosphonopyruvate or the thiophosphoenolpyruvate product and pyruvate intermediate would need to be developed.

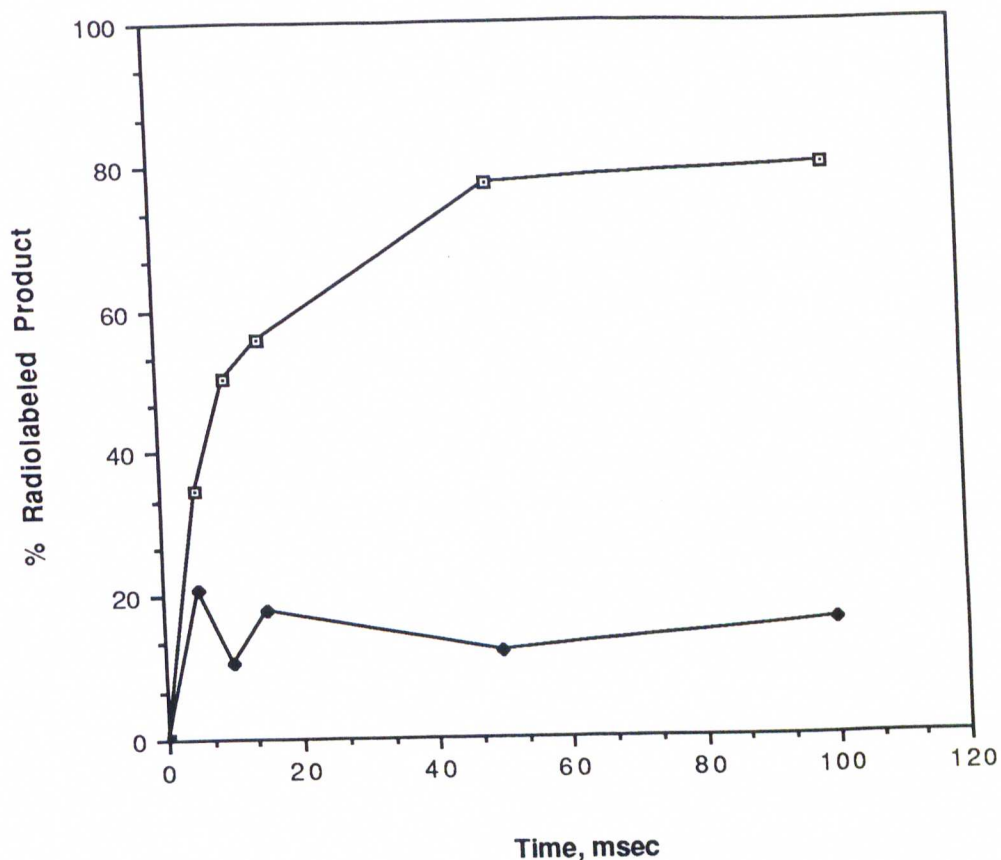


**Figure 16.** Time course for a single turnover of P-pyr in the active site of  $Mg^{2+}$ -activated PEP mutase at  $4^{\circ}C$ . The reaction contained  $5 \mu M$   $[^3H]P$ -pyr,  $50 \mu M$  PEP mutase (subunit Mol. Wt. 39000 Daltons),  $5 mM$   $MgCl_2$  and  $50 mM$   $K^+HEPES$  (pH 7.5): (□) PEP. Lactate (◆) was obtained from separate reaction containing  $5 \mu M$  P-pyr,  $50 \mu M$  PEP mutase,  $5 mM$   $MgCl_2$  and  $50 mM$   $K^+HEPES$ (pH 7.5), and trapped with the  $[^3H]NADH$ / lactate dehydrogenase system.

#### **4. Determination of the Internal Equilibrium of PEP and P-pyr Bound to PEP Mutase**

In order to measure the equilibrium of the substrates bound in the active site of PEP mutase a high concentration of pure PEP mutase relative to radiolabeled substrate was used and the ratio of enzyme bound P-pyr to PEP at equilibrium was measured. A control reaction containing 43  $\mu\text{M}$  of 100  $\mu\text{M}$  PEP mutase and 43  $\mu\text{M}$  of 10  $\mu\text{M}$  [ $^3\text{H}$ ]P-pyr was mixed in a rapid quench apparatus for 50 msec and quenched with 164  $\mu\text{l}$  HEPES adjusted to pH 1.6 with HCl. The [ $^3\text{H}$ ]P-pyr in the quenched reaction was reduced with 4 mM NaCNBH<sub>3</sub> for 15 min and then the solution was neutralized by the addition of 12  $\mu\text{L}$  of 1 M KOH. The HPLC-separated products were quantified by scintillation counting. The reaction produced [ $^3\text{H}$ ]PEP (40%), [ $^3\text{H}$ ]P-lactate (0%),  $^3\text{H}_2\text{O}$  (28%), and [ $^3\text{H}$ ]lactate (18%). The remaining 14% of the radioactivity derived from the unidentified contaminant in the [ $^3\text{H}$ ]P-pyr starting material. The control experiments carried out to test P-pyr and PEP hydrolysis under the quench conditions indicated that the [ $^3\text{H}$ ]lactate could in part (ca. 3-5%) be due to dephosphorylation of [ $^3\text{H}$ ]PEP during the quench and reduction reaction. The remaining (10%) of the pyruvate generated must be attributed to a minor dephosphorylase activity of the PEP mutase. This side reaction is not observed when the reaction is run with only a catalytic amount of PEP mutase. To circumvent this difficulty we decided to run a series of reactions for a fixed length of time and vary the PEP mutase concentration. We hoped we could find an ideal ratio of enzyme to substrate which minimized the dephosphorylase side activity, yet provide for maximum binding of the reactants to the enzyme.

Solutions of purified PEP mutase ranging from 2 to 200  $\mu\text{M}$  in 50 mM  $\text{K}^+\text{HEPES}$ , 10 mM  $\text{MgCl}_2$ , pH 7.5 were prepared. Forty-three microliters each of PEP mutase and 10  $\mu\text{M}$   $[^3\text{H}]\text{P-pyr}$  in 50 mM  $\text{K}^+\text{HEPES}$  (pH 7.5) were mixed in a rapid quench apparatus at 25°C for 50 ms, and worked up with  $\text{NaCNBH}_3$  as previously described. Three control reactions containing a catalytic amount of PEP mutase and 10  $\mu\text{M}$   $[^3\text{H}]\text{P-pyr}$ , were run at 25°C for 5 min and worked up as previously described. These controls should reflect the enzyme reaction in the absence of the dephosphorylase side activity. The control reaction product mixture consisted of PEP (60%), P-pyr (0%),  $^3\text{H}_2\text{O}$  (30%), and  $[^3\text{H}]\text{lactate}$  (0% to 3%). One control was run at the beginning of the experiment and two at the end of of the experiment. About 5% loss of label due to exchange with solvent occurred in between the time of the first and third control. The  $[^3\text{H}]\text{PEP}$ ,  $[^3\text{H}]\text{P-Pyr}$ , and  $^3\text{H}_2\text{O}$  were separated using an HPLC equipped with an anion exchange column as previously described (0.1 M  $\text{KH}_2\text{PO}_4$ , 0.4 M  $\text{KCl}$ , pH 2.75).  $[^3\text{H}]\text{lactate}$  coelutes with  $^3\text{H}_2\text{O}$  under these HPLC conditions. The amount of  $[^3\text{H}]\text{lactate}$  in the product was calculated by subtracting the amount of  $^3\text{H}_2\text{O}$  measured in the control reactions. The results are shown in Table 3 and a plot of  $[^3\text{H}]\text{PEP}$ ,  $[^3\text{H}]\text{P-Pyr}$ , and  $^3\text{H}_2\text{O}$  (and  $[^3\text{H}]\text{lactate}$ ) formed vs P-pyr to PEP mutase ratio is shown in Figure 17. The optimal ratio of PEP mutase active sites to  $[^3\text{H}]\text{P-pyr}$  was 2:1. At this ratio of enzyme to substrate the ratio of  $[^3\text{H}]\text{PEP}$  to  $[^3\text{H}]\text{P-pyr}$  is about 25:1.

Table 3: Amount of radioactivity associated with each product formed in the experiment determining the on-enzyme equilibrium of PEP mutase

Ratio Enz/P-pyr	Amounts of Products cpm(% of total)			Total
	[ <sup>3</sup> H]H <sub>2</sub> O & [ <sup>3</sup> H]lactate	[ <sup>3</sup> H]P-lac	[ <sup>3</sup> H]PEP	
Control 1	1659(27.4)		3674(60.7)	6044
20	2753(51.9)		1710(32.2)	5306
10	2554(46.0)		2257(40.1)	5557
4	2136(37.9)		2744(48.7)	5640
2	1785(32.6)	116(2.1)	2958(54.1)	5471
1	1703(31.0)	776(14.1)	2307(42.0)	5493
0.2	1462(31.5)	1835(15.6)	621(13.4)	4645
Control 2	2061(30.8)		3886(58.2)	6681
Control 3	1779(31.6)		3210(57.1)	5623

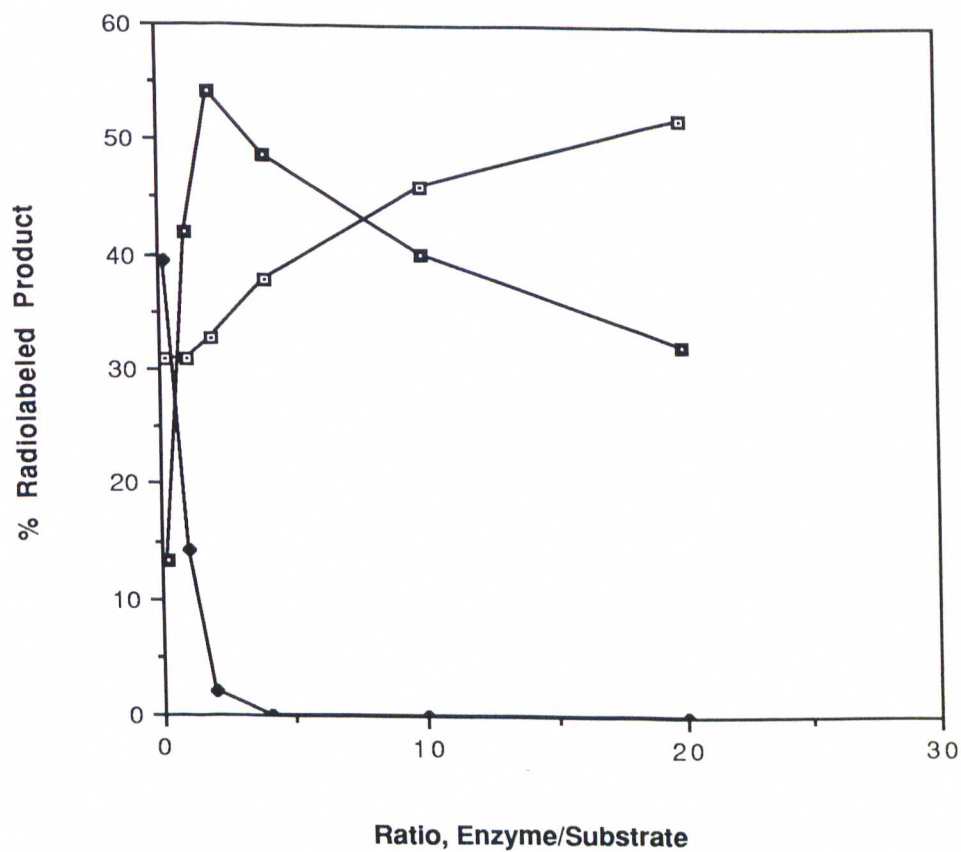


**Figure 17.** Plot of % substrates and products vs PEP mutase (subunit Molec Wt. 39000 daltons) concentration of 86  $\mu$ L reactions consisting of 5  $\mu$ M [<sup>3</sup>H]P-pyr 5 mM MgCl<sub>2</sub> in 50 mM K<sup>+</sup>HEPES buffer (pH 7.5) at 25°C, for 50 msec: (■)PEP, (●)P-pyr, (□) <sup>3</sup>H<sub>2</sub>O, lactate.

The methodology involving single turnover experiments consisting of [ $^3\text{H}$ ]P-pyr and PEP mutase were problematic. First, the [ $^3\text{H}$ ]P-pyr had a low specific activity (40 Ci/mol). This limitation precluded the direct observation of [ $^3\text{H}$ ]pyruvate produced from [ $^3\text{H}$ ]P-pyr. For example a typical reaction of 43  $\mu\text{L}$  of 10  $\mu\text{M}$  [ $^3\text{H}$ ]P-pyr contained 10000 cpm, a 1% yield of pyruvate would contain 100 cpm. The [ $^3\text{H}$ ]P-pyr contained a contaminant which eluted closely with [ $^3\text{H}$ ]P-lactate and exchange of the label from [ $^3\text{H}$ ]P-pyr with solvent during the experiments complicated the results. Trapping the putative pyruvate intermediate with [ $^3\text{H}$ ]NADH was unreliable due to the instability of [ $^3\text{H}$ ]NADH. The PEP mutase preparations also proved to be a critical limitation in these experiments. There appeared to be a dephosphorylase side reactivity when high concentrations of PEP mutase were used. Despite these complications some useful information could be extracted from these single turnover experiments. The  $\text{Mg}^{2+}$ -activated PEP mutase rearrangement of P-pyr to PEP in the enzyme active site at 25°C and 4°C were too fast to trap an intermediate. Using a manganese cofactor did not slow the reaction enough to allow for the accumulation of an intermediate. Although pyruvate is produced in these reactions it does not appear to be an intermediate. Further research into the intermediate in the P-pyr $\leftrightarrow$ PEP rearrangement may be best addressed by attempting to directly observe a phosphorylated-enzyme species using an phosphorus-labeled probe. The identification of the intermediate in the PEP mutase reaction remains for future study.

## CONCLUSION

The occurrence of PEP mutase in both eukaryotic, *T. pyriformis* and prokaryotic, *S. hygrosopicus*, organisms suggests that it is the entry point into the phosphonate class of natural products. However, PEP mutase is not the only P-C bond forming enzyme. The other P-C bond forming enzyme, found in the bialaphos pathway, carboxyphosphoenolpyruvate mutase, was recently discovered by Seto. Additionally, the P-C bond in fosfomycin is formed by an enzyme which is probably somewhat different than PEP mutase. The full spectrum of P-C bond forming enzymes has yet to be determined, but the two phosphonosynthases which are known are similar in that the rearrangement in the P-C bond formation direction appears to depend on decarboxylation.

Bialaphos contains a C-P-C moiety. The first P-C bond comes from the PEP mutase rearrangement of PEP to P-pyr. The second P-C bond is formed by the enzyme carboxyphosphoenolpyruvate (CPEP) mutase. CPEP mutase has been purified and has a specific activity of 217 U/mg. CPEP mutase is a homodimer with subunit molecular masses of 32,000. Although no mechanistic studies have been published on CPEP phosphonomutase its equilibrium apparently favors P-C bond formation, due to the thermodynamically favored decarboxylation.

Since PEP mutase was found in both eukaryotic and prokaryotic organisms Seto and coworkers also expected to find PEP mutase activity in fosfomycin biosynthetic pathway. It was known from fosfomycin pathway studies that there must be an enzyme activity that forms a P-C bond from

PEP and that produces P-ald. However, contrary to their expectations, PEP mutase activity could not be found in Fosfomycin-producing strains of *streptomyces*. Even the very high fosfomycin-producing organism, *S. wedmorensis* 209-97 did not show PEP mutase (P-pyr conversion to PEP) activity. Lack of observable P-pyr $\Rightarrow$ PEP activity in fosfomycin-producing bacteria may be rationalized if P-ald, and not P-Pyr, is the product of the P-C bond forming enzyme. Such a transformation could be catalyzed by an enzyme or enzyme complex which couples P-C bond formation with loss of CO<sub>2</sub>. Thus, another class of P-C bond forming enzymes may have evolved which combine P-C formation with decarboxylation.

In every known P-C forming pathway, the formation of a P-C bond seems to be always coupled to a subsequent decarboxylation. We have already suggested that the exergonic decarboxylation of P-pyr is what pulls the thermodynamic disfavored PEP $\Rightarrow$ P-pyr rearrangement forward in the AEP biosynthetic pathway. Perhaps the phosphosynthase in the fosfomycin pathway is a hybrid enzyme, similar to PEP mutase in that it forms the P-C bond from a rearrangement of PEP and similar to CPEP mutase in that the P-C bond formation is directly linked to decarboxylation.

The detailed mechanism of PEP mutase catalysis is still not known. We do know that PEP mutase catalyzes an intramolecular, stepwise rearrangement of P-pyr to PEP. The intermediate involved in that process remains to be identified. From the studies contained in this dissertation, one may speculate on the identity of the intermediate. Much of the data suggests the intermediate in the PEP $\Leftrightarrow$ P-pyr most likely resembles metaphosphate. Metaphosphate is a short-lived species. Its lifetime is enhanced if the phosphoryl group is substituted with a sulfur atom

(metathiophosphate). The rapid quench data indicate the intermediate involved in the PEP mutase reaction is very short-lived. Recall that thiophosphonopyruvate has a  $V_m$  which is on 80% that of the natural substrate. Usually thiophosphoryl analogs react with  $V_m$  on the order of 100- to 1000-fold slower than their phosphoryl counterparts. Additional support for the Metaphosphate intermediate is contained in a recent study by Freeman et. al.<sup>114</sup> which characterized the solution hydrolysis of phosphonopyruvate at pH 7.5. The mechanism was determined to be highly dissociative in nature, which is indicative of a metaphosphate intermediate.

## METHODS

**General.** PEP phosphomutase was prepared according to the method of Bowman.<sup>4</sup> Phosphonopyruvate was prepared from phosphonoalanine according to the method of Anderson.<sup>115</sup> Ninety eight percent enriched  $^{18}\text{O}$ -water was purchased from Cambridge Isotope Laboratories. The enzymes, buffers and substrates used were purchased from Sigma Chem. Co. Oxalyl chloride, (S)-(-)- $\alpha$ -phenethylamine,  $\text{D}_2\text{O}$  and  $\text{CuI}$  were purchased from Aldrich. Methylphosphonothioic dichloride was purchased from Alpha. The  $\text{H}_2^{18}\text{O}$  (containing 98 atom%  $^{18}\text{O}$ , 2 atom %  $^{16}\text{O}$ ) was obtained from Cambridge Isotope Laboratories. Methylphosphonothiodichloridate was purchased from Alpha, all other reagents were obtained from Aldrich and Sigma. All reagents were commercial grade and were used without further purification. Radioisotopes  $[^3\text{H}]\text{H}_2\text{O}$  (5Ci/mL) and  $[^3\text{H}]\text{Nicotinamide Adenine Dinucleotide}$  (1.61Ci/mmol) were purchased from Amersham. The following enzymes were purchased from Sigma: pyruvate kinase (rabbit muscle, 500U/mg), lactate dehydrogenase (pig muscle, 940 U/mg) myokinase (rabbit muscle, 1000 U/mg) and glyceraldehyde-3-phosphate dehydrogenase (4545 U/mg). Glyceraldehyde-3-phosphate dehydrogenase was obtained as an ammonium sulfate suspension and was dialyzed against  $\text{K}^+\text{HEPES}$  (50 mM, pH 8),  $\text{MgCl}_2$  (5 mM) for 2h before use.

Infrared spectra were measured on a Perkin-Elmer Model FT-IR spectrophotometer. Proton NMR spectral data were obtained on a Bruker AF 200, WP 200, or AM 400 spectrophotomer operatinag at 200 or 400

MHz. The chemical shifts are reported in parts per million (ppm) relative to chloroform ( $\delta=7.24$ ) as an internal standard for samples in  $\text{CDCl}_3$ , or relative to water ( $\delta=4.63$ ) for samples in  $\text{D}_2\text{O}$ . Coupling constants are given in hertz (Hz) and multiplicities are assigned as s (singlet), d (doublet), t (triplet), q (quartet), dd (doublet of doublets).  $^{13}\text{C}$  NMR were recorded at 50 MHz on a Bruker AF 200 spectrophotometer. The chemical shifts are reported in ppm relative to chloroform ( $\delta=77.0$ ) as an internal standard for samples in  $\text{CDCl}_3$  and relative to 1,4-dioxane ( $\delta=66.5$ ) as an external standard for samples in  $\text{D}_2\text{O}$ . The assignment of resonances is consistent with INEPT or DEPT results.  $^{31}\text{P}$  NMR spectra were obtained from a Bruker WP 200 or AM 400 spectrophotometers operating at 81 or 162 MHz. Chemical shifts are reported in ppm relative to 85% phosphoric acid ( $\delta=0.0$ ) as an external standard for samples in  $\text{CDCl}_3$  or  $\text{D}_2\text{O}$ . Low resolution mass spectral data were obtained on a Hitachi RMU-6E and high resolution mass spectral data were obtained from a VG-7070. Melting points were determined using a Mel-Temp apparatus.

Preparative chromatography separations were performed using the following absorbants: Dowex -1, diethylaminoethyl (DEAE) Sephadex A-25 or DEAE Cellulose (Whatman DE-52) for anion exchange; Dowex-50 for cation exchange, and Phenyl Sepharose for reverse phase separations. Flash chromatography was performed using

**Phosphonoacetaldehyde (P-ald)** Phosphonoacetaldehyde was prepared according to the method of La Nauze, *et al*<sup>116</sup>.  $\text{PCl}_5$  (85 g, 420 mmol) was added to 300 mL of  $\text{CCl}_4$  under an atmosphere of argon. After cooling to 0 °C, vinyl acetate (19 mL) was added over a one hour

period to the stirred reaction mixture, and a white precipitate gradually formed. After six hours of stirring at 0°C, SO<sub>2</sub> was bubbled through the mixture until the precipitate dissolved. The solvent and phosphorylchloride were removed *in vacuo*. and the SOCl<sub>2</sub> that still remained was removed *in vacuo* by repeated evaporation with benzene. THF (300 mL) and cold H<sub>2</sub>O (6 mL) were added to the reaction flask . The THF was removed by rotary evaporation yeilding a brown oil. Water (250 mL) was added to the crude product and the solution was adjusted to pH 9.0 with LiOH solution. The resulting LiPO<sub>4</sub> precipitate was removed by centrifugation and acetone (500 mL) was added to the supernatant top precipitate P-Ald.. The resulting precipitate was centrifuged, resuspended in water, and loaded onto a 1.5 x 100 cm Dowex-1 (Cl<sup>-</sup>) column. The column was eluted with a one liter linear gradient of LiCl (0.1 - 0.4M) in N-ethylmorpholine (5mM, pH 7.5). P-ald containing fractions were identified by measuring the change in absorbance at 253 nm of a 1 mL solution containing a 10 μL a1iquot of the fraction , 1% (w/v) semicarbazide-HCl and 2% (w/v) sodium acetate. Fractions containing P-ald were pooled and concentrated *in vacuo*. <sup>31</sup>P NMR (D<sub>2</sub>O, pH 8.0) 9.3 ppm (t, J = 19.9 Hz).

**Phosphonoalanine (P-ala)** Phosphonoacetaldehyde was prepared by the procedure described by Chambers and Isbell.<sup>117</sup> Acetamide (14.68 g, 250 mmol) was added to dry benzene (350 mL) containing pyruvic acid (13.2 g, 150 mmol). The mixture was refluxed under an atmosphere of argon. The benzene/water azeotrope was removed *via* a Dean-Stark trap. After cooling the reaction mixture to 25°C, trimethylphosphite (66 mL) and dimethylphosphite (59 mL) were added to

the mixture. The reaction mixture was refluxed for 3 hours, cooled to 25°C and then stirred for 12 hours. Excess phosphite and volatile compounds were removed by short path distillation (130°C, 0.7mm). The mixture was cooled to room temperature and concentrated HCl (250 mL) was added to the dark residue. The solution was refluxed for 48 hours. HCl was then removed by short path distillation. The residue was dissolved in a minimal amount of H<sub>2</sub>O and decolorized with activated carbon (2 g/mL) at 100 °C. The product was eluted on a 2.5 x 90 cm Dowex-50 (H<sup>+</sup>) column with deionized water. An aliquot from each fraction was spotted on a silica gel TLC plate. P-ala containing fractions were identified by visualization of the amine with ninhydrin spray. Fractions containing P-ala were pooled and concentrated *in vacuo*. The P-ala was then purified by recrystallization from cold water. <sup>31</sup>P NMR.(D<sub>2</sub>O, pH 8.0) 19.0 ppm (dd, 26.0, 27.3 Hz).

**Phosphonopyruvate (P-pyr).** Phosphonopyruvate was synthesized following the procedure of Anderson, *et al*<sup>115</sup>. P-ala (0.5 g, 3 mmol ) was added ,to 50 mL of freshly dried methanol containing 0.1 M HCl, under an atmosphere of argon. The reaction mixture was stirred for 40 hours at 40 °C. N-ethylmorpholine was added to the reaction mixture until a pH of 7.0 was achieved. 3,5-Ditertiarybutylbenzoquinone (0.65 g, 3 mmol) dissolved in 25 mL of dry methanol was added to the solution and stirred at room temperature for 4 hr. Fifteen mL of water were added to the reaction mixture and the pH of the solution was then adjusted to 4.0 with glacial acetic acid. After 12 hours, the reaction mixture was extracted with an equal volume of chloroform. The chloroform layer was washed with 3 equal volumes of 10 mM KHCO<sub>3</sub>. The aqueous layers were collected,

concentrated to 5 mL *in vacuo*, and neutralized with dilute KOH. The crude product was loaded onto a 2.5 x 20 cm Dowex-1 (Cl<sup>-</sup>) column. P-pyr was eluted from the column with a linear gradient of LiCl (0.1-0.4M) containing N-ethylmorpholine (5mM, pH=7.5). P-pyr containing fractions were identified by the change in absorbance at 253 nm of a 1 mL solution containing a 10 µl aliquot from each fraction, semicarbazide-HCl (1% w/v) and sodium acetate (2%w/v). P-pyr was purified by recrystallization from methanol. <sup>31</sup>P NMR.(D<sub>2</sub>O, pH 8.0) 10.5 ppm (t, J=19.8 Hz).

### ***Tetrahymena pyriformis* Media and Stock Cultures.**

Growth media consisted of Bactopeptone (20.0 g/L), yeast extract (5.0 g/L), CaCl<sub>2</sub> (0.008 g/L), NaCl (0.1 g/L), and KCl (0.004 g/L). Stock cultures of *Tetrahymena* were maintained in 18 X 150 mm culture tubes containing 5 mL of media and capped with stainless steel caps. Cultures were transferred to new tubes every four days at 5-10% dilutions.

**Large Scale Growth and Lysis.** Four-day-old stock cultures were used to inoculate 100 mL of media which was agitated on a gyratory shaker for 30 h, after which was added 1 L of media. After 20 h, an additional liter of media was added to the culture, and three hours later (OD<sub>530</sub> = 1.9) the culture was cooled to 4 °C and the cells harvested by centrifugation (3000 g X 10 min.) The cells were washed with a solution of sucrose (0.2 M) and NaCl (1.8%) 100 mL/L cell culture. The packed cells were cooled to 0 °C and suspended in a buffer (100 mL/16 mL cells) containing glycine (50 mM), EDTA (1 mM), β-mercaptoethanol (10 mM), BSA (1.6%), 1,10-phenanthroline (1 mM), benzamidine hydrochloride

hydrate (1 mM), phenylmethylsulfonylfluoride (50 mM), and trypsin inhibitor (50 mg/mL) at a pH of 9.4. For studies involving the elucidation of the biosynthetic pathway, cells were lysed in a tissue homogenizer fitted with a teflon pestel. For PEP phosphomutase purification and characterization studies, the cells were lysed using a French Pressure Cell Press operated at 9000 psi.

**Reactions with *Tetrahymena pyriformis* Homogenate and Homogenate Fractions.** Reactions consisted of 20 mL of a basal solution containing HEPES (50 mM), BSA (0.4%), MgCl<sub>2</sub> (10 mM), L-alanine (20 mM), pyridoxal phosphate and except where noted, thiamine pyrophosphate (2.5 mM) at pH 7.6 and 20 mL of cellular homogenate. Reactions were carried out at 27 °C on a gyratory shaker for *ca.* 12 h. Reactions were terminated by the addition of 40 mL trichloroacetic acid (20% w/v) and were subsequently centrifuged at 3000 g X 10 min. The resulting precipitant was twice washed with 40 mL trichloroacetic acid solution (5% w/v) and centrifuged at 3000 g X 10 minutes. The trichloroacetic acid solutions were the extracted three times with equivalent volumes of ethyl ether. To the ether was added one equivalent volume of absolute ethanol, and the mixture was centrifuged at 17,000 g X 10 minutes. The ether was then evaporated *in vacuo* and loaded on a Dowex-50 (H<sup>+</sup>) column (2.5 X 30 cm). The column was eluted with 300 ml of water and then with 300 mL 3 M NH<sub>4</sub>OH. The water fraction was dried *in vacuo* and rehydrated with D<sub>2</sub>O and analyzed for neutral or negatively charged phosphates and phosphonates by <sup>31</sup>P-NMR. The NH<sub>4</sub>OH fraction was concentrated to dryness and the residue rehydrated with a small

amount of water and loaded onto a Dowex-1 ( $\text{CH}_3\text{COO}^-$ ) column (18 X 40 cm). The column was eluted with 200 mL of water and then 250 mL acetic acid. The acetic acid fraction was concentrated to dryness and rehydrated with  $\text{D}_2\text{O}$  and analyzed by  $^{31}\text{P}$  NMR techniques.

**PEP Mutase Assay and Isolation.** PEP mutase was assayed by following the formation of PEP from P-pyr. An ADP-pyruvate kinase/NADH-lactate dehydrogenase coupled assay for PEP resulted in a decrease in absorbance at 340 nm. The assay solution contained HEPES (50 mM),  $\text{MgCl}_2$  (5 mM), ADP (5 mM), NADH (0.25 mM), LDH (80 units/mL), pyruvate kinase (20 units/mL), and P-pyr (1 mM). at pH 7.8, 25°C The enzyme was purified by the method described by Bowman with minor modifications.<sup>4</sup> Six grams of crude protein pellet was dissolved in 50 mM triethanolamine (pH 7.5), 5, mM  $\text{MgCl}_2$ , and 0.5 mM EDTA, 1,10-phenanthroline (1 mM), benzimidazole hydrochloride hydrate (1 mM), phenylmethylsulfonyl fluoride (50 mM), and trypsin inhibitor (50 mg/mL). and dialyzed for 9 h at 4°C against 2 L of buffer, which was replaced with fresh buffer every fifth hour. The remaining purification steps were carried out at 4°C. The dialyzed protein was loaded onto a 22 cm x 3.5 cm DEAE-cellulose column (Sigma Chemical Co.) that had been equilibrated with 50 mM triethanolamine (pH 7.5) containing 5 mM  $\text{MgCl}_2$  and 0.4 mM DTT. Isocratic elution of the PEP mutase from the column was carried out with the equilibration buffer.

The PEP mutase active fractions obtained from the DEAE-cellulose chromatography were made 25% (w/v) in ammonium sulfate and then applied to a 35 x 2.5 cm phenyl-Sepharose (CL-4b, Sigma Chemical Co.)

column equilibrated with 50 mM triethanolamine (pH 7.5) containing 25% (w/v) ammonium sulfate, 5 mM MgCl<sub>2</sub> and 0.5 mM DTT. The column was eluted with a 1.5 L linear gradient of 25% to 0% ammonium sulfate in 50 mM triethanolamine (pH 7.5), 5 mM MgCl<sub>2</sub>, and 0.5 mM DTT.

The PEP mutase containing fractions obtained from the phenyl Sepharose chromatography were pooled, concentrated to 2 mL with an Amicon ultrafiltration apparatus, and then loaded onto a 100 x 3 cm Bio-Gel P-200 (Bio-Rad Chemical Co.) column. The column was eluted with 50 mM triethanolamine (pH 7.5) containing 5 mM MgCl<sub>2</sub>, and 0.5 mM DTT. The PEP mutase containing fractions were made 10% (w/v) in glycerol and frozen in a dry ice-acetone bath before storing at -80°C.

**Thiophosphonopyruvate and Racemic [P=18O]Thiophosphonopyruvate.** To 80 mg (140 μmol) of a racemic mixture of the dicesium salt of phosphonamide **24** (1:1 **24a** and **24b**) were added 600 μl (30 mmol) of either 16O- or 18O-enriched (98%) H<sub>2</sub>O and 24 μl (288 μmol) of 12 N HCl. After 10 sec at 25 °C, 400 μl of K<sup>+</sup>Hepes (20 mM, pH 8) were added and the pH of the resulting solution was adjusted to 8 with 1 M KOH. The solutions were concentrated *in vacuo*. <sup>31</sup>P NMR analysis of the residues dissolved in D<sub>2</sub>O (pH 8.0) revealed that they contained 84% [S, 18O, 16O-P]thiophosphonopyruvate (t,+44.76 ppm, J = 18.2 Hz) and 16% [P=18O<sub>2</sub>]phosphonopyruvate (t,+10.50 ppm, J = 20.4 Hz), or 84% thiophosphonopyruvate (t,+44.80 ppm, J = 18.2 Hz) and 16% phosphonopyruvate (t, +10.55 ppm, J = 20.4 Hz), respectively. The [P=18O] and thiophosphonopyruvates were used in the

experiments described below without prior removal of the phosphonopyruvate contaminants unless otherwise stated.

**Kinetic Constants for Thiophosphonopyruvate vs. Phosphonopyruvate.** The initial velocities of PEP phosphomutase catalyzed conversion of phosphonopyruvate to PEP or thiophosphonopyruvate to thiophosphoenolpyruvate were measured at pH 8.0 as a function of the concentration of phosphonopyruvate or thiophosphonopyruvate. Thiophosphoenolpyruvate or PEP formation was monitored by using the pyruvate kinase - lactate dehydrogenase coupled assay. All reaction mixtures contained ADP (1 mM), MgCl<sub>2</sub> (5 mM), KCl (5 mM), NADH (0.3 mM), pyruvate kinase (750 U), and lactate dehydrogenase (30 U) in K<sup>+</sup>Hepes buffer (50 mM, pH 8). The  $K_m = 5 \mu\text{M}$  and  $V_m = 16 \text{ s}^{-1}$  values were evaluated from a Lineweaver-Burk plot of the initial velocity data. The  $K_m = 20 \mu\text{M}$  and  $V_m = 24 \text{ s}^{-1}$  values for phosphonopyruvate were evaluated under identical reaction conditions.

**[P=<sup>18</sup>O, C(2)-<sup>18</sup>O]Thiophosphonopyruvate (26) and [C(2)-<sup>18</sup>O]Thio-phosphonopyruvate (32).** Complete <sup>18</sup>O exchange at C<sub>2</sub> of either [P=<sup>18</sup>O]thiophosphonopyruvate (118  $\mu\text{mol}$ ) or thiophosphonopyruvate (59  $\mu\text{mol}$ ) was accomplished by separately incubating their potassium salts in 250  $\mu\text{l}$  of <sup>18</sup>O-enriched H<sub>2</sub>O (98%) for 24 hr at 4 °C.

**PEP Phosphomutase Catalyzed Reactions of [P=<sup>18</sup>O, C(2)-<sup>18</sup>O]Thiophos-phonopyruvate (26) and [C(2)-**

**$^{18}\text{O}$ Thiophosphonopyruvate (32) to the Corresponding Thiophosphoenolpyruvates.**  $[\text{C}(2)\text{-}^{18}\text{O}]$ Thiophosphonopyruvate (32) (59  $\mu\text{mol}$ ) or  $[\text{P}=\text{}^{18}\text{O}, \text{C}(2)\text{-}^{18}\text{O}]$ thiophosphonopyruvate (26) (118  $\mu\text{l}$ ) dissolved in 250  $\mu\text{l}$  of  $\text{H}_2^{18}\text{O}$  (98%) was added to 7.5 ml of 20 mM  $\text{K}^+$ Hepes buffer (pH 8) containing 2.5 mM  $\text{MgCl}_2$  and 5 units of PEP phosphomutase. The resulting solution was incubated for 10 min at  $25^\circ\text{C}$  and then passed through an amicon filter (DiaFlo, PM10, 10,000 MW cut off) under  $\text{N}_2$  pressure. The filtrate was concentrated *in vacuo* and the residue obtained was dissolved in a  $\text{D}_2\text{O}$  solution containing 20 mM  $\text{K}^+$ Hepes (pH 8) and 0.2 M EDTA. The  $^{31}\text{P}$  NMR spectrum of the mixture obtained from reaction of  $[\text{S}, \text{}^{16}\text{O}_2\text{-P}], [^{18}\text{O}\text{-C}_2]$ thiophosphonopyruvate (32) showed a phosphorus signal for (all- $^{16}\text{O}$ )thiophosphoenolpyruvate (27) (60%) at +39.443 ppm and for  $[\text{C}_2\text{-}^{18}\text{O}]$ thiophosphoenolpyruvate (28) (40%) at + 39.417 ppm. The  $^{31}\text{P}$  NMR spectrum of the product mixture obtained from the PEP phosphomutase catalyzed reaction of  $[\text{P}=\text{}^{18}\text{O}, \text{C}(2)\text{-}^{18}\text{O}]$ thiophosphonopyruvate (26) under the same conditions as described above showed a phosphorus signal at +39.397 ppm for  $[\text{P}=\text{}^{18}\text{O}]$ thiophosphoenolpyruvate (29) (60%) and at +39.368 ppm for  $[\text{P}=\text{}^{18}\text{O}, \text{C}(2)\text{-}^{18}\text{O}]$ thiophosphoenolpyruvate (30) (40%).

**PEP Phosphomutase Catalyzed Reaction of an Equimolar Mixture of Thiophosphonopyruvate and  $[\text{P}=\text{}^{18}\text{O}, \text{C}(2)\text{-}^{18}\text{O}]$ Thiophosphonopyruvate (32).** A mixture of 59  $\mu\text{mol}$  each of thiophosphonopyruvate and  $[\text{P}=\text{}^{18}\text{O}, \text{C}(2)\text{-}^{18}\text{O}]$ thiophosphonopyruvate (2) was reacted at  $25^\circ\text{C}$  for 10 min with 10 units of PEP phosphomutase in 5 ml of 20 mM  $\text{K}^+$ Hepes (pH 8) containing 2.5 mM  $\text{MgCl}_2$ . The reaction

mixture was subjected to the work-up procedure described above. The mixture obtained was analyzed by  $^{31}\text{P}$  NMR giving the spectrum displayed in Figure 5.

### **Op-(2-Trimethylsilylethyl)**

**Methylphosphonochloridothioate (20).** To a stirred solution of 2-trimethylsilylethanol (9.78 g, 82.7 mmol) in THF (150 mL) was added, dropwise, n-butyllithium (1.2 M, 75.2 mL, 90.2 mmol) at  $-78\text{ }^{\circ}\text{C}$ . The resulting solution was added to a stirred solution of methylphosphonothioic dichloride **8** (11.2 g, 75.2 mmol) in THF (40 mL) at  $-78\text{ }^{\circ}\text{C}$  over 1h. After 7 h at  $-78\text{ }^{\circ}\text{C}$ , the mixture was warmed to  $25\text{ }^{\circ}\text{C}$ , and diluted with ether (10 mL) and water (10 mL). The organic layer was separated, washed successively with water and brine, dried over anhydrous sodium sulfate, and concentrated *in vacuo*. The residue was subjected to distillation ( $80\text{ }^{\circ}\text{C}$ , 0.6 mm) to give 8.43 g (49%) of the silylethyl ester **20**. IR (neat) 2940 (C-H), 2880 (C-H), 620 (P=S)  $\text{cm}^{-1}$ ;  $^1\text{H}$  NMR ( $\text{CDCl}_3$ ) 0.05 (s,  $\text{SiCH}_3$ , 9H), 1.10 (t,  $J = 8.5\text{ Hz}$ ,  $\text{CH}_2\text{Si}$ , 2H), 2.26 (d,  $J = 15.4\text{ Hz}$ ,  $\text{PCH}_3$ , 3H), 4.30 (m,  $\text{POCH}_2$ , 2H) ppm;  $^{13}\text{C}$  NMR ( $\text{CDCl}_3$ ) -1.6 ( $\text{SiCH}_3$ ), 18.8 (d,  $J = 7.6\text{ Hz}$ ,  $\text{POCH}_2$ ), 29.8 (d,  $J = 103.0\text{ Hz}$ ,  $\text{PCH}_3$ ), 65.7 (d,  $J = 8.0\text{ Hz}$ ,  $\text{POCH}_2$ ) ppm;  $^{31}\text{P}$  NMR ( $\text{CDCl}_3$ ) +93.3 ppm; mass spectrum  $m/e$  (relative intensity) 203 ( $[\text{M}-28]^+$ , 100), 85 (15), 81 (13).

**Synthesis of (2-Trimethylsilylethyl)oxalyl Chloride.** To oxalyl chloride (13.6 g, 0.11 mol) was added 2-trimethylsilylethanol (12.5 g, 0.11 mol), dropwise, with stirring at  $0\text{ }^{\circ}\text{C}$ . The mixture was warmed to  $25\text{ }^{\circ}\text{C}$ , stirred for 15 h, concentrated *in vacuo* and subjected to distillation ( $56$

°C, 2.0 mm), to give 13.6 g (62%) of the mono-ester acid chloride. IR (neat) 2930 (C-H), 1780 (ClC=O), 1740 (OC=O), 1240 (Si-C)  $\text{cm}^{-1}$ ;  $^1\text{H}$  NMR ( $\text{CDCl}_3$ ) 0.05 (s, SiCH<sub>3</sub>, 9H), 1.12 (t, J = 8.6 Hz, SiCH<sub>2</sub>, 2H), 4.43 (t, J = 8.4 Hz, OCH<sub>2</sub>, 2H) ppm;  $^{13}\text{C}$  NMR ( $\text{CDCl}_3$ ) - 1.7 (SiCH<sub>3</sub>), 17.3 (s, SiCH<sub>2</sub>), 67.9 (s, OCH<sub>2</sub>), 155.8 (s, COOC), 161.2 (s, ClCO) ppm; mass spectrum, m/e (relative intensity) 163 ( $[\text{M}-42]^+$ , 100), 101 (41).

### Synthesis of (S)-(-)-N-Methyl-N-(1-Phenylethyl)amine

(21). To a stirred solution of (S)-(-)-N-(1-Phenyleth-1-yl)amine (14.1 g, 0.12 mol) and potassium carbonate (78.8 g, 0.57 mol) in THF (100 mL) was added a solution ethyl chloroformate (18.9 g, 0.18 mol) in THF (30 mL), dropwise, with stirring at 0 °C. After 2 h the reaction was warmed to 25 °C and stirred at this temperature for 6 h. Water (100 mL) was added and the organic layer was separated and washed with water. The aqueous extracts were washed ether. The ethereal extracts were dried over anhydrous sodium sulfate and concentrated *in vacuo* to yield 30.0 g (99%) of the corresponding carbamate.  $^1\text{H}$  NMR ( $\text{CDCl}_3$ ) 1.20 (t, J = 7 Hz, OCCH<sub>3</sub>, 3H), 1.48 (d, J = 6.6 Hz, PhCCH<sub>3</sub>, 3H), 4.08 (q, J = 7.0 Hz, OCH<sub>2</sub>, 2H), 4.82 (m, PhCH, 1H), 5.13 (s, NH, 1H), 7.30 (m, Aromatic, 5H) ppm;  $^{13}\text{C}$  NMR ( $\text{CDCl}_3$ ) 14.1 (CCH<sub>3</sub>), 21.9 (PhCCH<sub>3</sub>), 50.0 (PhCH), 60.1 (OCH<sub>2</sub>), 125.5, 126.5, 127.9 (aromatic CH), 143.7 (aromatic C), 155.6 (NCOO) ppm; mass spectrum m/e (relative intensity) 193 ( $\text{M}^+$ , 47), 178 (100), 164 (88), 120 (66), 106 (98), 77 (61).

To a stirred mixture of lithium aluminum hydride (4.7 g, 0.12 mol) in THF (100 mL) at 0 °C was added, dropwise, a solution of the carbamate (15.2 g, 79.2 mmol) in THF (40 mL). The solution was warmed to 25 °C

and stirred at this temperature for 7 h. Ether (200 mL), water (8 mL) and 0.1 N NaOH (7 mL) were successively added. The mixture was filtered through celite and the precipitate was washed with ether (160 mL) and chloroform (80 mL). The filtrate and washings were dried over anhydrous sodium sulfate and concentrated *in vacuo* giving a residue which was subjected to distillation (25 °C, 0.01 mm) to yield 9.7 g (91%) of the known (Cervinka et al., 1968) phenethyl amine **21**. IR (neat) 3280 (N-H), 3100 (aromatic C-H), 2940 (C-H)  $\text{cm}^{-1}$ ;  $^1\text{H}$  NMR ( $\text{CDCl}_3$ ) 1.33 (d,  $J = 6.7$  Hz  $\text{PhCCH}_3$ , 3H), 1.35 (s, NH, 1H), 2.29 (s,  $\text{NCH}_3$ , 3H), 3.62 (q,  $J = 6.6$  Hz,  $\text{PhCH}$ , 1H), 7.25 (m, aromatic H, 5H) ppm;  $^{13}\text{C}$  NMR ( $\text{CDCl}_3$ ) 23.8 ( $\text{PhCCH}_3$ ), 34.4 ( $\text{NCH}_3$ ), 60.2 ( $\text{PhCH}$ ), 126.5, 126.8, 128.3 (aromatic CH), 145.3 (aromatic C) ppm; mass spectrum  $m/e$  (relative intensity) 134 ( $[\text{M}+1]^+$ , 20), 120 (100), 105 (22), 77 (30).

**( $\text{S}_p, \text{S}_c$ )- and ( $\text{R}_p, \text{S}_c$ )-*N,P*-Dimethyl-*N*-(1-Phenylethyl)-*O*-[2-(Trimethylsilyl)ethyl Phosphoramidothioate (**22a** and **22b**).**

To a stirred solution of (*S*)-*N*-methyl-*N*-(1-phenylethyl)amine **21** (2.20 g, 16.3 mmol) in THF (100 mL) was added, dropwise, *n*-butyllithium (1.2 M, 11.3 mL, 13.6 mmol) at -78 °C. To this solution was added, dropwise, a solution of the methylphosphonochloridate **20** (3.13 g, 13.6 mmol) in THF (2 mL). The reaction mixture was stirred for 5 h. after which time ether (20 mL) and water (20 mL) were added. The organic layer was separated, washed successively with water and brine, dried over anhydrous sodium sulfate and concentrated *in vacuo*. The resulting residue was subjected to flash silica chromatography (4% ether in cyclohexane) affording 3.86 g (86%) of a mixture of the thiophosphoramidate diastereomers **22a** and **22b**. The diastereomeric mixture was then subjected to HPLC

chromatography (silica gel, 4% ether in cyclohexane) to give 1.53 g (34%) of the first eluting diastereomer, **22a**, and 1.34 g (30%) of the second eluting diastereomer, **22b**.

**22a**: IR (neat) 2920 (C-H), 1290 (P-C), 1050 (P-O-C), 970 (P-O-C), 620 (P=S)  $\text{cm}^{-1}$ ;  $^1\text{H}$  NMR ( $\text{CDCl}_3$ ) 0.02 (s,  $\text{SiCH}_3$ , 9H), 1.00 (m,  $\text{CH}_2\text{Si}$ , 2H), 1.48 (d,  $J = 7$  Hz  $\text{PhCH}_3$ , 3H), 1.73 (d,  $J = 14.6$  Hz,  $\text{PCH}_3$ , 3H), 2.36 (d,  $J = 10.0$  Hz,  $\text{NCH}_3$ , 3H), 3.80 (m,  $\text{POCH}_A$ , 1H), 4.11 (m,  $\text{POCH}_B$ , 1H), 5.58 (m,  $\text{PhCH}$ , 1H), 7.25 (m, aromatic H, 5H) ppm;  $^{13}\text{C}$  NMR ( $\text{CDCl}_3$ ) -1.4 ( $\text{SiCH}_3$ ), 16.8 ( $\text{PhCCH}_3$ ), 19.3 (d,  $J = 7.5$  Hz,  $\text{SiCH}_2$ ), 20.3 (d,  $J = 109.0$  Hz,  $\text{PCH}_3$ ), 26.9 (d,  $J = 15.3$  Hz,  $\text{PNCH}_3$ ), 53.2 (d,  $J = 6.1$  Hz,  $\text{PhC}$ ), 61.7 (d,  $J = 4.9$  Hz,  $\text{POCH}_2$ ), 127.0, 127.2, 128.2 (aromatic CH), 141.4 (d,  $J = 5.3$  Hz, aromatic C) ppm;  $^{31}\text{P}$  NMR ( $\text{CDCl}_3$ ) +85.2 ppm; mass spectrum  $m/e$  (relative intensity) 330 ( $[\text{M}+1]^+$ , 100) 113 (19), 85 (53), 81 (64); HRMS  $m/e$  330.1480 ( $\text{M}+1$ ) ( $\text{C}_{15}\text{H}_{28}\text{NOPSSi}$  requires 330.1477).

**22b**: IR (neat) 2920 (C-H), 1290 (P-C), 1050 (P-O-C), 970 (P-O-C), 620 (P=S)  $\text{cm}^{-1}$ ;  $^1\text{H}$  NMR ( $\text{CDCl}_3$ ) -0.03 (s,  $\text{SiCH}_3$ , 9H), 0.87 (m,  $\text{SiCH}_A$ , 1H), 1.00 (m,  $\text{SiCH}_B$ , 1H), 1.44 (d,  $J = 7.0$  Hz,  $\text{PhCCH}_3$ , 3H), 1.77 (d,  $J = 14.4$  Hz,  $\text{PCH}_3$ , 3H), 2.37 (d,  $J = 10.0$  Hz,  $\text{PNCH}_3$ , 3H), 3.68 (m,  $\text{POCH}_A$ , 1H), 4.09 (m,  $\text{POCH}_B$ , 1H), 5.53 (m,  $\text{PhCH}$ , 1H), 7.21 (aromatic H, 1H), 7.30 (aromatic H, 2H) 7.38 (aromatic H, 2H) ppm;  $^{13}\text{C}$  NMR ( $\text{CDCl}_3$ ) -1.6 ( $\text{SiCH}_3$ ), 16.3 (d,  $J=2.1$  Hz,  $\text{PhCCH}_3$ ), 18.9 (d,  $J= 7.5$  Hz,  $\text{SiCH}_3$ ), 21.2 (d,  $J=107.5$  Hz,  $\text{PCH}_3$ ), 26.7 (d,  $J=2.8$  Hz,  $\text{NCH}_3$ ), 53.3 (d,  $J=6.4$  Hz,  $\text{PhCH}$ ), 61.6 (d,  $J=6.9$  Hz,  $\text{POCH}_2$ ), 126.9, 127.4, 128.1 (aromatic), 141.5 (d,  $J=4.6$  Hz, aromatic), 186.4 (d,  $J = 5.3$  Hz,  $\text{PCCO}$ ) ppm;  $^{31}\text{P}$  NMR ( $\text{CDCl}_3$ ) + 84.5 ppm; mass spectrum  $m/e$  (relative intensity) 330 ( $[\text{M}+1]^+$ , 100), 302 (73),

113 (31), 85 (53), 81 (65); HRMS m/e 330.1480 (M+1)  
(C<sub>15</sub>H<sub>28</sub>NOPSSirequires 330.1477).

**(SP,SC)-N,P-Dimethyl-N-(1-Phenylethyl)-S-[2-(4-Nitrophenyl)-2-Oxoethyl] Phosphonamidothioate (40) for X-Ray**

**Analysis** To a stirred solution of the thiophosphonamidate diastereoisomer **22a** (0.32 g, 0.98 mmol) in acetonitrile (10 mL) was added cesium fluoride (0.74 g, 4.88 mmol). The mixture was stirred at reflux for 5 h. After cooling to 25 °C the solution was filtered through anhydrous sodium sulfate and concentrated *in vacuo* to yield 0.34 g (88%) of the cesium salt of desilyethylated **22a**.

**(SP,SC)-N,P-Dimethyl-N-(1-Phenylethyl) Phosphonamidothioic Acid.** IR (neat) 3300 (O-H), 3050 (aromatic C-H), 2980 (C-H), 620 (P=S) cm<sup>-1</sup>; <sup>1</sup>H NMR (CDCl<sub>3</sub>) 1.37 (d, J = 7.1 Hz, PhCCH<sub>3</sub>, 3H), 1.45 (d, J = 13.1 Hz, PCH<sub>3</sub>, 3H), 2.44 (d, J = 10.8 Hz, PNCH<sub>3</sub>, 3H), 5.11 (m, PhCH, 1H), 7.20 (m, aromatic H, 5H) ppm; <sup>13</sup>C NMR (CDCl<sub>3</sub>) 17.9 (PhCCH<sub>3</sub>), 25.2 (d, J = 92.2 Hz, PCH<sub>3</sub>), 27.9 (d, J = 5.3 Hz, PNCH), 52.6 (d, J = 3.3 Hz, PhCH), 126.6, 127.4, 128.3 (aromatic CH), 142.6 (aromatic C) ppm; <sup>31</sup>P NMR (CD<sub>3</sub>Cl) + 65.5 ppm.

To a solution of the cesium salt of desilyethylated **22a** (0.13 g, 0.32 mmol) in acetonitrile (4 mL) was added p-nitrophenacyl bromide (0.078 g, 0.32 mmol). The solution was stirred at 25 °C for 12 h. Water (1 mL) was added and the resulting solution was extracted with chloroform. The chloroform extracts were dried over anhydrous sodium sulfate and concentrated *in vacuo* to yield 0.13 g (93%) of the desired p-nitrophenacyl thioester **40** (mp, 106-108 °C, benzene). IR (CHCl<sub>3</sub>) 3050 (aromatic C-H), 2950 (C-H), 1690 (C=O), 1520 (ArN-O), 1340 (ArN-O) cm<sup>-1</sup>; <sup>1</sup>H NMR

(CDCl<sub>3</sub>) 1.57 (d, J = 6.9 Hz, PhCCH<sub>3</sub>, 3H), 1.89 (d, J = 14.4 Hz, PCH<sub>3</sub>, 3H), 2.50 (d, J = 11.7 Hz, PhNCH<sub>3</sub>, 3H), 4.16 (dd, J = 11.2, 15.8 Hz, PSCHA, 1H), 4.34 (dd, J = 11.2, 15.8 Hz, PSCHB, 1H), 5.03 (m, PhCH, 1H), 7.35 (m, aromatic CH, 5H), 8.12, 8.30 (m, NO<sub>2</sub>-aromatic CH, 4H) ppm; <sup>13</sup>C NMR (CDCl<sub>3</sub>) 17.6 (PhCH<sub>3</sub>), 19.9 (d, J = 99.5 Hz, PCH<sub>3</sub>), 27.1 (PNCH<sub>3</sub>), 36.7 (d, J = 3.7 Hz, PSCH<sub>2</sub>), 52.9 (d, J = 2.8 Hz, PhCH), 123.8, 127.3, 127.4, 128.5, 129.8 (aromatic CH), 139.8 (aromatic C), 140.7 (d, J = 3.9 Hz, aromatic C), 150.6 (aromatic C), 192.8 (d, J = 3.4 Hz, CO) ppm; <sup>31</sup>P NMR (CDCl<sub>3</sub>) + 45.6 ppm; mass spectrum m/e (relative intensity) 393 ([M+1]<sup>+</sup>, 23), 289 (21), 257 (44), 268 (100), 213 (41), 196 (74); HRMS m/e 393.1049 (M+1) (C<sub>18</sub>H<sub>21</sub>N<sub>2</sub>O<sub>4</sub>PS requires 393.1038).

**X-Ray Analysis of (SP,SC)-N,P-Dimethyl-N-(1-Phenylethyl)-S-[2-(4-Nitrophenyl)-2-Oxoethyl] Phosphonamidothioate (40).**<sup>103</sup> This compound was crystalized from benzene, providing a 0.1x0.2x0.4 mm specimen for X-ray crystallographic experiments. An Enraf-Nonius CAD4 diffractometer with CuK $\alpha$  radiation ( $\lambda=1.5418$  A<sup>0</sup>); incident beam graphite monochromator was used for data collection. The cell parameters and crystal orientation from 25 automatically centered reflections are: a=6.940(1), b=7.6412(6), c=36.356(6) A<sup>0</sup>; orthorhombic space group: P2<sub>1</sub>2<sub>1</sub>2<sub>1</sub>, Z=4.  $\rho_{\text{calcd}}=1.35$  g cm<sup>-3</sup> for C<sub>18</sub>H<sub>21</sub>N<sub>2</sub>O<sub>4</sub>PS (mol wt 392.4.  $\mu=24.5$  g cm<sup>-1</sup>. 2 $\theta$ - $\theta$  scans over  $\theta$  range of 1.5(0.7+0.14 tan  $\theta$ ); maximum  $\theta$  of 120<sup>0</sup>. The diffractometer was controlled by standard Enraf-Nonius programs (version 5.0); each scan was recorded in 96 steps with two outmost 16 step counts used for background calculations. Seven standard intensities were measured at 1 h

intervals of crystal X-ray exposure. The standard intensity change range and average was -1.9 to 0.6% and -0.5%. Eighteen hundred and fifty total data were measured (includes space group absences); 1731 unique data; 1498  $I > 3\sigma(I)$ . All crystallographic calculations were performed with the TEXSAN program system<sup>118</sup> on a DEC MicroVax II computer. The structure was solved with the MITHRIL<sup>119</sup> link incorporated in TEXSAN. Full matrix least squares refinement:  $\Sigma(\sigma^{-2}(F_o)(F_o-F_c)^2)$  minimized ; anisotropic temperature factors for C, O, N, P and S and isotropic terms for H; reflections with  $I < 3\sigma(I)$  excluded from refinement; final R,  $R_{wtd}$ , goodness-of-fit and  $\Delta/\sigma$  of 0.036, 0.042, 1.62 and 0.06. Maximum and minimum values in final  $\Delta\rho$  map of 0.18 and -0.17  $eA^{-3}$ . Atomic scattering factors were obtained from the International Tables for X-ray Crystallography (1974). A Table of atomic coordinates and temperature factors, bond lengths and angles and structure factors are given as supplementary material. The PLOTMD program<sup>120</sup> was used to display the ORTEP (Johnson, C. K. (1965) ORTEP, Report ORNL-3794, Oakridge National Laboratory, TN, USA) drawing on a VaxStation II monitor, to label the drawings and to prepare a print for a Hewlett-Packard Laser-Jet II printer. The structure is displayed in Figure 5.

**(S<sub>p</sub>,S<sub>c</sub>)- and (R<sub>p</sub>,S<sub>c</sub>)-3-[[Methyl(1-Phenylethyl)amino]][2-(trimethylsilyl)ethoxy]phosphinothioyl]-2-Oxo-2-(Trimethylsilyl)ethyl Propanoate (23a and 23b).** To each separate, stirred solution of the methylthiophosphonamidate diastereoisomer **22a** or **22b** (0.51 g, 156  $\mu$ mol) in THF (1 mL) was added, dropwise, n-butyllithium (1.2 M, 1.4 mL, 1.7  $\mu$ mol) in hexanes at -78 °C.

After 30 min, cuprous iodide (0.32 g, 1.67 mmol) in THF (5 mL) at  $-78\text{ }^{\circ}\text{C}$  was added to each of the reaction mixtures. The mixtures were warmed to  $-30\text{ }^{\circ}\text{C}$  over 1 h, and stirred at this temperature for 2 h. Solutions of O-(2-trimethylsilyl)ethyl)oxalyl chloride (0.49 g, 2.33 mmol) in ethyl ether (2 mL) were added dropwise to each solution. The reaction mixtures were stirred at  $-30\text{ }^{\circ}\text{C}$  for 7 h, and then warmed to  $25\text{ }^{\circ}\text{C}$ . Water (7 mL) was added and the resulting solutions were filtered through celite. The precipitates were washed with methylene chloride and refiltered. The methylene chloride layers of the filtrate were dried over anhydrous sodium sulfate and concentrated *in vacuo*. The resulting residues were subjected to chromatography on Florisil (25% ether in cyclohexane) yielding 0.32 g (41%) of desired thiophosphonamidates **23a** and **23b**, respectively.

**23a**: IR (neat) 3020 (aromatic C-H), 2940 (C-H), 2900 (C-H), 1720 (C=O)  $\text{cm}^{-1}$ ;  $^1\text{H}$  NMR ( $\text{CDCl}_3$ ) 0.01 (s, SiCH<sub>3</sub>, 9H), 0.02 (s, SiCH<sub>3</sub>, 9H), 1.00 (m, SiCH<sub>2</sub>, 2H), 1.11 (m, SiCH<sub>2</sub>, 2H), 1.51 (d,  $J = 7.0\text{ Hz}$ , PhCCH<sub>3</sub>, 3H), 2.44 (d,  $J = 10.5\text{ Hz}$ , NCH<sub>3</sub>, 3H), 3.62 (dd,  $J = 12.0\text{ Hz}$ ,  $J = 18.0\text{ Hz}$ , PCHA, 1H), 3.77 (dd,  $J = 12.0, 18.0\text{ Hz}$ , PCHB, 1H), 3.84 (m, POCHA, 1H), 4.11 (m, POCHB, 1H), 4.33 (m, COOCH<sub>2</sub>, 2H), 5.48 (m, PhCH, 1H), 7.30 (m, aromatic H, 5H) ppm;  $^{13}\text{C}$  NMR ( $\text{CDCl}_3$ ) -1.7 (SiCH<sub>3</sub>), -1.6 (SiCH<sub>3</sub>), 17.0 (d,  $J = 6.2\text{ Hz}$ , PhCCH<sub>3</sub>), 17.1 (s, SiCH<sub>2</sub>), 19.1 (d,  $J = 6.8\text{ Hz}$ , POCCH<sub>2</sub>), 27.2 (d,  $J = 3.0\text{ Hz}$ , PNCH<sub>3</sub>), 44.1 (d,  $J = 88.7\text{ Hz}$ , PCH<sub>2</sub>), 53.6 (d,  $J = 5.6\text{ Hz}$ , PhCH), 62.9 (d,  $J = 7.0\text{ Hz}$ , POCH<sub>2</sub>), 65.2 (SiC=O) 127.2, 127.3, 128.3 (aromatic CH), 140.5 (aromatic C), 160.9 (COOEtSi), 186.7 (d,  $J = 4.7\text{ Hz}$ , PCCO) ppm;  $^{31}\text{P}$  NMR ( $\text{CDCl}_3$ ) + 72.7 ppm; mass spectrum  $m/e$  (relative intensity) 502 ( $[\text{M}+1]^+$ , 11), 342 (15), 286 (47), 252 (65), 134

(99), 120 (100); HRMS  $m/e$  502.2006 ( $M+1$ ) ( $C_{22}H_{40}O_4NO_4PSSi_2$  requires 502.2033).

**23b:** IR (neat) 3020 (aromatic C-H), 2940 (C-H), 1720 (C=O)  $cm^{-1}$ ;  
 $^1H$  NMR ( $CDCl_3$ ) -0.04 (s,  $SiCH_3$ , 9H), 0.04 (s,  $SiCH_3$ , 9H), 0.85 (m,  $CH_2Si$ , 1H), 0.98 (m,  $CH_2Si$ , 1H), 1.12 (m,  $SiCH_2$ , 2H), 1.45 (d,  $J = 7.1$  Hz,  $PhCCH_3$ , 3H), 2.41 (d,  $J = 10.0$  Hz,  $PNCH_3$ , 3H), 3.60 (dd,  $J = 12.0, 19.9$  Hz,  $PCHA$ , 1H), 3.69 (m,  $POCHA$ , 1H) 3.94 (dd,  $J = 12.0, 19.9$  Hz,  $PCHB$ , 1H), 4.06 (m,  $SiCCH_2$ , 2H), 4.36 (m,  $SiCCH_2$ , 2H), 5.51 (m,  $PhCH$ , 1H), 7.23 (aromatic H, 1H), 7.30 (aromatic H, 2H), 7.39 (aromatic H, 2H) ppm;  
 $^{13}C$  NMR ( $CDCl_3$ ) -1.6 (s,  $SiCH_3$ ), 16.6 ( $PhCH_3$ ), 17.2 ( $SiCH_2$ ), 18.8 (d,  $J = 6.8$  Hz,  $POCCH_2$ ), 26.8 ( $NCH_3$ ) 45.0 (d, 88.8 Hz,  $PCH_2$ ), 53.3 (d,  $J = 6.8$  Hz,  $PhCH$ ), 62.6 (d,  $J = 7.1$  Hz,  $POCH_2$ ), 65.3 ( $SiCCH_2$ ), 127.2, 127.5, 128.2 (aromatic CH), 141.1 (d,  $J = 4.6$  Hz, aromatic C), 161.0 ( $COOEtSi$ ), 187.0 (d,  $J = 4.4$  Hz,  $PCCO$ ) ppm;  $^{31}P$  NMR ( $CDCl_3$ ) + 72.9 ppm; mass spectrum  $m/e$  (relative intensity) 502 ( $[M+1]^+$ , 0.3), 252 (33), 134 (100), 120 (51); HRMS  $m/e$  502.2027 ( $M+1$ ) ( $C_{22}H_{40}NO_4PSSi_2$  requires 502.2033).

(**SP, SC**)- and (**RP, SC**)-3-[[Methyl(1-Phenylethyl)amino]phosphinothioyl]-2-Oxo-2-Propanoic Acid (**24a** and **24b**). To each separate, stirred solution of **23a** or **23b** (0.32 g, 0.64 mmol) in dry acetonitrile (2 mL) was added a mixture of cesium fluoride (0.20 g, 1.30 mmol) and 18-crown-6 (0.17 g, 0.64 mmol) in acetonitrile (3 mL) under a nitrogen atmosphere. The mixtures were stirred at 25 °C for 24 h. The precipitates were separated by decantation and washed repetitively with dry acetonitrile to remove 18-crown-6. This

afforded 0.21 g (56%) of each of the pure deprotected thiophosphonamidate diastereomers, **24a** and **24b**.

**24a**:  $^1\text{H}$  NMR (DMSO- $d_6$ ) 1.36 (d,  $J = 7.0$  Hz, PhCCH $_3$ , 3H), 2.30 (d,  $J = 10.4$  Hz, PNCH $_3$ , 3H), 3.12 (dd,  $J = 10.6$  Hz,  $J = 15.5$  Hz, PCHA, 1H), 3.26 (dd,  $J = 10.6$  Hz,  $J = 15.5$  Hz, PCHB, 1H), 5.25 (m, PhCH, 1H), 7.30 (m, aromatic CH, 5H) ppm;  $^{31}\text{P}$  NMR (DMSO- $d_6$ ) + 57.2 ppm.

**24b**:  $^{31}\text{P}$  NMR (DMSO- $d_6$ ) +57.0 ppm.

**Preparation of the (Rp)- and (Sp)-[P= $^{18}\text{O}$ ]Thiophosphonopyruvates (31a and 31b) by Hydrolysis of 24a and 24b in [ $^{18}\text{O}$ ]H $_2\text{O}$ .** Compounds **24a** and **24b** (0.134 g, 0.24 mmol) were mixed with [ $^{18}\text{O}$ ] H $_2\text{O}$  (98%) (1250  $\mu\text{L}$ , 62.5 mmol) and HCl (12 M, 45  $\mu\text{L}$ , 0.54 mmol) then immediately quenched with 1.3 mL of D $_2\text{O}$  containing K $_2\text{HPO}_4$  (80 mM), MgCl $_2$  (5 mM), dithiothreitol (0.8 mM) and sufficient KOH to bring the pH of the resulting solutions 8.0. This procedure yielded from **24a** (Rp)-[P= $^{18}\text{O}$ ]thiophosphonopyruvate (**31a**) (0.17 mmol), and [P= $^{18}\text{O}_2$ ]phosphonopyruvate (0.07 mmol) and from **24b** (Sp)-[P= $^{18}\text{O}$ ]thiophosphonopyruvate **31b** (0.17 mmol) and [P= $^{18}\text{O}_2$ ]phosphonopyruvate (0.07 mmol).  $^{31}\text{P}$  NMR (D $_2\text{O}$ ) + 44.8 ppm (t,  $J = 18.2$  Hz) for **31a** and **31b** and +10.6 ppm (t,  $J=20.4$  Hz) for the phosphonopyruvate. These samples were used without purification.

**Selective Op-Detrimethylsilylethylation of 23a.** To a stirred mixture of cesium fluoride (0.11g, 657  $\mu\text{mol}$ ) and 18-crown-6 (0.17 g, 657  $\mu\text{mol}$ ) in dry acetonitrile (5 mL) was added a solution of thiophosphonamidate **23a** (0.33 g, 657  $\mu\text{mol}$ ) in dry acetonitrile (3 mL).

The reaction mixture was stirred at 25 °C for 3 h and then centrifuged (14,000 g X 2 min). The supernatant was concentrated *in vacuo* to yield a residue containing the desired mono-deblocked thiophosphonamidate (**42a**) (61%) ( $^{31}\text{P}$  NMR ( $\text{CDCl}_3$ ) +53.7 and +62.4 ppm for the keto and enol forms), the enol form of unreacted **23a** (25%) ( $^{31}\text{P}$  NMR ( $\text{CDCl}_3$ ) +81.1 ppm) and the OC-detrimethylsilylethylated derivative (**43a**) (12%) ( $^{31}\text{P}$  NMR( $\text{CDCl}_3$ ) +76.3 ppm).

**[P= $^{18}\text{O}$ ]Thiophosphonopyruvates (31a and 31b) by Hydrolysis of OP-Desilylethyl-23a (42a) in [ $^{18}\text{O}$ ]H $_2\text{O}$ .** To the mixture containing OP-desilylethyl 12a (400  $\mu\text{mol}$ ) was added [ $^{18}\text{O}$ ] H $_2\text{O}$  (98%) (69  $\mu\text{L}$ ) and *p*-toluenesulfonic acid (0.122 g, 640  $\mu\text{mmol}$ ). After 20 min at 25 °C the mixture was diluted with 100 mL of Hepes buffer (100 mM) and the pH of the resulting solution was adjusted to 8 with KOH solution.  $^{31}\text{P}$  NMR ( $\text{D}_2\text{O}$ ) analysis the product mixture revealed that it contained 10% of the desired [P= $^{18}\text{O}$ ]thiophosphonopyruvate (+44.8 ppm) along with the OP-trimethylsilylethyl ester of [P= $^{18}\text{O}$ ]thiophosphonopyruvate (35%, +64.0 ppm), thiophosphate (34%, +35.6 ppm) and phosphonopyruvate (12%, +10.6 ppm).

**( $\text{S}_\text{p}, \text{S}_\text{c}$ )- and ( $\text{R}_\text{p}, \text{S}_\text{c}$ )-3-[[Methyl(1-Phenylethyl)amino]][2-(Trimethylsilyl)ethoxy]phosphinothioyl]-2-Oxo-(2-Propyl)propanoate (45a and 45b).**

To each stirred solution of **22a** and **22b** (0.20 g, 0.61 mmol) in THF (1 mL) was added, dropwise, *n*-butyllithium (1.2 M, 0.56 mL, 0.67 mmol) in hexanes at -78 °C. After 30 min, cuprous iodide (0.13 g, 0.67 mmol) in

THF (5 mL) was added. The mixtures were warmed to  $-30\text{ }^{\circ}\text{C}$  over 1 h, and stirred at this temperature for 2 h. Solutions of the known  $^{11}\text{B}$  2-propyl oxalyl chloride (0.12 g, 0.8 mmol) in ether (2 mL) were added dropwise to the mixtures, and each was stirred at  $-30\text{ }^{\circ}\text{C}$  for 7 h and then warmed to  $25\text{ }^{\circ}\text{C}$ . Water (7 mL) was added and the resulting solutions were filtered through celite. The precipitates were washed with methylene chloride (20 mL) and the filtrates were refiltered. The methylene chloride layers were separated, dried over anhydrous sodium sulfate and concentrated *in vacuo*. The resulting residues were subjected to chromatography on Florisil (30% ether in cyclohexane) to yield (40%) in pure form the individual thiophosphonamidate esters **45a** and **45b**.

**45a**: IR (neat) 3020 (aromatic C-H), 2940 (C-H), 1750 (C=O), 1720 (O=C-OR)  $\text{cm}^{-1}$ ;  $^1\text{H}$  NMR ( $\text{CDCl}_3$ ) -0.01 (s,  $\text{Si}(\text{CH}_3)_3$ , 9H), 1.00 (m,  $\text{SiCH}_2$ , 2H), 1.33 (d,  $J = 6.3\text{ Hz}$ ,  $\text{COC}(\text{CH}_3)_2$ , 6H), 1.49 (d,  $J = 7.0\text{ Hz}$ ,  $\text{PhCCH}_3$ , 3H), 2.42 (d,  $J = 10.5\text{ Hz}$ ,  $\text{PNCH}_3$ , 3H), 3.59 (dd,  $J = 20.6, 12.0\text{ Hz}$ ,  $\text{PCH}_2$ , 1H), 3.76 (dd,  $J = 20.6, 12.0\text{ Hz}$ ,  $\text{PCH}_2$ , 1H), 3.84 (m,  $\text{POCH}_A$ , 1H), 4.10 (m,  $\text{POCH}_B$ , 1H), 5.12 (m,  $\text{COCH}$ , 1H), 5.48 (m,  $\text{PhCH}$ , 1H), 7.30 (m, aromatic H, 5H) ppm;  $^{13}\text{C}$  NMR ( $\text{CDCl}_3$ ) - 1.6 ( $\text{SiCH}_3$ ), 17.0 (d,  $J=2.5\text{ Hz}$ ,  $\text{PhCCH}_3$ ), 19.0 (d,  $J = 6.5\text{ Hz}$ ,  $\text{SiCH}_2$ ), 21.4 (d,  $J=2.8\text{ Hz}$ ,  $\text{COCCH}_3$ ), 27.2 (d,  $J = 2.8\text{ Hz}$ ,  $\text{PNCH}_3$ ), 44.9 (d,  $J = 88.2\text{ Hz}$ ,  $\text{PCH}_2$ ), 53.6 (d,  $J = 6.5\text{ Hz}$ ,  $\text{PhCH}$ ), 62.8 (d,  $J = 7.1\text{ Hz}$ ,  $\text{POCH}$ ), 70.9 ( $\text{COCH}$ ), 127.3, 128.3 (aromatic CH), 140.6 (d,  $J = 4.9\text{ Hz}$ , aromatic C), 160.3 ( $\text{CO}_2$ ), 186.9 (d,  $J = 4.4\text{ Hz}$ ,  $\text{PCCO}$ ) ppm;  $^{31}\text{P}$  NMR ( $\text{CDCl}_3$ ) +76.4 ppm; mass spectrum; HRMS  $m/e$  444.1787 ( $\text{M}+1$ ) ( $\text{C}_{20}\text{H}_{34}\text{NO}_4\text{PSSi}$  requires 444.1794).

**45b**: IR (neat) 3050 (aromatic C-H), 2950 (CH), 1750 (C=O), 1720 (O=C-OR)  $\text{cm}^{-1}$ ;  $^1\text{H}$  NMR ( $\text{CDCl}_3$ ) 0.08 (s,  $\text{Si}(\text{CH}_3)_3$ , 9H), 0.88 (m,  $\text{CH}_2\text{Si}$ ,

2H), 1.31 (d, J = 6.3, OC(CH<sub>3</sub>)<sub>2</sub>, 6H), 1.42 (d, J = 7.1 Hz, PhCHCH<sub>3</sub>, 3H), 2.37 (d, J = 10.1 Hz NCH<sub>3</sub>, 3H), 3.57 (dd, J = 19.4, 12.0 Hz, PCH<sub>2</sub>, 1H), 3.65 (m, POCH<sub>2</sub>, 1H), 3.91 (dd, J = 19.9, 12.0 Hz, PCH<sub>2</sub>, 1H), 4.05 (m, POCH<sub>2</sub>, 1H), 5.64 (m, PhCH, 1H), 7.28 (m, aromatic CH, 5H) ppm. <sup>13</sup>C NMR (CDCl<sub>3</sub>) -1.62 (s, SiCH<sub>3</sub>), 16.1 (d, J = 2.1, PhCH<sub>3</sub>), 18.9 (d, J = 6.4 Hz, CH<sub>2</sub>Si), 21.5 (s, OCH(CH<sub>3</sub>)<sub>2</sub>), 26.8 (s, NCH<sub>3</sub>), 45.1 (d, J = 88.1 Hz, PCH<sub>2</sub>), 53.6 (d, J = 6.9 Hz, PhCH), 62.6 (d, J = 7.4 Hz, POCH<sub>2</sub>), 71.1 (s, OCC<sub>2</sub>H<sub>3</sub>), 127.2, 127.6, 128.2 (aromatic CH), 141.1 (d, J = 4.5 Hz, aromatic C), 160.4 (s, CO<sub>2</sub>), 187.2 (d, J = 4.6 Hz, PCCO) ppm; <sup>31</sup>P NMR (CDCl<sub>3</sub>) +75.8 ppm; mass spectrum m/e (relative intensity) 502 ([M+1]<sup>+</sup>, 11), 342 (15), 286 (47), 252 (65), 134 (99), 120 (100); HRMS m/e 444.1777 (M+1) (C<sub>20</sub>H<sub>34</sub>NO<sub>4</sub>PSSi requires 444.1794).

**(S<sub>P</sub>, S<sub>C</sub>)- and (R<sub>P</sub>, S<sub>C</sub>)-3-[[Methyl(1-Phenylethyl)amino]phosphinothioyl]-2-Oxo-(2-Propyl)propanoate (46a and 46b).** To each stirred solution of **45a** and **45b** (90 mg, 0.20 mmol) in dry acetonitrile (2mL) were added cesium fluoride (32 mg, 0.21 mmol) and 18-crown-6 (54 mg, 0.20 mmol) in dry acetonitrile (3 mL) under a nitrogen atmospheres. The reaction mixtures were stirred for 30 h at 25 °C and concentrated *in vacuo* to afford the crude thiophosphonamidate esters **46a** and **46b** (85%), respectively.

**46a** (ca. 1:1 mixture of enol and keto tautomers): <sup>1</sup>H NMR (CDCl<sub>3</sub>) 1.18 (d, J = 1.7 Hz, CCH<sub>3</sub>, 3H), 1.20 (d, J = 1.7 Hz, CCH<sub>3</sub>, 3H), 1.26 (d, J = 2.4 Hz, CCH<sub>3</sub>, 3H), 1.27 (d, J = 2.4 Hz, CCH<sub>3</sub>, 3H), 1.43 (d, J = 7.0 Hz, PhCCH<sub>3</sub>, 6H, both tautomers), 2.39 (d, J=10.7 Hz, NCH<sub>3</sub>, 3H), 2.46 (d, J=10.9 Hz, NCH<sub>3</sub>, 3H), 3.48 (dd, J=10.4, 17.7 Hz, PCHA, keto form, 1H),

3.71 (dd,  $J=10.4, 15.2$  Hz, PCHB, keto form, 1H), 4.98 (m, OCH, 1H) and 5.05 (m, OCH, 1H), 5.50 (m, PhCH, 2H), 5.76 (d,  $J = 16.2$  Hz, PCH, enol form, 1H), 7.23 (m, aromatic CH, 10H, both tautomers);  $^{13}\text{C}$  NMR ( $\text{CDCl}_3$ ) 17.0 (PhCCH<sub>3</sub>), 17.4 (PhCCH<sub>3</sub>), 21.5 (CCH<sub>3</sub>), 21.7 (CCH<sub>3</sub>), 27.1 (d,  $J = 4.9$  Hz, NCH<sub>3</sub>), 27.5 (d,  $J = 4.9$  Hz, NCH<sub>3</sub>), 50.8 (d,  $J = 63.0$  Hz, PCH<sub>2</sub>), 52.3 (PhCH, both tautomers), 69.5 (OCH, both tautomers), 107.0 (d,  $J = 118$  Hz, PCH enol form), 125.8, 126.5, 127.2, 127.6, 127.7, 128.3 (aromatic C-H, both tautomers), 143.6 (aromatic C), 150.8 (aromatic C), 161.7 (CO<sub>2</sub>), 163.8 (d,  $J = 18.7$ , PCCO, enol form), 190.8 (d,  $J = 5.3$ , PCCO, keto form) ppm;  $^{31}\text{P}$  NMR ( $\text{CH}_3\text{CN}$ ) +54.2, +61.8 ppm. (keto and enol forms).

**46b** (ca. 1:1 mixture of enol and keto tautomers):  $^1\text{H}$  NMR ( $\text{CDCl}_3$ ) 1.24 (d,  $J = 6.2$  Hz, OCHCH<sub>3</sub>, 6H), 1.28 (d,  $J = 6.2$  Hz, COCHCH<sub>3</sub>, 3H), 1.29 (d,  $J = 6.2$  Hz, COCHCH<sub>3</sub>, 3H), 1.46 (d,  $J=6.9$  Hz, PhCCH<sub>3</sub>, 3H), 1.47 (d,  $J=7.0$  Hz, PhCCH<sub>3</sub>, 3H), 2.38 (d,  $J = 10.4$  Hz, NCH<sub>3</sub>, 3H), 2.43 (d,  $J = 10.7$ , NCH<sub>3</sub>, 3H), 3.66 (dd,  $J=10.5, 19.2$  Hz, PCHA, keto form, 1H), 3.71 (dd,  $J=10.5, 19.2$ , PCHB, keto form, 1H), 5.05, (m, OCH, 2H), 5.55 (m, PhCH, 2H), 5.80 (d,  $J = 16.5$  Hz, PCH enol form, 1H), 7.25 (m, aromatic CH, 10H) ppm;  $^{13}\text{C}$  NMR ( $\text{CDCl}_3$ );  $^{31}\text{P}$  NMR ( $\text{CDCl}_3$ ) +55.0 (keto form) and +61.6 ppm (enol form).

**Formation of the  $[\text{P}=\text{}^{18}\text{O}]$ Thiophosphonopyruvates (31a and 31b) by Hydrolysis of 46a and 46b in  $\text{H}_2^{18}\text{O}$ .** The monocationic salts **46a** and **46b** were separately dissolved in mixtures of  $\text{H}_2^{18}\text{O}$  (250  $\mu\text{l}$ ) and THF (25  $\mu\text{l}$ ). The resulting solutions were added to 1 mL of Dowex-50 [ $\text{H}^+$ ] resin to which HCl (22  $\mu\text{l}$ , 12 M, 90  $\mu\text{mol}$ ) had been added. The mixtures were incubated at 4° C for 40 min and then diluted

with 250  $\mu\text{L}$  of HEPES solution (200 mM) and the pH of the resulting solutions was adjusted to 8.  $^{31}\text{P}$ -NMR analysis of the product mixtures revealed that the desired [S,  $^{18}\text{O}$ ,  $^{16}\text{O}$ -P]thiophosphonopyruvates **31a** and **31b** were formed in an *ca.* 10% yield. These compounds were used in subsequent experiments without purification.

**Enzymatic Conversion of the (Rp)- and (Sp)-[P= $^{18}\text{O}$ ]Thiophosphonopyruvates (31a and 31b) to the [P= $^{18}\text{O}$ ]Thiophosphoenolpyruvates (29a and 29b).** The (Sp)- and (Rp)-[P= $^{18}\text{O}$ ]thiophosphonopyruvates (**31a** and **31b**) (170  $\mu\text{mol}$ ), derived from the  $\text{H}_2^{18}\text{O}$  hydrolysis of either **24a** and **24b** (170  $\mu\text{mol}$ ) or **46a** and **46b** (17  $\mu\text{mol}$ ), were separately reacted at 25°C with 1.8 units of PEP phosphomutase in a 5 mL solution of 5 mM  $\text{MgCl}_2$ , 0.8 mM dithiothreitol and 50 mM  $\text{K}^+$ HEPES (pH 8.0) in 50%  $\text{D}_2\text{O}$ . The formation of thiophosphoenolpyruvates **29a** and/or **29b** was complete within 7 h ( $^{31}\text{P}$  NMR). In the case of the catalyzed reaction of the (Sp)-[P= $^{18}\text{O}$ ]thiophosphonopyruvate generated from the  $\text{H}_2^{18}\text{O}$  hydrolysis of OP-desilylethyl-**23a** (**42a**),  $\text{MgCl}_2$  (to a final concentration of 2.5 mM) and PEP phosphomutase (0.08U) were added directly to the buffered hydrolysate. The  $^{31}\text{P}$  NMR ( $\text{D}_2\text{O}$ , pH 8) analysis of the resulting reaction mixtures revealed that they contained both [P= $^{18}\text{O}$ ]thiophosphoenolpyruvate (+39.4 ppm) (12%) and PEP (-0.2 ppm) ( 3 9 % ) .

**Enzymatic Conversion of [P= $^{18}\text{O}$ ]Thiophosphoenolpyruvates 29a and/or 29b to [ $\gamma$ - $^{18}\text{O}$ -**

**P]ATPS.** Samples of [ $P=^{18}O$ ]thiophosphoenolpyruvate (17 - 170  $\mu\text{mol}$ ) generated by reaction of **31a** and **31b** with PEP phosphomutase were converted directly to [ $\gamma\text{-}^{18}O\text{-P}$ ]ATP $\gamma\text{S}$  by incubation with ADP (15 - 25 mM),  $\text{MgCl}_2$  (2.5 mM) and pyruvate kinase (250 - 2000 units) in 1 mL  $\text{K}^+\text{HEPES}$  (50 mM, pH 8.0) at 25  $^\circ\text{C}$  for 12 h. The [ $\gamma\text{-}^{18}O\text{-P}$ ]ATP $\gamma\text{S}$  was purified from the reaction mixture by chromatography on a (2 x 40 cm) DEAE Sephadex A-25 column with 1.5 L of a linear gradient of TEAB, 0.15 M to 0.70 M at pH 8.1 serving as the eluant. Fractions containing [ $\gamma\text{-}^{18}O\text{-P}$ ]ATP $\gamma\text{S}$  were pooled and concentrated *in vacuo*. The residue was dissolved in 10 mL of water and concentrated. This process was repeated four times in order to remove residual TEAB. The yield of the [ $\gamma\text{-}^{18}O$ ]ATP $\gamma\text{S}$  was estimated by  $^{31}\text{P}$ -NMR to be ca. 70%.

The [ $\gamma\text{-}^{18}O\text{-P}$ ]ATP $\gamma\text{S}$  (15 - 110  $\mu\text{mol}$ ) was converted to [ $\beta\text{-}^{18}O\text{-P}$ ]ADP $\beta\text{S}$  by reaction with myokinase (500 units) in a 5 mL solution containing 10 mM  $\text{MgCl}_2$ , 0.1 mM dithiothreitol, 15-120 mM AMP and 50 mM Tris-HCl (pH 8.0). The progress of the reaction was monitored by  $^{31}\text{P}$  NMR. After 1 h at 25  $^\circ\text{C}$  the reaction was ca. 80% complete. The [ $\beta\text{-}^{18}O\text{-P}$ ]ADP $\beta\text{S}$  was purified from the reaction mixture by chromatography on a DEAE Sephadex A-25 column (1.5 x 35 cm) equilibrated with 0.10 M TEAB (pH 8.1). The column was eluted with a 1.5 L linear gradient of TEAB (0.10 M to 0.4 M) . Fractions containing [ $\beta\text{-}^{18}O\text{-P}$ ]ADP $\beta\text{S}$  were pooled and concentrated *in vacuo*. Residual TEAB was removed by dissolving the residue in 10 mL of water followed by concentration *in vacuo*. The yield of [ $\beta\text{-}^{18}O\text{-P}$ ]ADP $\beta\text{S}$  was estimated by  $^{31}\text{P}$  NMR analysis to be ca. 60%. The [ $\beta\text{-}^{18}O\text{-P}$ ]ADP $\beta\text{S}$  (7-70  $\mu\text{mol}$ ) was converted to (SP)-[ $\beta\text{-}^{18}O\text{-P}$ ]ATP $\beta\text{S}$  by incubation in a 5 mL (50%  $\text{D}_2\text{O}$ , 25  $^\circ\text{C}$ ) solution containing  $\text{MgCl}_2$  (4 mM),

KCL (380 mM), dithiothreitol (0.8 mM), TRIS-HCl (40 mM, pH 8), PEP (10 - 70  $\mu$ mol) and 250 units of pyruvate kinase. The reaction, monitored by  $^{31}\text{P}$  NMR, and was found to be complete in 12 h. The reaction mixture was concentrated *in vacuo* and the residue obtained was dissolved in 0.5 mL of  $\text{D}_2\text{O}$  containing EDTA (0.2 M) and TRIS-HCl (1 M, pH 8.0) and subjected to  $^{31}\text{P}$  NMR analysis. The spectrum of this substance was obtained on a Bruker AM 400 instrument at 160 MHz with a deuterium field lock; spectral width 11363 Hz; acquisition time 1.44 s; pulse width 8  $\mu$ s; relaxation delay 5s; number of transients, 3000.

**Rapid Quench Experiments.** All solutions were buffered with K<sup>+</sup>HEPES (50 mM, pH 7.5). A buffered solution (43  $\mu$ L) containing PEP mutase, MgCl<sub>2</sub> was mixed via the rapid quench instrument with a buffered solution (43 $\mu$ L) containing [<sup>3</sup>H]P-pyr to give final concentrations after mixing of PEP mutase (20-25  $\mu$ M, Mol. Wt. 78,000), MgCl<sub>2</sub> (5 mM), [<sup>3</sup>H]P-pyr (5  $\mu$ M, specific activity, 40 Ci/mol) After a specified time the solution was quenched with 164  $\mu$ L of K<sup>+</sup>HEPES (20 mM, pH 1.6). Two  $\mu$ L of NaCNBH<sub>3</sub> (1M solution in THF, 2  $\mu$ L, 2  $\mu$ mol) were added to the reaction mixture. After 15 min the pH of the reaction mixture was neutralized with KOH (1M, 10  $\mu$ L). Fifty  $\mu$ L of CCl<sub>4</sub> were added to the resulting solution and it was vortexed to precipitate the protein. After centrifugation the total supernatant was analyzed for radioactive PEP, P-Lac, and lactate by separation using HPLC and quantitation using liquid scintillation counting.

**Control studies to test the efficiency of NaCNBH<sub>3</sub> Reduction of P-pyr and pyruvate** Phosphonopyruvate (75 mM) and phosphoenolpyruvate (75 mM) were reacted separately with 75 mM NaCNBH<sub>3</sub> at 25°C for 15 min at pH 2. After adjusting the pH of the solutions to 8 the reaction products were concentrated *in vacuo* and dissolved in D<sub>2</sub>O.

**Synthesis and Analysis of [<sup>3</sup>H]P-pyr** The phosphonopyruvate was labeled with tritium by exchange of the C-2 protons in 110 Ci/mol [<sup>3</sup>H]water at 25°C at pH 9 (the pH of a solution of Li<sub>3</sub>P-pyr). After 24 h the [<sup>3</sup>H]P-pyr was precipitated with ethanol and dried *in vacuo*, thus producing [<sup>3</sup>H]P-pyr with a specific activity of 40 Ci/mol. A 10  $\mu$ M solution of [<sup>3</sup>H]P-pyr

in 50 mM K<sup>+</sup>HEPES (pH 7.5) was prepared immediately before use in the rapid quench experiments.

The specific activity of the [<sup>3</sup>H]P-pyr was determined to be 40 Ci/mol by spectrophotometric-based analysis of the P-pyr (340 nm, pyruvate kinase/ ADP coupling to PEP mutase catalyzed PEP formation and NADH/ lactate dehydrogenase coupling to pyruvate formation) and tritium counting at an efficiency of 56%.

# APPENDIX

Bond angles ( $^{\circ}$ ) and estimated standard deviations (in parentheses) for compound 40

atom	atom	atom	angle	atom	atom	atom	angle
C8	S	P	99.3(1)	C3	C4	N2	118.8(4)
O1	P	N1	111.6(2)	C5	C4	N2	117.8(4)
O1	P	C18	114.9(3)	C4	C5	C6	117.7(4)
O1	P	S	114.1(1)	C5	C6	C1	121.1(4)
N1	P	C18	109.4(3)	O2	C7	C1	120.1(4)
N1	P	S	107.9(1)	O2	C7	C8	120.9(4)
C18	P	S	98.1(2)	C1	C7	C8	118.9(4)
C9	N1	C11	117.2(3)	C7	C8	S	109.9(3)
C9	N1	P	121.5(3)	N1	C11	C12	110.2(3)
C11	N1	P	120.9(3)	N1	C11	C10	110.8(4)
O4	N2	O3	124.0(5)	C12	C11	C10	114.4(4)
O4	N2	C4	118.1(4)	C13	C12	C17	117.6(5)
O3	N2	C4	117.9(5)	C13	C12	C11	122.9(4)
C6	C1	C2	118.5(4)	C17	C12	C11	119.4(4)
C6	C1	C7	118.7(4)	C14	C13	C12	120.8(5)
C2	C1	C7	122.8(4)	C15	C14	C13	120.8(5)
C3	C2	C1	121.1(4)	C14	C15	C16	119.4(5)
C4	C3	C2	118.1(4)	C17	C16	C15	119.9(5)
C3	C4	C5	123.4(4)	C16	C17	C12	121.5(5)

Table. Bonds distances (Å) and estimated standard deviations (in parentheses) for compound 40

atom	atom	distance	atom	atom	distance
S	C8	1.804(4)	C2	C3	1.373(6)
S	P	2.089(2)	C3	C4	1.366(6)
P	O1	1.472(3)	C4	C5	1.377(6)
P	N1	1.636(3)	C5	C6	1.377(6)
P	C18	1.794(5)	C7	C8	1.499(6)
O2	C7	1.202(5)	C10	C11	1.525(7)
O3	N2	1.205(5)	C11	C12	1.523(6)
O4	N2	1.197(6)	C12	C13	1.380(6)
N1	C9	1.463(6)	C12	C17	1.394(6)
N1	C11	1.490(5)	C13	C14	1.378(7)
N2	C4	1.480(6)	C14	C15	1.364(7)
C1	C6	1.392(5)	C15	C16	1.383(7)
C1	C2	1.397(5)	C16	C17	1.365(7)
C1	C7	1.489(6)			

Table. Fractional coordinates, equivalent isotropic temperature factors ( $\text{\AA}^2$ ) and estimated standard deviations (in parentheses) for compound 40

atom	x	y	z	B
S	0.4746(2)	0.1350(1)	0.36276(3)	5.35(5)
P	0.5540(1)	0.0271(1)	0.31219(3)	4.04(4)
O1	0.4148(4)	-0.1002(4)	0.29747(8)	5.4(1)
O2	0.428(1)	0.1336(4)	0.43958(9)	10.0(3)
O3	0.441(1)	-0.5039(6)	0.57121(9)	11.3(3)
O4	0.438(1)	-0.7007(5)	0.5301(1)	12.5(4)
N1	0.7682(4)	-0.0592(4)	0.31688(9)	4.1(1)
N2	0.441(1)	-0.5507(7)	0.5396(1)	7.6(3)
C1	0.4473(7)	-0.1591(5)	0.4578(1)	4.6(2)
C2	0.4483(8)	-0.3362(5)	0.4482(1)	4.9(2)
C3	0.4469(8)	-0.4645(6)	0.4747(1)	5.1(2)
C4	0.4446(7)	-0.4141(6)	0.5107(1)	5.1(2)
C5	0.4448(8)	-0.2418(7)	0.5218(1)	5.1(2)
C6	0.4446(8)	-0.1148(6)	0.4949(1)	5.0(2)
C7	0.4451(8)	-0.0161(6)	0.4300(1)	5.5(2)
C8	0.4715(9)	-0.0618(6)	0.3902(1)	4.8(2)
C9	0.9292(8)	0.0409(7)	0.3322(2)	4.9(2)
C10	0.932(1)	-0.2231(8)	0.2669(1)	5.8(3)
C11	0.8120(6)	-0.2363(6)	0.3020(1)	4.0(2)
C12	0.9004(6)	-0.3510(6)	0.3318(1)	4.1(2)
C13	1.0963(7)	-0.3782(7)	0.3350(1)	4.8(2)
C14	1.1695(8)	-0.4820(7)	0.3626(2)	6.1(3)
C15	1.0504(9)	-0.5576(6)	0.3879(1)	5.8(3)
C16	0.8537(9)	-0.5320(7)	0.3852(1)	5.7(3)

C17	0.7808 (7)	-0.4309 (6)	0.3576 (1)	4.8 (2)
C18	0.572 (1)	0.2270 (9)	0.2865 (2)	6.3 (3)
H2	0.439 (6)	-0.368 (5)	0.421 (1)	6 (1)
H3	0.455 (7)	-0.589 (6)	0.468 (1)	6 (1)
H5	0.441 (6)	-0.215 (4)	0.547 (1)	3.6 (8)
H6	0.458 (7)	0.002 (5)	0.500 (1)	5 (1)
H8A	0.373 (6)	-0.125 (6)	0.383 (1)	5 (1)
H8B	0.605 (7)	-0.130 (7)	0.386 (1)	7 (1)
H9A	0.961 (8)	0.003 (7)	0.357 (2)	9 (2)
H9B	1.02 (1)	0.01 (1)	0.319 (2)	13 (3)
H9C	0.89 (1)	0.157 (8)	0.331 (1)	9 (2)
H10A	0.868 (7)	-0.161 (7)	0.250 (1)	7 (1)
H10B	1.054 (9)	-0.173 (7)	0.273 (1)	8 (2)
H10C	0.963 (8)	-0.349 (7)	0.258 (1)	8 (1)
H11	0.688 (6)	-0.286 (5)	0.297 (1)	3.8 (9)
H13	1.170 (6)	-0.326 (6)	0.318 (1)	5 (1)
H14	1.295 (7)	-0.501 (7)	0.365 (1)	7 (1)
H15	1.101 (7)	-0.624 (6)	0.406 (1)	6 (1)
H16	0.778 (7)	-0.581 (7)	0.402 (1)	6 (1)
H17	0.659 (6)	-0.414 (6)	0.354 (1)	5 (1)
H18A	0.46 (1)	0.279 (7)	0.289 (1)	8 (2)
H18B	0.68 (1)	0.30 (1)	0.294 (2)	10 (2)
H18C	0.588 (7)	0.192 (6)	0.261 (1)	7 (1)

## REFERENCES

1. *The Role of Phosphonates in Living Systems*; Hildebrand, R. L.; CRC Press: Boca Raton, 1983.
2. Horiguchi, M.; and Kandatsu, M. *Nature* **1959** *184*, 901.
3. Barry, R. J.; Bowman, E.; McQueney, M.; Dunaway-Mariano, D. *Biochem. Biophys. Res. Commun.* **1988** *153*, 177.
4. Bowman, E. D.; McQueney, M. S.; Scholten, J. D.; Dunaway-Mariano, D. *Biochemistry*, **1990** *29*, 7059.
5. Seidel, H. M.; Freeman, S.; Seto, H.; Knowles, J. R. *Nature* (London) **1988** *335*, 457.
6. Brink, J. W. *Phosphorus in the Environment; Its Chemistry and Biochemistry*; Ciba Foundation Symposium No. 57; Elsevier: Amsterdam, 1978; p 23.
7. Van Wazer, J. R. *Phosphorus and Its Compounds*, vol 1; Interscience Publishers Inc: New York, 1951; p 887.
8. Hildebrand R. L.; Henderson, T. O.; Glonek, T. C. *Fed. Proc. Abstr.* **1971**, *30*, 1072.
9. Miceli, M. V.; Henderson, T. O.; Meyers, T. C. *Science* **1980** *209*, 1245.
10. Kandatsu, M.; Horiguchi, M. *Agric. Biol. Chem.* **1962** *26*, 721.
11. Rosenberg, H. *Nature* **1964** *203*, 299.
12. Komai, Y.; Matskawa, S.; Satake, M. *Biochim. Biophys. Acta* **1973** *316*, 271.
13. Kitteredge, J. S. *7th Int. Congr. biochem.* (Jpn) **1967** 453.
14. Dawson, R. M. C.; Kemp, P. *Biochem J.* **1977** *102*, 873.
15. Steiner, S.; Conti, S. F.; Lester, R. L. *J. Bacteriol.* **1973** *116*, 1199.

16. Wassef, M. K.; Hendreix, J. W. *Biochim. Biophys. Acta* **1977** *486*, 172.
17. Hendlin, D.; Stapley, E. O.; Jackson, M.; Wallick, H.; Miller, A. K.; Wolk, F. J.; Miller, T. W.; Chalet, L.; Kahan, F. M.; Foltz, E. L.; Woodruff, F. J.; Matta, J. M.; Hernandez, S.; Mochales, S. *Science* **1969** *166*, 122.
18. Okuhara, M.; Kuroda, Y.; Goto, T.; Okamoto, M.; Terano, H.; Kohsaka, M.; Aoki, H.; Imanaka, H. *J. Antibiot.* **1980** *33*, 24.
19. Bayer, E.; Gugel, K. H.; Hagele, K.; Hagenmaier, H.; Jessipow, S.; Konig, W. A.; Zahne, H. *Helv. Chim. Acta* **1972** *55*, 224.
20. *The Role of Phosphonates in Living Systems*; Hildebrand, R. L.; CRC Press: Boca Raton, 1983.
21. Rosenberg, H.; La Nauze, J. M. *Biochim Biophys. Acta* **1967**, *141*, 79.
22. Shames, S. L.; Wackett, L. P.; Labarge, M. S.; Kuczkowski, R. L.; Walsh C. T. *Bioorg. Chem.* **1987**, *15*, 366.
23. Fitzgibbon, J.; Braymer, H. D. *Appl. Environ. Microbiol.* **1988**, *54*, 1886.
24. La Nauze, J. M.; Rosenberg, H. *Biochim. Biophys. Acta* **1968**, *165*, 438.
25. Dumora, C.; Lacoste, A. M.; Cassaigne, A. *Eur. J. Biochem.* **1983**, *133*, 119.
26. La Nauze, J. M.; Lacoste, A. M.; Cassaigne, A. *Biochim. Biophys. Acta* **1989**, *997*, 193.
27. Dumora, C.; Lacoste, A. M.; Cassaigne, A. *Biochim. Biophys. Acta* **1989**, *997*, 193.

28. Cook, A. M.; Daughton, C. G.; Alexander, M. *J. Bacteriol.* **1978**, *133*, 85.
29. Cook, A. M.; Daughton, C. G.; Alexander, M. *Biochem J.* **1979**, *184*, 453.
30. Daughton, C. G.; Cook, A. M.; Alexander, M. *FEMS Microbiol. Lett.* **1979**, *5*, 91.
31. Daughton, C. G.; Cook, A. M.; Alexander, M. *J. Agric. Food Chem.* **1979**, *27*, 1375.
32. Cook, A. M.; Daughton, C. G.; Alexander, M. *Appl. Environ. Microbiol.* **1978**, *36*, 668.
33. Sinabargarer, D. L.; Braymer, H. D.; Larson, A. D. *Appl. Environ. Microbiol.* **1984**, *48*, 1049.
34. Zelznick, L. D.; Meyers, T. C.; Titchner, E. B. *Biochim. Biophys. Acta* **1963**, *78*, 546.
35. Wackett, L. P.; Shames, S. L.; Venditti, C. P.; Walsh, C. T. *J. Bacteriol.* **1987**, *169*, 710.
36. Bengelsdorf, I. S. *J. Amer. Chem. Soc.* **1955**, *77*, 6611.
37. Barthel, W. F.; Alexander, B. H.; Giang, P. A.; Hall, S. A. *J. Amer. Chem. Soc.* **1955**, *77*, 2424.
38. Eto, M. *Organophosphorus Pesticides: Organic and Biological Chemistry*; CRC Press: Boca Raton, 1979; p 77.
39. Martell, A. E.; Langohr, M. F.; Tatsumoto, K. *Inorg. Chim. Acta* **1985**, *108*, 2166.
40. Frost, J. W. ; Loo, S.; Cordeiro, M. L.; Li, D. *J. Amer. Chem. Soc.* **1987**, *109*, 2166.
41. Avila, L. E.; Frost, J. W. *J. Am. Chem. Soc.* **1988**, *110*, 7904.

42. Walsh, C. T. *Enzymatic Reaction Mechanisms*; Freeman: New York, 1979; p 669.
43. Olsen, D. B.; Hepburn, T. P.; Moos, M. ; Mariano, P. S.; Dunway-Mariano, D. *Biochemistry* **1988**, *27*, 2229.
44. Lee, S.-L.; Hepburn, T. W.; Mariano, P. S.; Dunaway-Mariano, D. *J. Org. Chem.* **1990**, *55*, 5435.
45. Westheimer, F. H. *Acc. Chem. Res.* **1968**, *1*, 70.
46. Chen, C.-M.; Ye, Q. Z.; Zhu, Z.; Wanner, B. L.; Walsh, C. T. *J. Biol. Chem.* **1990**, *265*, 4461.
47. Elliott, A. M. *Biology of Tetrahymena*, Dowden, Hutchinson & Ross: Stroudsburg, PA, 1973; p 45-47.
48. Horiguchi, M.; Kittredge, J. S.; Roberts, E.; *Biochim Biophys. Acta.* **1968**, *165*, 164.
49. Trebst, A.; Geike, F. *Z. Naturforsch*, **1967**, *22b*, 989.
50. Laing, C. R., Rosenberg, H., *Biochem Biophys. Acta.*, **1968**, *156*, 437.
51. Warren, W. A. *Biochim. Biophys. Acta.* **1968**, *156*, 340.
52. Horiguchi, M. *Biochem. Biophys. Acta.* **1972**, *261*, 102.
53. Horiguchi, M.; Rosenberg, H. *Biochim. Biophys. Acta.* **1975**, *404*, 333.
54. Takada, T.; Horiguchi, M. *Biochim. Biophys. Acta.* **1988**, *964*, 113.
55. Kahan, F. M.; Kahan, J. S.; Cassidy, P. J.; Kropp, H. *Ann. NY. Acad. Sci.* **1974**, *235*, 364.
56. Rogers, T. O.; Birnbaum, J. *Antimicrob. Agents Chemother.* **1974**, *5*, 121.

57. Rogers, T. O.; Birnbaum, J.; Demain, A. *Bacteriol Proc.* **A42** (Abstr), 1971.
58. White, R. F.; Birnbaum, J.; Meyer, R. T.; ten Broeke, J.; Chemerda, J. M.; Domain, A. L.; *Appl. Microbiol.* **1971**, *22*, 55.
59. Hammerschmidt, F.; Bayer, B.; Bovermann, G. *Liebigs. Ann. Chem.* **1990**, 1055.
60. Hammeschmidt, f.; Kahlig, H. *J. Org. Chem.* **1991**, *56*, 2364.
61. Hadika, T.; Mori, M.; Imai, S.; Hara, O.; Nagaoka, K.; Seto, H., *J. Antibiot.* **1989**, *42*, 491.
62. Hidaka, T.; Seto, H. *J. Am. Chem. Soc.* **1989**, *111*, 8012.
63. Hidaka, T.; Imai, S.; Hara, O.; Anzai, H.; Murakami, T.; Nagaoka, K.; Seto, H. *J. Bacteriol.* **1990** *172*, 3066.
64. Seto, H. In *Mycotoxins and Phycotoxins*; Steyn, P. S.; Vlegaar, R. Eds.; Elsevier: Amsterdam, 1986; p 77.
65. Adams, F.; and Conrad, J. P. *Soil Sci.* **1953** *75*, 361.
66. Casida, L. E. *J. Bacteriol.* **1960** *80*, 237.
67. Malacinski, G. M.; Konetzka, W. A. *J. Bacteriol.* **1967** *93*, 1906.
68. Elmsley, J.; Hall, D. *The Chemistry of Phosphorus*; John Wiley and Sons: New York, 1976; p 133.
- 69.. Melvin, L. S. *Tetrahedron Lett.* **1981**, *22*, 3375.
70. Calogeropoulou, T.; Hammond, G. B.; Weimer, D. F. *J. Org. Chem.* **1987**, *52*, 4185.
71. Jackson, J. A.; Hammond, G. B.; Weimer, D. F. *J. Org. Chem.* **1989**, *54*, 4750.
72. Welch, S. C.; Levine, J. A.; Bernal, I.; Cetrullof, J. *J. Org. Chem.* **1990**, *55*, 5991.

73. Machleidt, H.; Strehlke, G. U. *Agrew. Chem. Internat. Edit.* **1964**, *3*, 443.
74. Knowles, J. R. *Ann. Rev. Biochem.* **1980**, *49*, 877.
75. Zimmerman, H. E. in *Pericyclic Reactions, vol 1*; Marchland, A. P.; Lehr, R. E. Eds.; Academic Press: New York, p 53.
76. Webb, T. C. *Eur. J. Biochem.* **1990**, *187*, 278.
77. Barry, R. Ph. D. Dissertation, University of Maryland at College Park, 1987.
78. Walsh, C. T. *Enzymatic Reaction Mechanisms* W. H. Freeman and Company: New York; 1979, p 686-689.
79. Bowman, E.; McQueney, M.; Barry, B.; Dunaway-Mariano, D. J. *Amer. Chem. Soc.* **1988**, *110*, 5575.
80. Walsh, C. T. *Enzymatic Reaction Mechanisms* W. H. Freeman and Company: New York; 1979, p 686-689.
81. Huheey, J. E. *Inorganic Chemistry* 3rd Ed.; Harper and Row; New York, **1983**; p A-31. Tarr, A. M.; Whittle, E. *Trans. Faraday. Soc.* **1964**, *60*, 2039.
82. Atkinson, M. R.; Morton, R. K. in *Comparative Biochemistry*; Florin, M.; Mason, H. S., Eds.; Academic Press: New York, 1963, Vol. II, p 1.
83. Schwalbe, C. H.; Freeman, S. J. *Chem. Soc. Chem. Commun.*, **1990**, 251.
84. Srere, P. A., *Ann. Rev. Biochem.* **1987**, *56*, 89.
85. Frey, P. A.; Sammons, R. D. *Science* **1985** *228*, 541.
86. Liang, C.; Allen, L. C. *J. Amer. Chem. Soc.* **1987**, *109*, 6449.
87. Baraniak, J.; Frey, P. A. *J. Am. Chem. Soc.* **1988**, *110*, 4059.

88. Varlet, J., Collignon, N.; Savinac, P. *Can. J. Chem.* **1979**, *57*, 3216.
89. Gatehouse, J. A.; Knowles, J. R. *Biochemistry* **1977**, *16*, 3045.
90. Rose, Z. B. *Arch. Biochem. Biophys.* **1970**, *140*, 508.
91. Seidel, H. M.; Freeman, S.; Schwalbe, C. H.; Knowles, J. R. *J. Amer. Chem. Soc.* **1990**, *112*, 8149.
92. a) Edwards, J. M.; Jackman, L. M. *Aust. J. Chem.* **1965**, *18*, 1227. b) Andrews, P. R.; Smith, G. D.; Young, I. G. *Biochemistry* **1973**, *12*, 3492.
93. a) Feldman, F.; Butler, L. *Biochem. Biophys. Res. Commun.* **1969**, *119*, 36. b) Schwartz, J.; Lipmann, F. *Proc. Natl. Acad. Sci.* **1961**, *47*, 1996.
94. Ray, W.; Peck, E. In *The Enzymes vol. 6.*; Boyer, P. Ed; Academic Press.
95. a) Dahl, J.; Hokin, L. *Ann. Rev. Biochem.* **1974**, *43*, 327.  
b) Degani, C.; Boyer, P. *J. Biol. Chem.* **1973**, *248*, 8222.  
c) MacLennan, D. *J. Biol. Chem.* **1975**, *249*, 974, 980
96. Rose, I. A. *J. Biol. Chem.* **1960**, *235*, 1170.
97. Moskovitz, B.; Wood, H. G. *J. Biol. Chem.* **1978**, *253*, 884.
98. Berson, J. A. *Acc. Chem. Res.* **1968**, *1*, 152.
99. DeBruin, K. E.; Tang, C.W.; Johnson, D. M.; Wilde, R. L. *J. Amer. Chem. Soc.* **1989**, *111*, 5871.
100. Vedejs, E.; Marth, C. F. *J. Amer. Chem. Soc.* **1989**, *111*, 151.
101. Baraniak, J.; Kinas, R. W.; Lesiak, K.; Stec, W. J. *J. Amer. Chem. Soc. Chem. Commun.* **1978**, *100*, 940.
102. Gerlt, J. A.; Coderre, J. A. *J. Amer. Chem. Soc.* **1980**, *102*, 4531.

103. The X-ray analysis was performed by Dr. H. Ammon, University of Maryland at College Park.
104. Sheu, K. -F.; Ho, H. -T.; Nolan, L. D.; Markovitz; P. Richard, J. P.; Utter, M. F.; Frey, P. A. *Biochemistry* **1984**, *23*, 1779.
105. Richard, J. P.; Ho, H. -T.; Frey, P. A. *J. Amer. Chem. Soc.* **1978**, *100*, 7756.
106. Cooper, D. B.; Harrison, J. M.; Inch, T. D. *Tetrahedron Lett.* **1974**, *31*, 2697.
107. Harrison, J. M.; Inch, T. D.; Lewis, G. I. *J. Chem. Soc., Perkin Trans. 1* , **1975**, 1982.
108. McQueney, M. S.; Lee, S-L.; Bowman, E.; Mariano, P. S.; Dunaway-Mariano, D. *J. Amer. Chem. Soc.* **1989**, *111*, 6885.
109. (a) McQueney, M. S., Lee, S-l., Bowman, E., Mariano, P. S., and Dunaway-Mariano, D. *J. Amer. Chem. Soc.* **1989**, *111*, 9280.
110. Schray, K. J.; Benkovic, S. J. *J. Amer. Chem. Soc.* **1971**, *93*, 2522.
111. Hepburn T. Ph. D. Thesis, University of Maryland at College Park, 1988.
112. Freeman, S.; Seidel, H. M.; Schwalbe, C. H.; Knowles, J. R. *J. Amer. Chem. Soc.* **1989**, *111*, 9233.; Seidel, H. M.; Freeman, S.; Schwalbe, C. H.; Knowles, J. R. *J. Amer. Chem. Soc.* **1990**, *112*, 8149.
113. Breslow, R.; Katz, I. *J. Amer. Soc.* **1969**, *90*, 7376.
114. Freeman, S.; Irwin, W. J.; Schwalbe, C. H. *J. Chem. Soc. Perkin Trans. II*, **1991**, 263.

115. Anderson, V. E.; Wies, P. M.; Cleland, W. W.; *Biochemistry* **1984**, *23*, 409.
116. La Nauze, J. M.; Coggins, J. R.; Dixon, H. B. F. *Biochem. J.* **1977**, *165*, 409.
117. Chambers, J. R.; Isbell, A. F.; *J Org. Chem.* **1964** *29*, 832.
118. TEXRAY *Structure Analysis System*, **1989**, ver. 5.0, Molecular Structure Corp., 3200a Research Forest Dr., The Woodlands, TX 77381.
119. Gilmore, MITHRIL, *A Computer Program for the Automatic Solution of Crystal Structures*, **1983**, Univ. of Glasgow, Scotland.
120. Luo, J.; Ammon, H. L.; Gilliland, G. L. *J. Appl. Cryst.* **1989**, *22*, 186.